การประยุกต์ระบบเฝ้าระวังแบบพื้นที่กว้างเพื่อรักษาเสถียรภาพแรงดัน

นายเลสนานโต มัลตา ปูตานโต

วิทยานิพนธ์นี้เป็นส่วนหนึ่งของการศึกษาตามหลักสูตรปริญญาวิศวกรรมศาสตรมหาบัณฑิต
สาขาวิชาวิศวกรรมไฟฟ้า ภาควิชาวิศวกรรมไฟฟ้า
คณะวิศวกรรมศาสตร์ จุฬาลงกรณ์มหาวิทยาลัย
ปีการศึกษา 2554

APPLICATION OF WIDE AREA MONITORING SYSTEM FOR SECURING VOLTAGE STABILITY

Mr. Lesnanto Multa Putranto

A Thesis Submitted in Partial Fulfillment of the Requirements
for the Degree of Master of Engineering Program in Electrical Engineering
Department of Electrical Engineering
Faculty of Engineering
Chulalongkorn University
Academic Year 2011

Thesis Title	APPLICATION OF WIDE AREA MONITORING SYSTEM FOR SECURING VOLTAGE STABILITY
By	Mr. Lesnanto Multa Putranto
Field of Study	Electrical Engineering
Thesis Advisor	Assistant Professor Naebboon Hoonchareon, Ph.D.

Accepted by the Faculty of Engineering, Chulalongkorn University in Partial Fulfillment of the Requirements for the Master's Degree

……Dean of the Faculty of Engineering
(Associate Professor Boonsom Lerdhirunwong, Dr.Ing.)

THESIS COMMITTEE

…….. Chairman
(Assistant Professor Kulyos Audomvongseree, Ph.D.)

…….……. Thesis Advisor
(Assistant Professor Naebboon Hoonchareon, Ph.D.)

…….. Examiner
(Surachai Chaitusaney , Ph.D.)

…….. External Examiner
(Associate Professor Issarachai Ngamroo, Ph.D.)

เลสนานโต มัลตา ปูตานโต: การประยุกต์ระบบเฝ้าระวังแบบพื้นที่กว้างเพื่อรักษาเสถียรภาพแรงดัน (APPLICATION OF WIDE AREA MONITORING SYSTEM FOR SECURING VOLTAGE STABILITY) อ.ที่ปรึกษาวิทยานิพนธ์หลัก: ผศ.ดร.แนบบุญ หุนเจริญ, 92 หน้า

ระบบเฝ้าระวังแบบพื้นที่กว้างโดยใช้เครื่องวัดเฟสเซอร์เป็นเครื่องมือขั้นสูงที่สามารถช่วยผู้ปฏิบัติการเฝ้าระวังสถานะของระบบไฟฟ้ากำลัง โดยรวมถึงสมรรถนะของเสถียรภาพเชิงแรงดันในเวลาจริง วัตถุประสงค์ของวิทยานิพนธ์นี้คือการหาจำนวนเครื่องวัดเฟสเซอร์ที่น้อยที่สุดและตำแหน่งติดตั้งในโครงข่ายไฟฟ้าที่กำหนด และนำเสนอการประยุกต์ใช้ระบบเฝ้าระวังแบบพื้นที่กว้างเพื่อแสดงสมรรถนะเสถียรภาพเชิงแรงดัน วิธีการหาจำนวนเครื่องวัดเฟสเซอร์ที่น้อยที่สุดและจุดติดตั้งคัดเลือกจากการเปรียบเทียบประสิทธิผลทั้งหมดสามวิธี ได้แก่ ขั้นตอนทฤษฎีกราฟ ระเบียบวิธีวนซ้ำแบบเอ็น และวิธีกำหนดการเชิงเส้นแบบจำนวนเต็ม โดยเลือกวิธีสุดท้ายเมื่อพิจารณาจากความสามารถในการประเมินสถานะของระบบ ถัดมาเป็นการพัฒนาระบบเฝ้าระวังแบบพื้นที่กว้าง ประกอบด้วยการเลือกดัชนีชี้วัดเสถียรภาพเชิงแรงดันที่เหมาะสม การใช้เทคนิคการประมาณสถานะแบบเชิงเส้น และการออกแบบส่วนต่อประสานเชิงกราฟฟิกกับผู้ใช้ ใช้ดัชนีชี้วัดเสถียรภาพเชิงแรงดันแบบซิงโครเฟสเซอร์และแบบ PQ ซึ่งเหมาะกับการประยุกต์ใช้แบบออนไลน์ เพื่อจัดลำดับความอ่อนแอของบัสและสายส่งตามลำดับ ประสิทธิผลของการพัฒนาระบบเฝ้าระวังแบบพื้นที่กว้างนี้ได้ถูกแสดงให้เห็นโดยใช้ข้อมูลของระบบทดสอบ IEEE 14 บัส ภายใต้ 4 กรณีศึกษา ภายใต้ผลจากการเพิ่มโหลดต่อเนื่องหลายบัสในเวลาพร้อมกัน และจากความผิดพร่องอันเนื่องมาจากการลัดวงจรในระบบ ดัชนีสมรรถนะที่คำนวณได้ในเวลาจริง รวมทั้งจุดวิกฤตบนเส้นโค้ง PV ที่แสดงผลในส่วนต่อประสานเชิงกราฟฟิกกับผู้ใช้ ได้รับการตรวจสอบกับค่าที่แท้จริงในภายหลัง โดยใช้การจำลองแบบเชิงพลวัตของระบบภายใต้เงื่อนไขที่สอดคล้องกัน

ภาควิชา วิศวกรรมไฟฟ้า ลายมือชื่อนิสิต .....

สาขาวิชา วิศวกรรมไฟฟ้า ลายมือชื่อ อ.ที่ปรึกษาวิทยานิพนธ์หลัก .....

ปีการศึกษา 2554

537 06088 21 : MAJOR ELECTRICAL ENGINEERING

KEYWORDS: PHASOR MEASUREMENT UNIT / WIDE AREA MONITORING SYSTEMS / VOLTAGE STABILITY INDEX / STATE ESTIMATION

LESNANTO MULTA PUTRANTO: APPLICATION OF WIDE AREA MONITORING SYSTEM FOR SECURING VOLTAGE STABILITY. ADVISOR: ASST. PROF. NAEBBOON HOONCHAREON, Ph.D.,92 pp.

Wide Area Monitoring System (WAMS) using Phasor Measurement Unit (PMU) as the input devices is an advanced tool, which can help system operators monitor a power system condition, including voltage stability performance, in real time. The objectives of this thesis have two folds which are to determine the minimum number and location of the PMU to be installed given power network topology, and to propose the application of WAMS for monitoring voltage stability performance. The solution method of determining the minimum number and location of the PMU has been selected by comparing the effectiveness of the three methods proposed in the literatures, which are the Graph Theoretic Procedure, the Recursive N Method and the Generalized Integer Linear Programming. In this thesis, the Generalized Integer Linear Programming is chosen in regard to the observability performance. Then, the implementation of WAMS consisting of selecting suitable voltage stability indexes (VSI), employing linearly formulated state estimation technique, and designing graphic user interface (GUI) has been developed. The Synchrophasor-Based Real-Time Voltage Stability Index (SBRT VSI) and the PQ Voltage Stability Index (PQVSI), which suit well for on-line application, are used to identify the weak bus and the weak line rankings, respectively. The effectiveness of the developed WAMS has been successfully demonstrated using the simulated data of the IEEE 14-bus test system under four scenarios combining the effects of continued load increases at various load buses simultaneously, and short circuit faults. All the computed, on-line performance indexes including the critical point on the PV curve shown in the GUI have been verified against the actual values obtained later from the dynamic simulation of the system for the corresponding conditions.

Department : Electrical Engineering Student's Signature .....

Field of Study : Electrical Engineering Advisor's Signature .....

Academic Year : 2011

ACKNOWLEDGEMENTS

First of all, I would like to take this opportunity to express my deepest gratitude to my thesis supervisor, Assistant Professor Naebboon Honchareon, for all his careful guidance and considerable support during my study at Chulalongkorn University. This thesis would not have been possible without his great encouragement and enthusiastic supervision.

I am thankful to Chulalongkorn University, especially the Power System Research Laboratory, for making an excellent and professional working environment. I am indebted to Associate Professor Boonchai Techaumnat, Assistant Professor Assistant Professor Kulyos Audomvongseree, Dr. Surachai Chaitusaney, Professor David Banjerdpongchai and Professor Bundhit Eua-arporn and all of electrical engineering lecturers, for proving me the fundamental background involving the field of Power Systems. The knowledge that I gained from their lectures is particularly useful not only for the work in this thesis but also for my future research.

I greatly appreciate the considerable effort of all the committee members including Assistant Professor Kulyos Audomvongseree, Associate Professor Issarachai Ngamroo, Dr. Surachai Chaitusaney and Assistant Professor Naebboon Honchareon who have spent time in reading the manuscript of the thesis and attending the thesis defence. Their useful comments and constructive advices are absolutely invaluable. My thanks also go to everyone at Chulalongkorn University, especially students and staffs of Power System Research Laboratory, for their great friendship and enthusiastic help.

I gratefully acknowledge the full financial support from the ASEAN University Network/Southeast Asia Engineering Education Development Network (AUN/SEED-Net) for my Master's program in Thailand. My sincere thanks are also extended to the International School of Engineering (ISE), Chulalongkorn University for their care and help during my study.

Finally, I would like to dedicate this thesis to all members in my family and friends for their endless love and support.

CONTENTS

Page

Page

Page

LIST OF TABLES

Page

LIST OF FIGURES

Page

Page

CHAPTER I
INTRODUCTION

1.1 Motivation

Nowadays, the power system is growing bigger and more complex. The power system growth is caused by the load demand growth. Fulfilling load demand growth, not only the number of the generation is increased but also the number of the station (bus) and the transmission-line is increased. Moreover the reliability design philosophy and the electricity market lead the power systems to operate close to the capacity limit[1]. Consequently, the risk of suffering disturbance is increasing in bigger power system.

Wide Area Monitoring System (WAMS) is the new concept in the power system that will provide us a real time monitoring of the whole system. WAMS has been applied in worldwide power system especially in USA and Europe in some applications. WAMS records the real time data, computes the real time data and provides real time information pertinent to the operating system condition.

Having the fast response [2] against disturbance, WAMS is applicable to prevent the power system from the collapse (black out) by applying on-line monitoring. Based on the WAMS monitoring, proper action can be taken to provide good anticipation.

One of the WAMS applications is to monitor the voltage stability performance. Various voltage stability indexes (VSI) have been developed to assess the voltage stability performance. Applying the voltage stability index calculation in WAMS [3, 4] the voltage stability performance can be well observed. Based on the real time monitoring information, system utility operator can applied some action to prevent voltage collapse.

1.2 Specific Objective

The work in this thesis to build the WAMS for securing the voltage stability of the power systems transmission. There are two specific detail objective of this work:

1. Determine sufficient number of Phasor Measurement Unit (PMU) and location in power system to warrant full observable condition.

   In the real application, PMU cannot be installed in every station in power system network. Sufficient number of PMU is needed to be determined by certain algorithm to warrant the power system operation in the full observable condition.

2. Build WAMS to monitor the voltage stability performance in real time and show the result in user interface tool.

WAMS has the capability to do real time monitoring, voltage profile and voltage stability index are shown to give the power system operating condition simultaneously.

1.3 Scope of Work

1. Input data are voltages and line currents from certain busses and line recorded by PMU.
2. The disturbance in the power system is the combination of continued load increases at various load buses simultaneously, and short circuit faults.
3. Load models are modeled using constant power model and constant shunt admittance
4. In the simulation, the delay in the communication system is neglected.
5. Computation:
   a. PMU number and location determination
   b. State estimation
   c. Voltage stability indexes calculation
6. Develop Graphic User Interface for real time monitoring

1.4 Methodology

1. Literature survey
2. Determine the specific objective and scope of work
3. Formulate the problem
4. Determine the solution method
5. Build and test the power system and WAMS model
6. Analyze and conclude the result

1.5 Expected Contribution

1. Dynamic security assessment, in this case Voltage stability assessment of the power system network can be done using the real time WAMS

   When WAMS implemented in the power system utility, the power system utility have the system to do on-line monitoring. The display of the WAMS helps the system operator identify whether the power system is in the secure or insecure condition

2. Danger due to voltage stability problem can be reduced.

   On-line monitoring gives the updated information about the voltage stability performance of WAMS. Information from WAMS can be used to assess the voltage stability performance. Based on the assessment proper

action can be done immediately to prevent the danger due to the voltage stability problem.

The report consists of six chapters. The other chapters, except the Chapter I, are described as follow.

Chapter II, the background knowledge of WAMS is described. In this chapter, the definition, PMU as input device, application of WAMS and the state estimation are elaborated.

Chapter III presents the method of VSI calculation that in this work such as Synchrophasor-Based Real-Time Voltage Stability Index (SBRT VSI) and PQ Voltage Stability Index (PQVSI).

Chapter IV explains the problem formulation and methodology. In this chapter, the input, process including the selected techniques and output of the WAMS are elaborated.

Chapter V describe about the test procedure and the test result. Discussion part is also presented to emphasize the importance of WAMS result.

Chapter VI gives the future work and the conclusion of this work.

.

CHAPTER II
WIDE AREA MONITORING SYSTEM

2.1 Overview of Wide Area Monitoring System

2.1.1 Definition

Wide Area Monitoring System (WAMS) is a new concept in modern power system transmission. WAMS is defined (by Machowski, 2008) as measurement systems based on the transmission of analogue and/or digital information using telecommunication systems and allowing synchronization (time stamping) of the measurements using a common time reference [5].

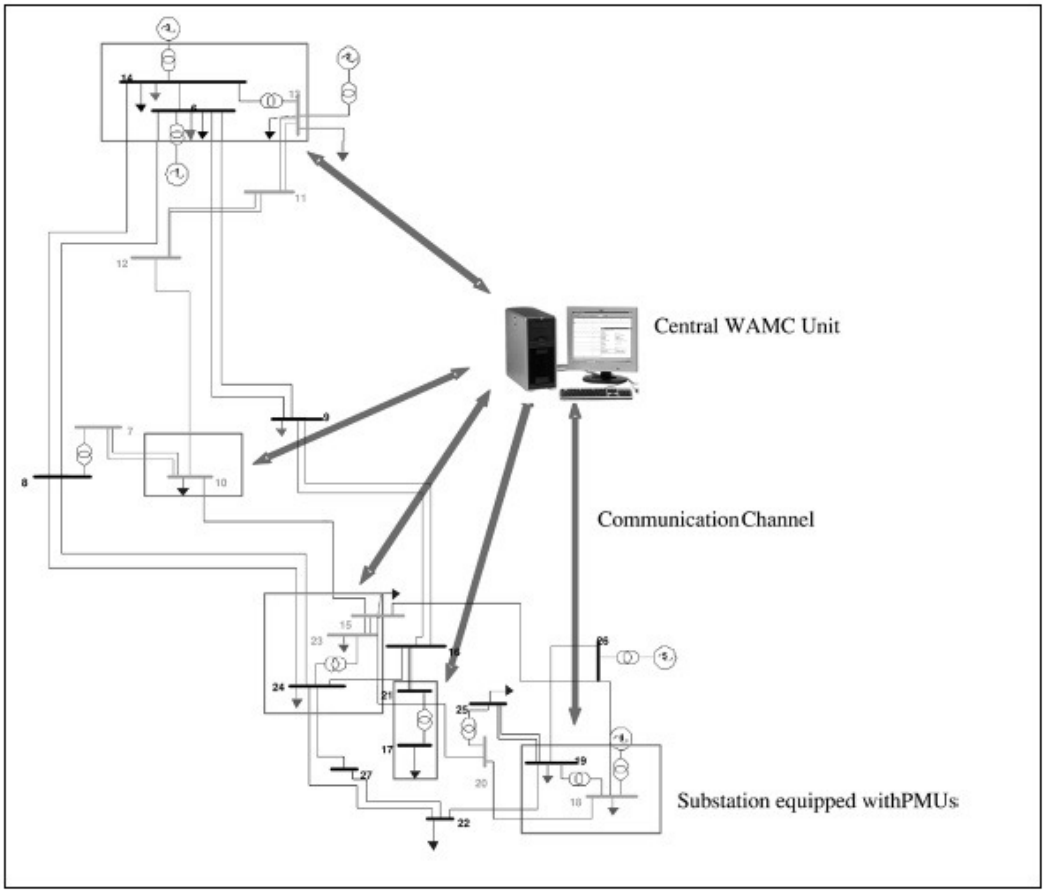

Figure 2.1 The Topology of Wide Area Monitoring in Power Systems [2].

Vladimir Terzija also define WAMS a new concept that measure and monitor the whole of the system at the same time by using the telecommunication technology so that the accuracy of the measurement is better than the conventional measurement[4]. By each definition WAMS can be divided into several parts such input device, communication, algorithm, output device and application.

The topology of WAMS can be seen in Figure 2.1. WAMS monitors all of the bus and line in the power system in the same time reference (real time). The input devices take the data from selected bus and line and then through the communication devices the data is collected into the data center. In the data center, certain algorithm is applied to calculate the data become useful information.

All of the WAMS part is important such input devices, communication devices, data center and also the output device. The topology of the WAMS is shown below as described in reference[2].

2.1.2 Input Device

Input devices are part of the WAMS structure. Accuracy and response of input devices is the compulsory requirement to be used in WAMS. The devices used for input devices must have fast response to the signal changes, real time capability and synchronized with the other input devices.

There are several kinds of metering used in WAMS such as using the relay metering, Phasor Measurement Unit (PMU) or Digital Fault Recorder (DFR). Among these three kinds of metering base, the most common device used in the application is PMU.

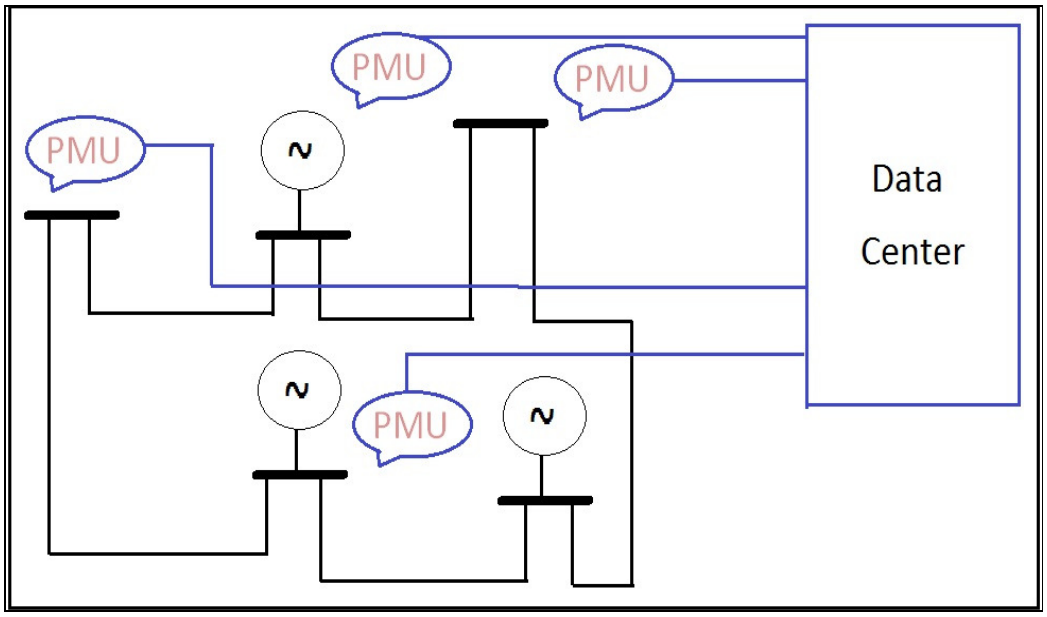

Figure 2.2 PMU as Input Devices in WAMS

Phasor Measurement Unit (PMU) is commonly used in WAMS. PMU usually is placed in bus or line of the power system. All of the PMU in the power system must be synchronized each other. Global Positioning Unit (GPS) is commonly used to synchronize the reference time of PMU.

PMU is measured the voltage (V), voltage angle (θ), current (I), current angle (ϕ) [6]. In practical, PMU is located in bus and measure the bus voltage and line current from/to immediately adjacent bus with the bus that PMU installed on.

2.1.3 Communication

There are various kinds of information that can be provided by the WAMS depend on the information needed. The data from the input devices from various locations will be collected centrally in a data center. Then the data is used for evaluating the actual power system operation conditions respect to the stability limits[2].

WAMS use the concept that involves the use of system-wide information and the communication of selected local information to a remote location [4]. This concept can see all the power system area and can monitor the transmission-lines as unit protection so that disturbance monitoring can be done well [6].

Based on reference [3], due to potential loss of communication, the relay of communication system must be designed well to detect failures and tolerate noise. The communication network needs to be designed for fast, robust and reliable operation.

Synchronous optical network (Sonet/SDH) is communication protocol commonly used for WAMS. Self-healing (or survivability) capability is a distinctive feature of Sonet/SDH networks is possible because of ring topology. This means that if communication between two nodes is lost, the traffic among them switches over to the protected path of the ring.

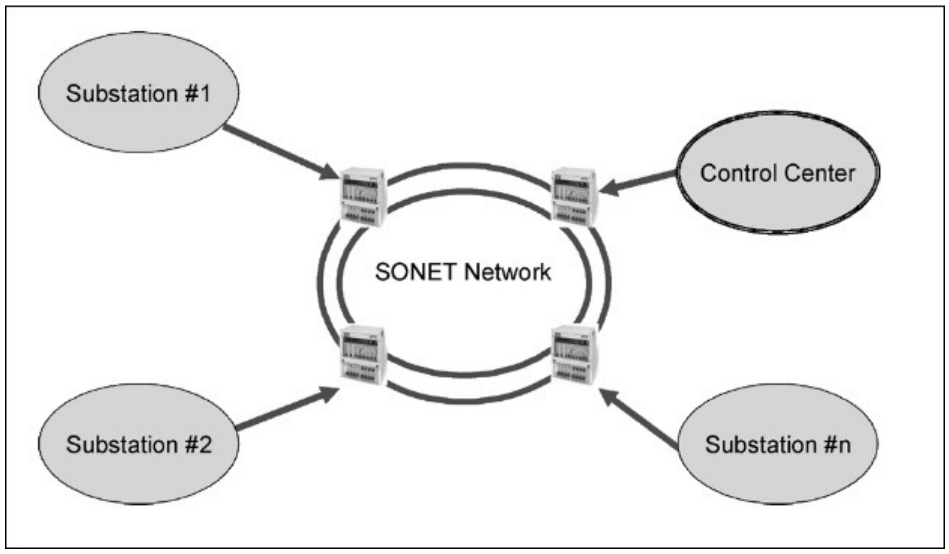

Figure 2.3 Sonet Communication System Architechture [3]

2.1.4 Application

Algorithm of the WAMS is the key to perform specific application. WAMS is specific for each system and can be designed into different specific purpose (among WAMSs). Algorithm is strictly depended on the application of the WAMS that also affects input variable and the desired output [2].

WAMS can be designed to protect all over the transmission system by developing interconnected system protection terminals. WAMS is designed centralized that all data from the input devices is sent to the control center for process in to useful information. In the control center, some algorithm and model are applied to the specific objective. The result of algorithm and modeling then send to the system operator or control some indicators[2].

WAMS has already been applied in some electrical transmission network in the world into several applications. The final objective of installing WAMS is to make the power system more powerful by giving real time monitoring information. The WAMS can be applied in to several applications [2, 7, 8] such as:

- Frequency stability assessment
- Oscillation stability assessment
- Voltage stability assessment
- Line temperature monitoring
- State estimator
- Parallel application with FACTS devices

2.1.4.1 WAMS for Improving Voltage Stability in Southern Sweden

The WAMS in Southern Sweden is called the Special Protection System (SPS)[3]. The main function of this system is to avoid voltage collapse after the disturbance. The WAMS can help the network to increase the voltage stability by increasing the power transfer limit from north Sweden.

Some input measurement such as low voltage level, high reactive power generation and generator current limiters hitting limits are used as inputs for the systems that using the SCADA. Data from the input measurement is calculated with specific algorithm to do the voltage stability assessment.

Proper commands are then ordered from the existing SCADA system to the system operator for increase the power transfer from the north Sweden utility. The amount of the transferable power is also determined. The detail of the process can be shown in Figure 2.4.

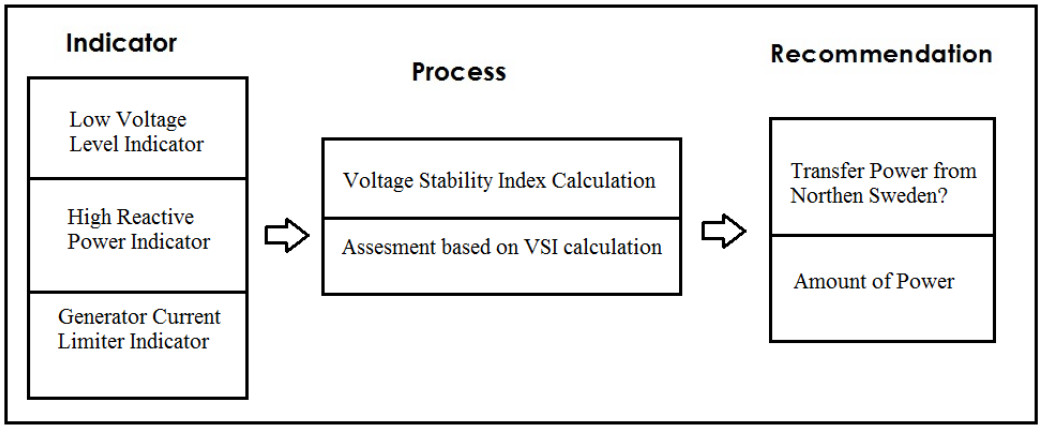

Figure 2.4 Scheme of WAMS in Sweden

2.1.4.2 WAMS for Setting the Automatic Load Shedding for Avoiding Voltage Collapse

BC Hydro has developed an automatic load shedding remedial action scheme to protect the system against voltage collapse[3]. A closed-loop feedback scheme will monitor the system condition and determine the necessity of load shedding. The scheme is based on a centralized feedback system.

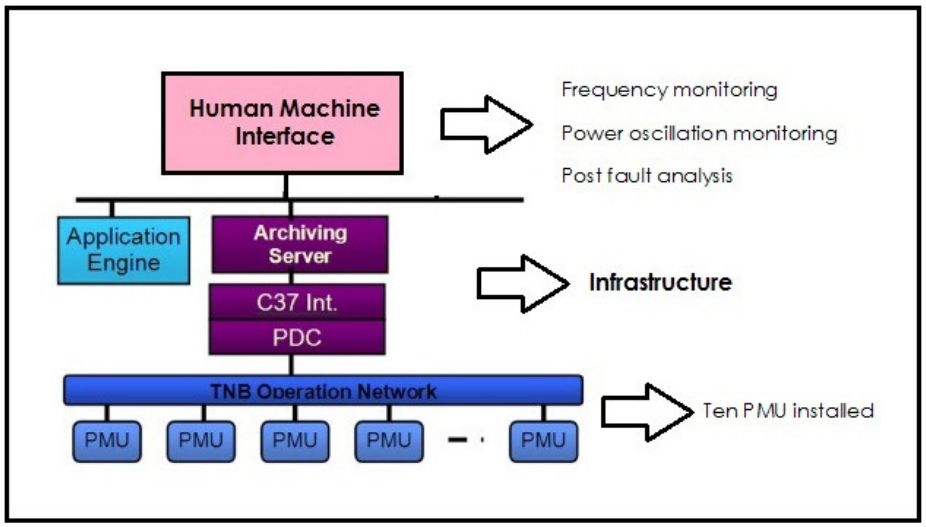

Figure 2.5 WAMS in TNB Malaysia [8]

The system is continually assesses the entire system condition using the actual dynamic response of the system voltages at weak buses and dynamic VAR reserves of two large reactive power sources in the load area. These methods is to identify the voltage instability and then sheds predetermined loads in steps recursively until the potential for voltage collapse is eliminated.

The weak voltage buses are selected based on their sufficiently high fault levels and having multiple low-impedance connections to load centers so that local system outages will not affect the voltages significantly to cause disoperation. The VAR sources are selected based on their large capacity relative to the total load area dynamic VAR capacity.

2.1.4.3 Wide Area Monitoring in Tenaga National Berhad Malaysia

Wide area monitoring system in TNB Malaysia [8] is for wide frequency monitoring, power oscillation monitoring and post-fault analysis. WAMS structure in the TNB power system is consisted of the input, process and the output. The input of WAMS in TNB Malaysia is the PMU, there is ten PMU installed to measure the voltage in certain buses in power system network. The process of WAMS in TNB network consists of the Process Data Concentrator (PDC), application engine and the server. Data is collected from several stations in the power system in the PDC. From PDC the data will be calculated or formulated into useful information like the frequency and power oscillation as an output.

In power system network it is important to maintain the frequency value stable like the TNB power system that maintains the frequency in 50 Hz. Under steady-state condition the frequency must be maintained within ±1% (between 49.5 Hz and 50.5 Hz). During emergency conditions (when the power imbalance happened), the low frequency demand corrective control (LFDC) is often used as the last measure to prevent total system collapse under the WAMS. Ten PMU is installed to support the WAMS. In TNB, the power imbalanced is predicted to maintain the frequency stability.

2.1.4.4 The Application of WAMS in Commission Federal de Electricidad Mexico

In the Commission Federal de Electricidad (CFE) Mexico [9], there are PMUs equipped with the GPS supporting the WAMS. The WAMS applications in CFE is for Post-Fault Analysis and Real Time monitoring.

In post-fault analysis, data such as voltage, current and frequency are recorded by the PMUs in selected station. These information is used for model validation and updating the data base. Moreover, the data recorded are used to make the Q-V, P-V, R-X and P-f curves during the disturbance. The analysis is very important due to the interconnection with the North-West and National systems.

The example of the graph of the post disturbance analysis is shown in in Figure 2.6 a, b and c. Figure 2.6 a show the P-V characteristic of several station in CFE during the synchronization test. Figure 2.6 b shows the P-f curve of several generator buse in CFE also during synchronization. Figure 2.6 c shows the R-X characteristic during the disturbance in CFE. The last is Figure 2.6 d show the power system

network in CFE that consist of three regions that with the WAMS the three areas of CFE regions can be communicate each other.

In real time monitoring, WAMS is used to provide the system operator with the adequate signals of bus voltage and line current in critical location. Preventive action is taken by analyze those signals.

2.2 Phasor Measurement Unit

Phasor Measurement Unit (PMU) is the measuring device that is used for collecting the data from several stations in the power system transmission network. PMU can support the power system In order to perform the real time voltage stability monitoring. Phasor Measurement Unit (PMU) is the most commonly devices use as the input devices of the WAMS. PMU has the entire requirement as mentioned above. Data measured by the PMU is in phasor based that consist of magnitude and angle. In this work the input devices is set to be a PMU [4].

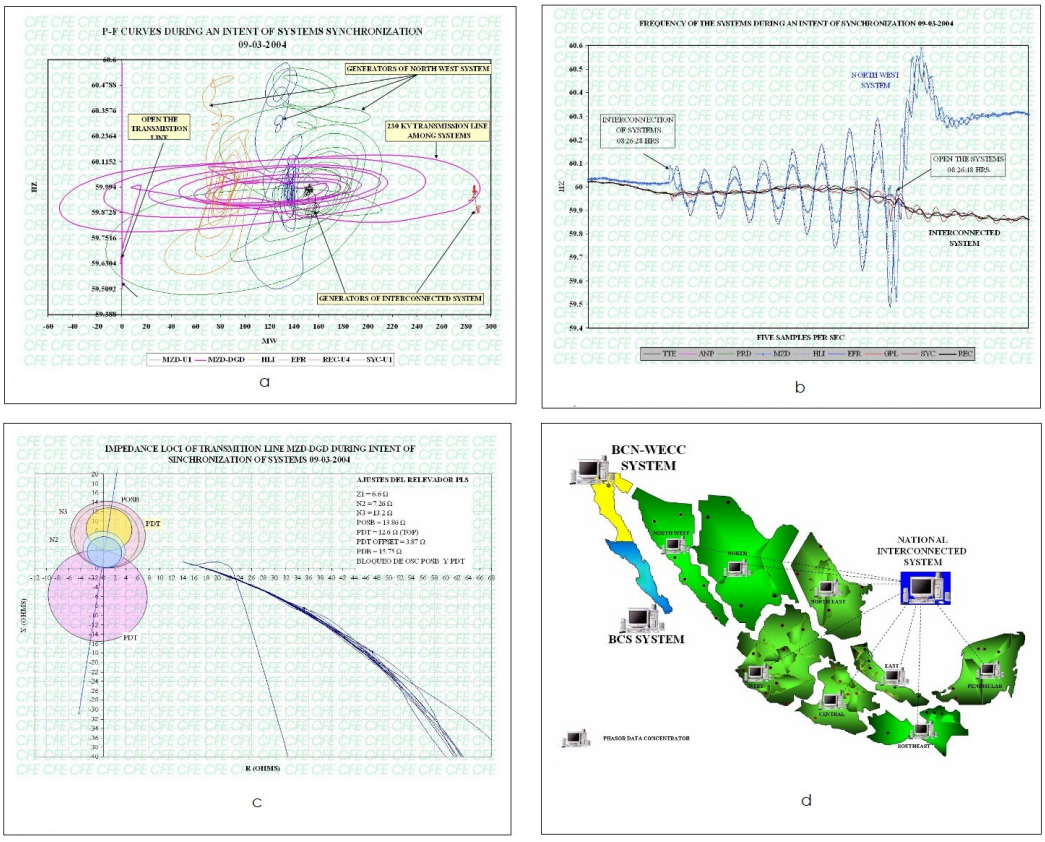

Figure 2.6 a. P-V curves of station in CFE, b. Frequency monitoring, c. Impedance analysis post fault and d. Topology of Mexico WAMS [9]

2.2.1 Feature of Phasor Measurement Unit

PMU's are commonly used in the WAMS as an input device. Some advantages of using PMU as input devices are the high sample rate, high precision, selective to the noise and the synchronization time [4]. The methodology of WAMS measurement based on the chosen of common coordinates for a power system. The common coordinates for the whole WAMS are obtained by synchronizing the measurement using the Global Positioning Systems (GPS).

The measurement system allows measurement of the phasors of voltage and currents in power system is referred to as PMU [5]. The voltage measured by the PMU is in the bus that PMU installed on. Line current measured by PMU is line current that flows from/to the bus that PMU installed on. Voltages in the bus that does not have PMU can be calculated by the measured data from PMU (voltage bus and current line).

PMU installed in the station of power system network must be integrated to the user interface system and communication system. As mentioned is reference [10], PMU must require:

1. at least have 15 inputs and 8 outputs
2. compatible with Personal Computer (PC)
3. has plot data to remote control operation
4. sample rate at least 10 per second
5. interfacing with satellite clock
6. phase angle accuracy within 1 degree.

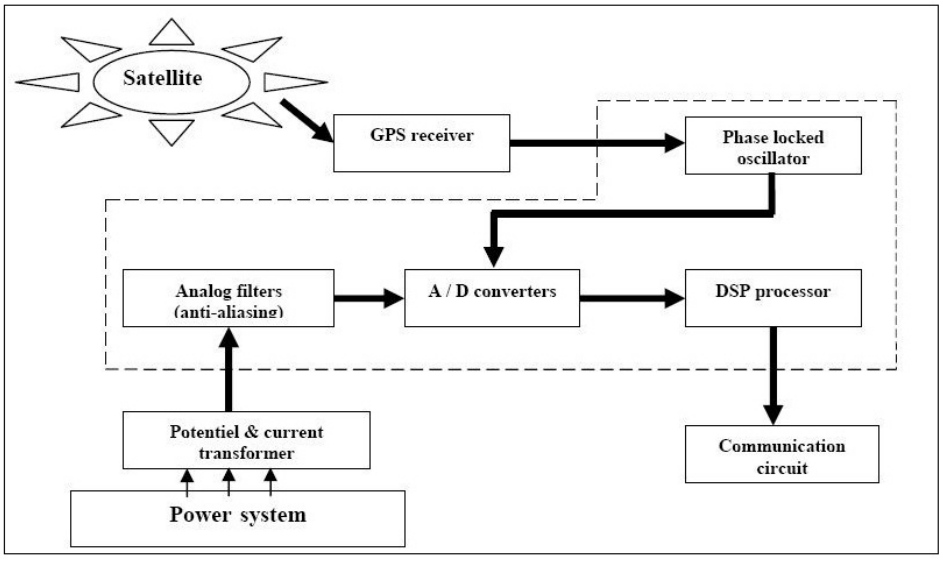

Figure 2.7 Functional Diagram of PMU [11]

In a power system several number of PMU are installed in the station (bus). In application, data collected from all PMU in network send to the data center. In data center the collected data is computed by some algorithm and model to be a specific application such as for maintaining voltage stability. The output of the computation is useful information that is user friendly for the system operator [11].

Voltage and line current can be monitored by PMU. PMU provides two types of measurement, bus voltage phasors and line current phasors. Assuming the channel is sufficient, PMU record the voltage phasor and line current phasors flowing from/to PMU bus [12].

The advantage of PMU measurement, the signal measured is only the fundamental so that the higher harmonics and the DC component are washed out. The three phase phasor of the signal are replaced by their positive sequence components. Positive sequence of phasor is measured every 10 ms, 40 ms or 100 ms depend on the needs. The measured data is stored into the appropriate data format and telecommunication media.

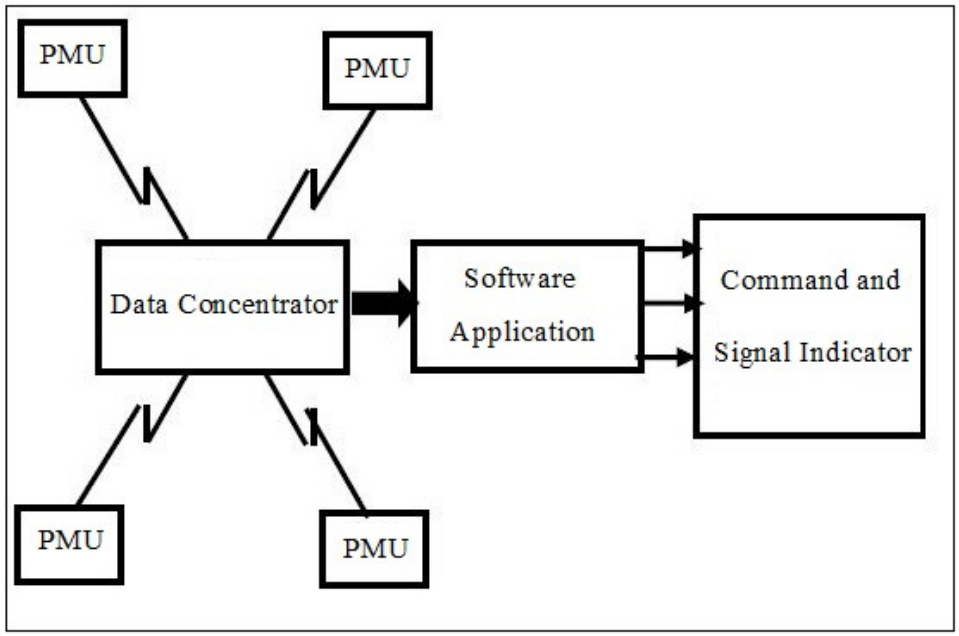

Figure 2.8 Application PMU in Power System Network [11]

2.2.2 Phasor Measurement Unit Placement Methods

The cost of PMU limits the number of PMU installed in the power system. PMU has to be installed in certain station in the power system. The sufficient number of the PMU should be calculated to warrant the observability of the entire power system network. The concept of observability means the location of station is observable in the power system. This concept is called with the topologically observable [13].

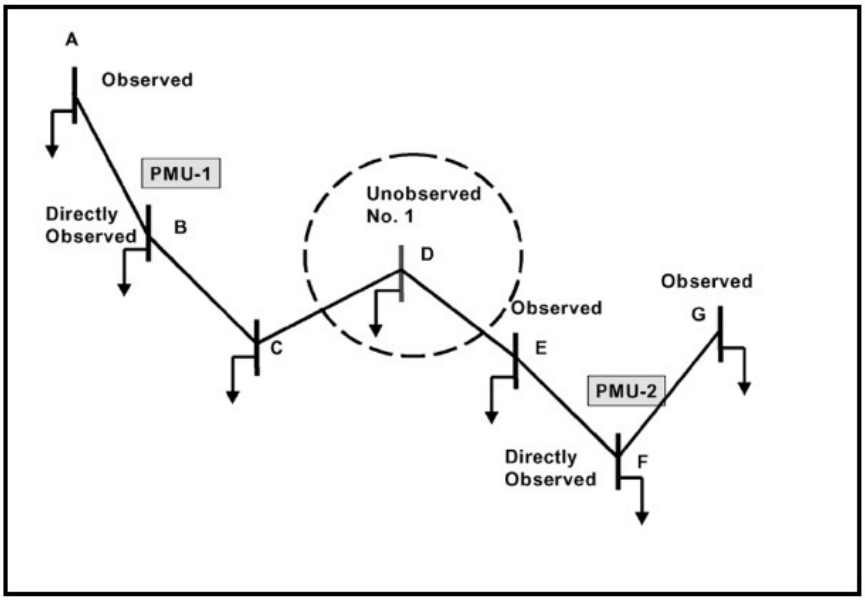

Figure 2.9 Ilustration of Observable and Unobservable of PMU [13]

There are three kinds of condition of a bus/station that are directly observed, observed and unobserved. These three criteria are defined by the topological of the bus in the power system.

Bus is called directly observe when the PMU is installed on that bus and the bus is called PMU bus. However, bus is called observed when the bus is stand next to the PMU bus. Bus stands next to the PMU bus is often called by immediately adjacent bus or calculated bus. The other bus condition is on the unobservable. The bus is unobservable when the bus is immediately adjacent to the PMU bus and the PMU bus as shown in Figure 2.9.

Method for determining number and location of PMU is well established and vary depends on the computation and the consideration. Concepts of all the method is developed by the following step:

Step 1: Place PMU at certain bus (PMU bus) so that the voltage at that bus and current line (according to this bus) can be measured.

Step 2: Get the bus that connected to the PMU buses (Calculated bus) by the measured current line so that the voltage at that bus can be calculated.

Step 3: Find the line that connected two calculated buses so that the current line can be calculated

Step 4: Calculate the current from/to the indirect bus using the Kirchhoff Current Law (KCL)

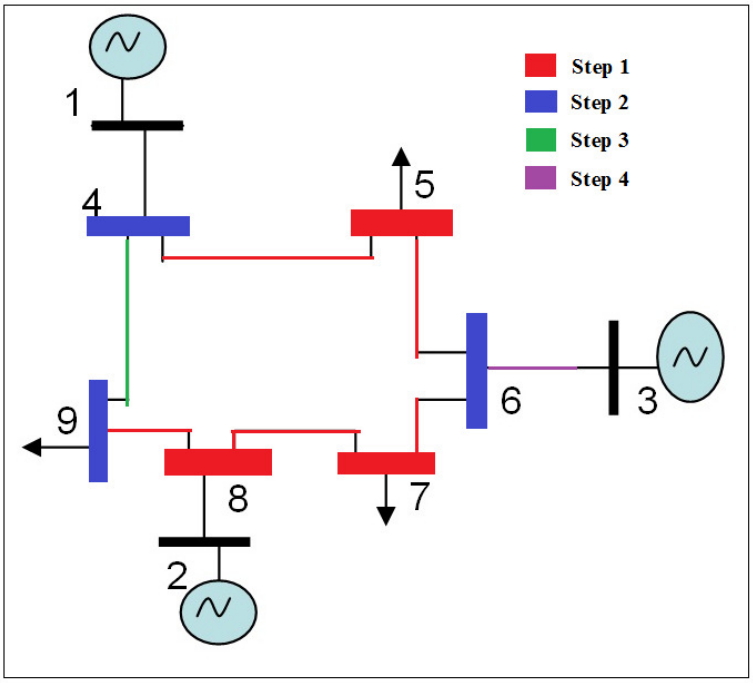

Figure 2.10 Basic Rule in Determining the PMU Number and Location

In determining the PMU number and location in the power system network there are some well-known methods. The Graph Theoretic Procedure, The Recursive Security N Method, The Generalized Integer Linear Programming, etc. are widely used method in determining the number and the location of PMU [14-16].

Some of the method can be easily derived by the Power System Analysis Toolbox (PSAT) such as the Graph Theoretic Procedure and the Recursive N Method. PSAT is the MATLAB Extension software built especially in Power System Analysis problem and solution.

2.2.2.1 Graph Theoretic Procedure

Graph theoretic procedure is based on the system topology. Sub graph is built using the following steps[16]:

Step 1 : Place a PMU at the bus with the highest number of incident lines in the unobservable region

Step 2 : Determine the region observed by the current PMU placement set

Step 3 : If the observed region does not cover the whole system go to step 2, otherwise stop.

Graph theoretic procedure takes the ability of the PMU to measure the entire incident currents. Algorithm of the Graph theoretic procedure can be shown in the Figure 2.11.

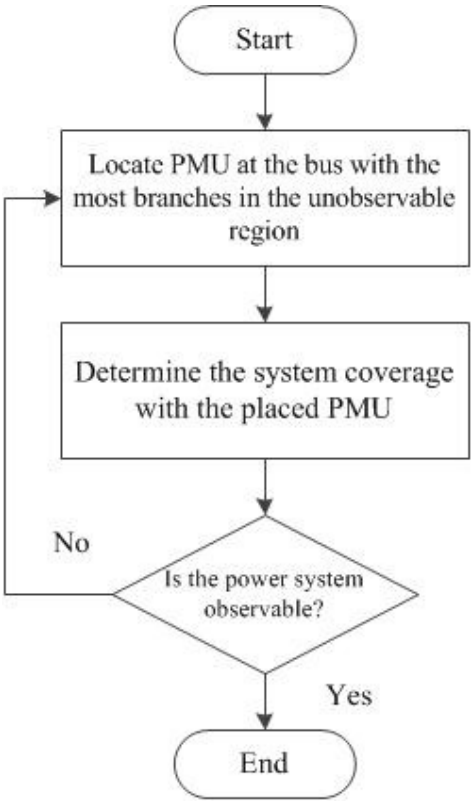

Figure 2.11 Flowchart of Graph Theoretic Procedure

2.2.2.2 Recursive N Method

Based on the PMU placement rule on the reference [16], the Recursive Security N Method has three main steps [14] as described below and also shown in Figure 2.12:

Step 1: Generation of minimum spanning trees

First step in building the minimum spanning tree can be obtained by put the PMU in certain bus and make the spanning tree. If in the network there are N buses so there are N step of putting the PMU in the first steps. After choosing the first PMU, the remaining PMU are recursively set in the nodes which are found both to be closer to the observability region and to provide the

higher number of observed buses. The process will be ended after the network is observable.

Step 2: Search another pattern of solution

The set obtained by the previous step can be re-designed using another pattern for further improvement elaboration. Applying this step means that each PMU of each set is replaced at the buses connected with the node where a PMU originally set. PMU located on busses connected to the grid by single lines are replaced on the neighboring buses since this operation provides more direct current measurements which can reduce the error variance.

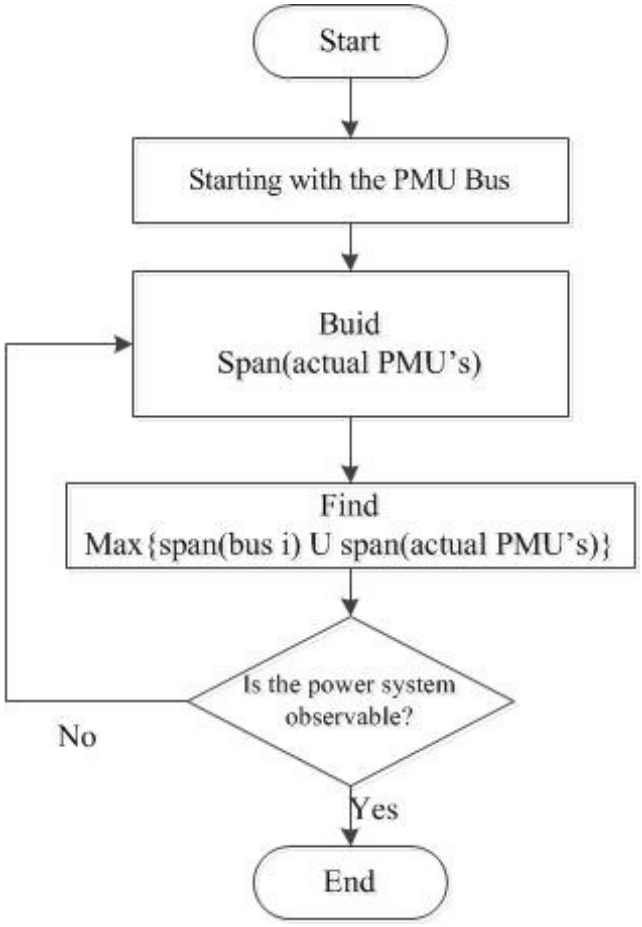

Figure 2.12 Flowchart of Recursive N Method

Step 3: Reducing PMU number in case of pure transit nodes

Considering the indirect bus, can reduce the PMU number in the network. The indirect bus means zero injection buses in the network.

2.2.2.3 Generalized Integer Linear Programming

Generalized Integer Linear Programming can determine the PMU location in the network by applying the computation in the power system network [17]. The objective function is to minimize the set of the PMU bus that define in x_k, subject to the objective function as described below.

$$\begin{aligned} &Min \sum_{k=1}^{N} x_k \\ &S.T.\ T\ X \geq b_{PMU} \end{aligned} \qquad (2.1)$$

With:

T = Network Incident Matrix Connecting the Bus

$\therefore t_{ij}$ is the element of T

$$\therefore t_{ij} = \begin{cases} 1, \text{ if } i = j \\ 1, \text{ if } i \text{ and } j \text{ are connected} \\ 0, \text{ the other} \end{cases}$$

X is the state variable representing power system buses

$$\therefore X = [x_1\ x_2 \ldots\ldots\ldots x_n]^T$$

$$\therefore x_i = \begin{cases} 0, \text{if no PMU installed in this bus} \\ 1, \text{if PMU installed in this bus} \end{cases}$$

b_{PMU} is the PMU placement variable

$$\therefore b_{PMU} = [1\ 1 \ldots\ldots 1]^T_{Nx1}$$

The matrix T is the incidence matrix connected buses in power system of the desired network. The T matrix shows the connection between buses in the power system. If the network has N bus the matrix T will have N x N element. The value of the matrix T is 0 or 1. Letters i and j is the bus indexes corresponding to the matrix T itself.

X is the vector that contain of N element that represent the bus number of the network. X is state variable and in this equation (2.1) x_i represent the bus number i. X will be obtained from the optimization computation. The value of X will tell which station in the network the PMU will be installed on. When the value of the element in the computation result is equal to 1, it means that One PMU is installed on that bus.

In the equation (2.1) in the right hand side there is vector b_{PMU} there. This vector contain of N element that represent the number of the bus. The value of this element is remained 1 for representing that all of the bus is on the observable state. The value of b_{PMU} can be seen as the reference value, to measure the solution satisfaction. The solution of the optimization is satisfied when the multiplication between T and the X is greater than the reference value.

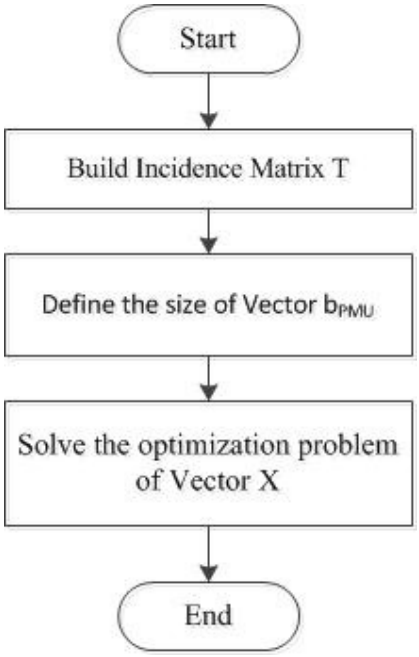

Figure 2.13 Flowchart of Generalized Integer Linear Programming

2.3 State Estimation

In power system, certain state variable can be computed using set of measurement data [18]. State estimation is needed because in the real case the state variable must be known as soon as possible while the measurement device at that point cannot provide the value on time. Another case is when it is not possible to install the measurement device in all of station of the state variable needed.

In this work, the state variable is the voltage magnitude and angle of each bus. This state variable can be estimated using set of measurement. The measurement can be vary and depend the formulation used to estimate the state variable. The measurement can be the voltage phasor, injected power, power flow or even current flow. There is a very well-known method called The Weighted Least Squared State Estimation Method that often used to estimate the bus voltage of the power system network. This method will be described below along with the Linear Formulation of State Estimation Method.

WLS state estimation method is widely used in power system problem because the system model information and measurement are part of the constraint of this method [18]. WLS state estimation method can solve the estimation function by minimizing the weighted error square. In practical, the WLS is solved by iteration using the Gauss Newton method or by linearization depend on the measurement function.

2.3.1 Iterative Weighted Least Squared State Estimation Method

In iterative WLS state estimation the set of measurement in given by the equation:

$$z = \begin{bmatrix} z_1 \\ z_2 \\ . \\ . \\ z_k \end{bmatrix} = \begin{bmatrix} h_1(x_1, x_2, \ldots, x_n) \\ h_2(x_1, x_2, \ldots, x_n) \\ . \\ . \\ h_k(x_1, x_2, \ldots, x_n) \end{bmatrix} + \begin{bmatrix} e_1 \\ e_2 \\ . \\ . \\ e_k \end{bmatrix} = h(x) + e \qquad (2.2)$$

Where:

z = measurement vector

$x^T = [x_1, x_2, \ldots, x_n]$ is system state vector

$e^T = [e_1, e_2, \ldots, e_k]$ is the vector measurement error

$h_i(x)$ = is the non-linear measurement i relating to the state vector x, $i \in k$

There is an assumption that the mean of the measurement error is r and the measurement error is independent. The $Cov(e)$ is equal to R ($R = \text{diag}(\sigma_1^2, \sigma_2^2, \ldots, \sigma_k^2)$). The standard deviation σ of each measurement is calculated to reflect the accuracy of the corresponding meter used.

The WLS estimator minimizes weighted error by solving the following objective function:

$$J(x) = \sum_{i=1}^{k} (z_i - h_i(x))^2 / R_{ii}$$
$$S.t. \quad J(x) = \left[z - h(x)\right]^T \left[R\right]^{-1} \left[z - h(x)\right] \qquad (2.3)$$

To get the minimum error, the partial derivative value of equation (2.3) has to be set equal to zero as following:

$$\frac{\partial J(x)}{\partial x} = -H^T \left[R\right]^{-1} \left[z - h(x)\right] = 0$$
$$H = \frac{\partial h(x)}{\partial x} \qquad (2.4)$$

The expanding Taylor series:

$$g(x) = g(x^k) + G(x^k)(x - x^k) + \ldots = 0$$

where (2.5)

$$G(x) = \frac{\partial g(x)}{\partial x} = -H^T(x)\left[R\right]^{-1} H(x) = 0$$

From the Taylor series from equation (2.5) and neglecting the higher order that term, the Gauss-Newton iterative method can be applied as following

$$x^{k+1} = x^k - \left[G(x^k)\right]^{-1} g(x) \qquad (2.6)$$

The tolerance is set to end the iteration and to yield the result. When the difference value of state variable x^{k+1} and x^k (Δx^{k+1}) is greater than the tolerance, the iteration can be stopped. And the value of Δx^{k+1} can be calculated as following:

$$\Delta x^{k+1} = \left[G(x^k)\right]^{-1} H^T(x^k) R^{-1} \left[z - h(x^k)\right]$$

Where (2.7)

$G(x^k)$ is gain matrix

The gain matrix is sparse, positive definite and symmetric, that warranty that the power system is fully observable.

The non-linear measurement function can be seen by set the non-linear variable of measurement vector. The example case is how to estimate all of the bus voltage in power system using injected real power (P), injected reactive power (Q), real power flow (P_{ij}), reactive power flow (Q_{ij}) and current flow (I_{ij}) as an input.

$$z^T = \left[\hat{P}_i \quad \hat{Q}_i \quad \hat{P}_{ij} \quad \hat{Q}_{ij} \quad \hat{I}_{ij}\right] \; i, j \in N$$
$$x^T = \left[\theta_2, \theta_3, \ldots, \theta_N \quad V_1, V_2, V_3, \ldots, V_N\right] \qquad (2.8)$$

N is all of the bus in the power system

The measurement function can be formulated from the state variable equation x. The measurement vector can be calculated by the equation below type of measurement from the known state variables is described below corresponding to the z order.

$$
\begin{aligned}
P_i &= V_i \sum_{j=1}^{N} V_j (G_{ij} \cos\theta_{ij} + B_{ij} \sin\theta_{ij}) \\
Q_i &= V_i \sum_{j=1}^{N} V_j (G_{ij} \sin\theta_{ij} + B_{ij} \cos\theta_{ij}) \\
P_{ij} &= V_i^2 (g_i + g_{ij}) - V_i V_j (g_{ij} \cos\theta_{ij} + b_{ij} \sin\theta_{ij}) \\
Q_{ij} &= -V_i^2 (b_i + b_{ij}) - V_i V_j (g_{ij} \sin\theta_{ij} - b_{ij} \cos\theta_{ij}) \\
I_{ij} &= \sqrt{(g_{ij}^2 + b_{ij}^2)(V_i^2 + V_j^2 - 2V_i V_j \cos\theta_{ij})}
\end{aligned}
\qquad (2.9)
$$

Where:

V_i, θ_i is the voltage magnitude and phase angle at bus i

$\theta_{ij} = \theta_i - \theta_j$

$G_{ij} + jB_{ij}$ is the ij^{th} element of complex bus admitance

$g_{ij} + jb_{ij}$ is the admittance of series branch connecting bus i - j

For this case, the matrix H can be solved using the following equation:

$$
\frac{\partial h(x)}{\partial x} = H(x) = \begin{bmatrix}
\frac{\partial P_{inj}}{\partial \theta} & \frac{\partial P_{inj}}{\partial V} \\
\frac{\partial P_{flow}}{\partial \theta} & \frac{\partial P_{flow}}{\partial V} \\
\frac{\partial Q_{inj}}{\partial \theta} & \frac{\partial Q_{inj}}{\partial V} \\
\frac{\partial Q_{flow}}{\partial \theta} & \frac{\partial Q_{flow}}{\partial V} \\
0 & \frac{\partial V_{mag}}{\partial V}
\end{bmatrix} \qquad (2.10)
$$

The solution for the state variable vector can be obtained by the equation (2.5) to the equation (2.7).

2.3.2 Linear Formulation of State Estimation

Linear Formulation of State Estimation method is development method of WLS state estimation. In this method the measurement function is linear equation so that there is no iteration in the solution process. As described in the previous subchapter, Phasor Measurement Unit (PMU) has the sampling rate less than 100 ms so that the recorded data from PMU is needed to process in the fast mode. Because of that reason, the computation time for WAMS need to be faster. Using non-iterative state

estimation, the time consumption for state estimation part is faster than using iterative state estimation.

Using idea of the WLS state estimation, voltage and current data PMU can be used to estimate the state variable consisted of voltage magnitude and voltage angle [19]. If the data are consisted of voltage and current the state estimation can be formulated as a linear problem.

In this method, the function is modeled as the linear function as shown following[20].

$$\hat{z} = H\hat{x} + \hat{e}$$
$$\hat{e} = \hat{z} - H\hat{x} \qquad (2.11)$$

In this case the data measurement and the state variable can be expressed in rectangular form. The voltage measurement ($V_i = |V_i|\angle\theta$) can be expressed in the form of ($V_i = E_i + jF_i$) and current measurement can be expressed as ($I_i = C_i + jD_i$). The measurement vector z and the state variable x can be expressed as following. Letter i and j represent the bus number of the network.

$$\hat{z} = \left[[E_k]^T \quad [C_{ki}]^T \quad [F_k]^T \quad [D_{ki}]^T \right]^T$$
$$\hat{x} = \left[[E_k]^T \quad [E_j]^T \quad [F_k]^T \quad [F_j]^T \right]^T \qquad (2.12)$$

Where

E_k is Real part of PMU Bus Voltage, $k \in$ PMU Bus

F_k is Imaginary part of PMU Bus Voltage

C_{ki} is Real part of Line Current from PMU bus, $k \in$ PMU Bus,

$i \in$ Immediately Adjacent PMU Bus

D_{ki} is Imaginary part of Line Current from PMU bus

E_j is Real part of non-PMU Bus Voltage, $j \in$ PMU Bus

F_j is Imaginary part of non-PMU Bus Voltage

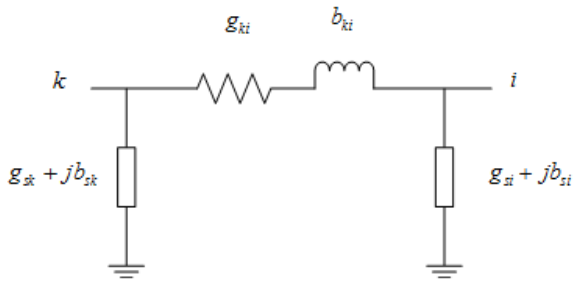

Figure 2.14 Transmission-line Model

Where

$g_{ki} + jb_{ki}$ is the series admittance of transmission line

$g_{si} + jb_{si}$ is the shunt admittance of transmission line

Based on the Figure 2.14 the equation of the line current flow can be expressed as linear function. Where y_{ki} is series admittance of the network with $y_{ki} = g_{ki} + jb_{\mathrm{ki}}$ and y_{si} is the shunt admittance of the network with $y_{si} = g_{si} + jb_{si}$. The measurement function of the current line can be computed as following:

$$C_{ki} + jD_{ki} = \left[\left(g_{ki} + jb_{ki}\right) + \left(g_{si} + jb_{si}\right)\right]\left(E_k + jF_k\right) - \left(g_{ki} + jb_{ki}\right)\left(E_j + jF_j\right) \quad (2.13)$$

The Measurement Jacobian Matrix H for Linear Formulation of state estimation is determined as the following.

$$H = \begin{bmatrix}
\frac{\partial E_{k_1}}{\partial E_{k_1}} & \cdots & \frac{\partial E_{k_1}}{\partial E_{k_m}} & \frac{\partial E_{k_1}}{\partial E_{j_1}} & \cdots & \frac{\partial E_{k_1}}{\partial E_{j_n}} & \frac{\partial E_{k_1}}{\partial F_{k_1}} & \cdots & \frac{\partial E_{k_1}}{\partial F_{k_m}} & \frac{\partial E_{k_1}}{\partial F_{j_1}} & \cdots & \frac{\partial E_{k_1}}{\partial F_{j_n}} \\
\vdots & \ddots & \vdots & \vdots & \ddots & \vdots & \vdots & \ddots & \vdots & \vdots & \ddots & \vdots \\
\frac{\partial E_{k_m}}{\partial E_{k_1}} & \cdots & \frac{\partial E_{k_m}}{\partial E_{k_m}} & \frac{\partial E_{k_m}}{\partial E_{j_1}} & \cdots & \frac{\partial E_{k_m}}{\partial E_{j_n}} & \frac{\partial E_{k_m}}{\partial F_{k_1}} & \cdots & \frac{\partial E_{k_m}}{\partial F_{k_m}} & \frac{\partial E_{k_m}}{\partial F_{j_1}} & \cdots & \frac{\partial E_{k_m}}{\partial F_{j_n}} \\
\frac{\partial C_{k_1 i}}{\partial E_{k_1}} & \cdots & \frac{\partial C_{k_1 i}}{\partial E_{k_m}} & \frac{\partial C_{k_1 i}}{\partial E_{j_1}} & \cdots & \frac{\partial C_{k_1 i}}{\partial E_{j_n}} & \frac{\partial C_{k_1 i}}{\partial F_{k_1}} & \cdots & \frac{\partial C_{k_1 i}}{\partial F_{k_m}} & \frac{\partial C_{k_1 i}}{\partial F_{j_1}} & \cdots & \frac{\partial C_{k_1 i}}{\partial F_{j_n}} \\
\vdots & \ddots & \vdots & \vdots & \ddots & \vdots & \vdots & \ddots & \vdots & \vdots & \ddots & \vdots \\
\frac{\partial C_{k_m i}}{\partial E_{k_1}} & \cdots & \frac{\partial C_{k_m i}}{\partial E_{k_m}} & \frac{\partial C_{k_m i}}{\partial E_{j_1}} & \cdots & \frac{\partial C_{k_m i}}{\partial E_{j_n}} & \frac{\partial C_{k_m i}}{\partial F_{k_1}} & \cdots & \frac{\partial C_{k_m i}}{\partial F_{k_m}} & \frac{\partial C_{k_m i}}{\partial F_{j_1}} & \cdots & \frac{\partial C_{k_m i}}{\partial F_{j_n}} \\
\frac{\partial F_{k_1}}{\partial E_{k_1}} & \cdots & \frac{\partial F_{k_1}}{\partial E_{k_m}} & \frac{\partial F_{k_1}}{\partial E_{j_1}} & \cdots & \frac{\partial F_{k_1}}{\partial E_{j_n}} & \frac{\partial F_{k_1}}{\partial F_{k_1}} & \cdots & \frac{\partial F_{k_1}}{\partial F_{k_m}} & \frac{\partial F_{k_1}}{\partial F_{j_1}} & \cdots & \frac{\partial F_{k_1}}{\partial F_{j_n}} \\
\vdots & \ddots & \vdots & \vdots & \ddots & \vdots & \vdots & \ddots & \vdots & \vdots & \ddots & \vdots \\
\frac{\partial F_{k_m}}{\partial E_{k_1}} & \cdots & \frac{\partial F_{k_m}}{\partial E_{k_m}} & \frac{\partial F_{k_m}}{\partial E_{j_1}} & \cdots & \frac{\partial F_{k_m}}{\partial E_{j_n}} & \frac{\partial F_{k_m}}{\partial F_{k_1}} & \cdots & \frac{\partial F_{k_m}}{\partial F_{k_m}} & \frac{\partial F_{k_m}}{\partial F_{j_1}} & \cdots & \frac{\partial F_{k_m}}{\partial F_{j_n}} \\
\frac{\partial D_{k_1 i}}{\partial E_{k_1}} & \cdots & \frac{\partial D_{k_1 i}}{\partial E_{k_m}} & \frac{\partial D_{k_1 i}}{\partial E_{j_1}} & \cdots & \frac{\partial D_{k_m i}}{\partial E_{j_1}} & \frac{\partial D_{k_1 i}}{\partial F_{k_1}} & \cdots & \frac{\partial D_{k_1 i}}{\partial F_{k_m}} & \frac{\partial D_{k_1 i}}{\partial F_{j_1}} & \cdots & \frac{\partial D_{k_m i}}{\partial F_{j_1}} \\
\vdots & \ddots & \vdots & \vdots & \ddots & \vdots & \vdots & \ddots & \vdots & \vdots & \ddots & \vdots \\
\frac{\partial D_{k_m i}}{\partial E_{k_1}} & \cdots & \frac{\partial D_{k_m i}}{\partial E_{k_m}} & \frac{\partial D_{k_m i}}{\partial E_{j_1}} & \cdots & \frac{\partial D_{k_m i}}{\partial E_{j_n}} & \frac{\partial D_{k_m i}}{\partial F_{k_1}} & \cdots & \frac{\partial D_{k_m i}}{\partial F_{k_m}} & \frac{\partial D_{k_m i}}{\partial F_{j_1}} & \cdots & \frac{\partial D_{k_m i}}{\partial F_{j_n}}
\end{bmatrix} \quad (2.14)$$

Where

$j = [j_1, j_2, \ldots, j_n]$

$i = [i_1, i_2, \ldots, i_p]$

With index i is the PMU bus index and j is non-PMU bus index. The value of each component can be calculated using the following equation.

$$\frac{\partial E_{k_x}}{\partial E_{k_y}} = \begin{cases} 1, x = y \\ 0, x \neq y \end{cases}; \quad \frac{\partial E_{k_x}}{\partial E_{j_y}} = 0; \quad \frac{\partial E_{k_x}}{\partial F_{k_y}} = 0; \quad \frac{\partial E_{k_x}}{\partial F_{j_y}} = 0$$

$$\frac{\partial C_{ij}}{\partial E_i} = g_{ij} + g_{si}; \quad \frac{\partial C_{ij}}{\partial E_j} = -g_{ij}; \quad \frac{\partial C_{ij}}{\partial F_i} = -b_{ij} + -b_{si}; \quad \frac{\partial C_{ij}}{\partial F_j} = b_{ij}$$

$$\frac{\partial F_i}{\partial E_i} = 0; \quad \frac{\partial F_i}{\partial E_j} = 0; \quad \frac{\partial F_i}{\partial F_i} = 1; \quad \frac{\partial F_i}{\partial F_j} = 0$$

$$\frac{\partial D_{ij}}{\partial E_i} = b_{ij} + b_{si}; \quad \frac{\partial D_{ij}}{\partial E_j} = -b_{ij}; \quad \frac{\partial D_{ij}}{\partial F_i} = g_{ij} + g_{si}; \quad \frac{\partial D_{ij}}{\partial F_j} = -g_{ij}$$

The estimated value of $V_i = E_i + jF_i$ can be obtained by solving the weighted error square as described below:

$$\begin{aligned} &J(x) = \left(\hat{z} - H\hat{x}\right)^T R^{-1} \left(\hat{z} - H\hat{x}\right) \\ &S.t.\ \hat{z} = H\hat{x} + \hat{e} \\ &J(x) = \hat{z}^T R^{-1} \hat{z} - \hat{x}^T H^T R^{-1} \hat{z} - \hat{z}^T R^{-1} H\hat{x} + \hat{x}^T H^T R^{-1} H\hat{x} \end{aligned} \tag{2.15}$$

To minimize the objective function of *J(x)*, the compute the partial derivative of J(x) and set the value equal to zero

$$\frac{\partial J(x)}{\partial x} = -2\hat{z}^T R^{-1} H + 2\hat{x}^T H^T R^{-1} H = 0 \tag{2.16}$$

Then, find the estimated value of the state variable by solving the equation (2.16)

$$\hat{x} = (H^T R^{-1} H)^{-1} H^T R^{-1} \hat{z} \tag{2.17}$$

The computation is very simple and fast and does not have iteration. *R* is formulated from the variance of each measurement function, which the value of variance, represent the accuracy against the measurement error. *R* is the sparse matrix with the value of the diagonal value is the variance of each measurement.

$$R = \begin{bmatrix} \sigma_1^2 & 0 & \cdots & 0 \\ 0 & \sigma_2^2 & \cdots & 0 \\ \vdots & \ddots & \ddots & \vdots \\ 0 & 0 & \cdots & \sigma_n^2 \end{bmatrix}$$

with σ_n^2 is error measurement number n

CHAPTER III
VOLTAGE STABILITY

Voltage stability is part of power system stability so that the definition and classification of power system stability must be defined previously. Power system stability is defined as characteristic for a power system to remain in a state of equilibrium at normal operating conditions and to restore an acceptable state of equilibrium after a disturbance [21].

The power system stability consists of rotor angle stability, voltage stability and frequency stability. Voltage stability will be significantly described in this work. Reference [22] defines the voltage stability as the ability of a power system to maintain the steady state acceptable voltages at all buses in the system at normal operating conditions and after being subjected to a disturbance

Power system stability is classified as rotor angle stability, voltage stability and frequency stability. Classification of power system stability is divided into two criteria that are time scale and driving force criteria.

Table 3.1 Classification of Power Systems Stability

<table>
<tr><td>Time scale</td><td colspan="2">Generator – driven</td><td colspan="2">Load – driven</td></tr>
<tr><td rowspan="2">Short-term</td><td colspan="2">Rotor angle stability</td><td colspan="2" rowspan="2">Short-term voltage stability</td></tr>
<tr><td>Small-signal</td><td>transient</td></tr>
<tr><td rowspan="2">Long-term</td><td colspan="2" rowspan="2">Frequency stability</td><td colspan="2">Long-term voltage stability</td></tr>
<tr><td>Small disturbance</td><td>Large disturbance</td></tr>
</table>

3.1 Definition

The voltage stable power system is the power system is the power system that the voltages are close to the voltages at normal operating condition after the disturbance happened. Unstable condition will happen in power system when the voltages uncontrollably decrease because of the outage of equipment (generator, line, transformer and bus bar), increment of load, etc. Voltage instability stems from the attempt of load dynamics to restore power consumption beyond the capability of the combined transmission and generation system [21].

The voltage stability of a power system is greatly dependent upon the amount, location and type of reactive power sources available. If the reactive power support is

far away, insufficient in size, or too dependent on shunt capacitors, a relatively normal contingency (such as a line outage or a sudden increase in load) can trigger a large system voltage drop [1]. The effect if the voltage instability can affect the entire of the power system.

Voltage collapse might be happened due to the voltage instability. A voltage collapse is defined as being the process by which voltage instability leads to a very low voltage profile in a significant part of the system. A voltage collapse may occur rapidly or more slowly, depending on the system dynamics. It may be caused by a variety of single or multiple contingencies. These may be the sudden removal of generation or a transmission element (a transformer or a transmission-line), an increase of load without an adequate increase of reactive power, or the slow clearing of a system fault. Voltage collapse is more likely when transmission-lines are heavily loaded [1].

3.2 Analysis of Power System Voltage Stability

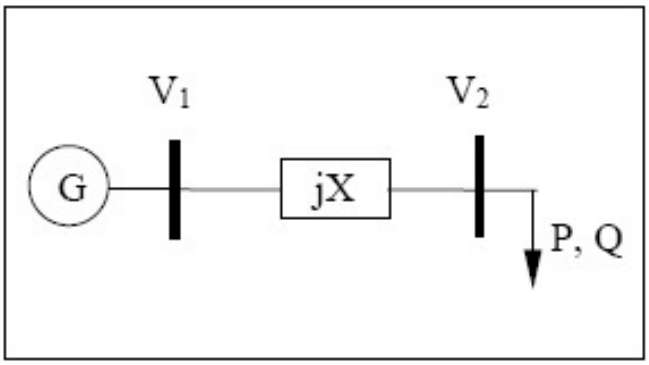

Figure 3.1 Two bus test system [22]

Voltage stability charactheristic can be described by the Figure 3.1 below. In this figure there is a simplified two-bus test system. Generator produces active power, which is transferred through a transmission-line to the load. The reactive power capability of generator is infinite so that the generator terminal voltage V_1 is constant. The transmission-line is shown by the reactance (jX). The load is constant power load including active and reactive Q parts.

The observation bus is bus 2, V_2 in bus 2 is calculated with the different value of load. The value of the V_2 can be calculated by equation below.

$$V_2 = \sqrt{\frac{(V_1 - 2QX) \pm \sqrt{V_1^4 - 4QXV_1^2 - 4P^2X^2}}{2}} \qquad (3.1)$$

The solution of (3.1) is often presented as PV-curve (Figure 3.2). The PV-curve presents the voltage of the load bus as a function of load or sum of loads. The solution is stated that it has low current-high voltage and high current-low voltage. The shape of the P-V curve is strongly depended on the load, each value of the power factor gives different characteristic of the P-V curve.

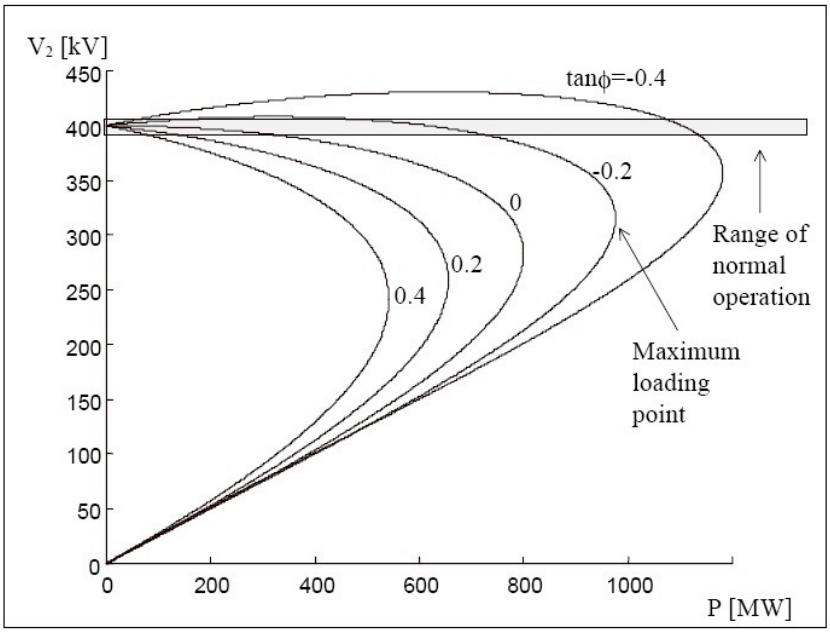

Figure 3.2 P-V Curve Generated by Different Operating Condition [22]

Secure operating condition in power system network is upper the nose of P-V curve that is maintain the bus voltage above the limit. This part of PV-curve is statically and dynamically stable. The nose of the curve is called the maximum loading point. Maximum loading point is the critical point where the solutions unite is the voltage collapse point [21]

The maximum loading point is the voltage collapse point when constant power loads are considered. The power systems become voltage unstable at the voltage collapse point. The lower part of the PV-curve (left from the voltage collapse point) is statically stable, but dynamically unstable [22]. Five PV-curves are described in Figure 3.2 for the test system. The test system variables are V_1 = 400 kV and the X = 100Ω. The P-V curves represent different load compensation cases (tanϕ=Q/P). The decrement value of tanϕ is beneficial for the power system because the more power can be operated. The load compensation increases the loading of the power systems according to voltage stability.

3.3 Voltage Stability Index

3.3.1 Synchrophasor-Based Real-Time Voltage Stability Index

Voltage Stability Index (VSI) can give the assessment of the power system security pertinent to the voltage stability. In WAMS, dynamic computation of VSI is needed to give the accurate value of the voltage stability condition in order to make the preventive action in the power system.

Synchrophasor-Based Real-Time Voltage Stability Index (SBRT VSI) is one of the VSI that can compute the accurate real time voltage stability indexes[23]. SBRT VSI can compute the on-line VSI accurately. Moreover SBRT VSI can compute the power system voltage stability margin so that the voltage collapse can be prevented.

The first step to do the SBRT VSI calculation is to compute the power (active and reactive power) in each load bus of the power system. In SBRT-VSI calculation the index is computed based on bus location. VSI is computed locally in the load bus. To derive the calculation of SBRT VSI, the simplified model of power system is shown in Figure 3.3 below

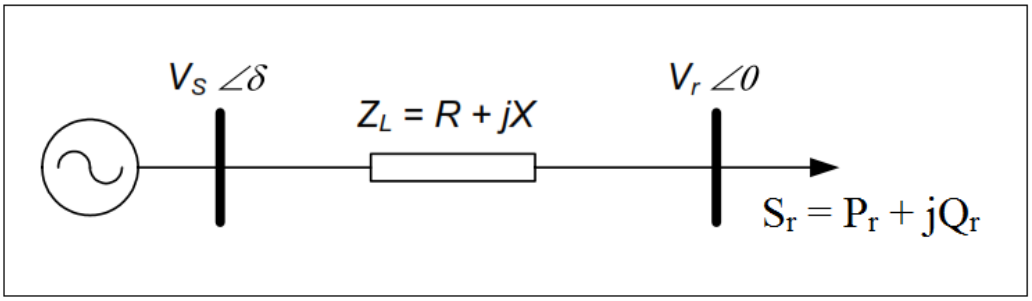

Figure 3.3 Simplified Power System Model [23]

Where

Vs isVoltage at generator terminal

Vr isVoltage at load bus terminal

δ is Voltage angle difference of generator terminal and load bus terminal

$Z_L$is Line Impedance

S is Apparent Power of Load bus

From the Figure 3.3, the VSI of the load bus *r* is computed by firstly compute the active (*P*) and reactive (*Q*) power of the load bus *r*. The active and reactive power of load bus *r* can be calculated by the equation (3.2) and 3.3).

$$P_r = V_r \left[(V_s \cos\delta - V_r) \frac{R}{R^2 + X^2} + V_s \sin\delta \frac{X}{R^2 + X^2} \right] \tag{3.2}$$

$$Q_r = V_r \left[(V_s \cos\delta - V_r) \frac{X}{R^2 + X^2} + V_s \sin\delta \frac{R}{R^2 + X^2} \right] \quad (3.3)$$

From those two equations, the Load Bus Voltage V_r equation should be computed. Based on the voltage value we can obtain limit voltage prediction based on the actual condition. The limit voltage V_r leads the computation to find the maximum active power of P_r. The equation (3.4) shows the value of the computed Voltage at load bus R.

$$V_r = \sqrt{\frac{V_s^2}{2} - (Q_r X + P_r R) \pm \sqrt{\frac{V_s^4}{4} - (Q_r X + P_r R) V_s^2 - (P_r X - Q_r R)^2}} \quad (3.4)$$

From the (3.4), there are two value of computed V_r. The biggest is called V_{r1} and the others is V_{r2}. Whenever the power system operate at the secure condition the actual value of the Voltage is close to the V_{r1}.

$$\begin{aligned} A &= \frac{V_s^4}{4} - (Q_r X + P_r R) V_s^2 - (P_r X - Q_r R)^2 \\ A &= (X - R\tan\theta)^2 P^2 + V_s^2 (X\tan\theta + R) P - \frac{V_s^4}{4} \end{aligned} \quad (3.5)$$

Let's recall the determinant value of equation (3.4) with the symbol A. This equation is a quadratic equation with the V_s^2 as the variable. This equation can be rearranged as another quadratic function with P as the variable.

The power system is in the stable condition when the value of A is greater than zero. When the value of A is equal to zero, there is only one value of V_r that represent the collapse point of the nose curve.

By solving the quadratic equation A equal to zero the maximum value of P can be computed. Inserting the power system parameter of R, X and Z_L and assuming that the power system has the constant value of the power factor at the load bus, the P_{max} value can be define as follow:

$$\begin{aligned} P_{\max} &= \frac{Q_r R}{X} - \frac{V_s^2 R}{2X^2} + \frac{|Z_L| V_s \sqrt{V_s^2 - 4Q_r X}}{2X^2} \\ &\text{where} \\ Z_L &= \sqrt{R^2 + X^2} \end{aligned} \quad (3.6)$$

From the equation (3.6) the power margin and the SBRT VSI at bus R can be computed as follow

$$P_{\text{margin}} = P_{\max} - P_r$$

$$SBRT\ VSI = \frac{P_{\text{margin}}}{P_{\max}} \tag{3.7}$$

$$SBRT\ VSI > 0$$

Where

$P_{\max}$ is computed maximum active power (MW) at load bus

P_r is actual active power of the load bus r

The operating point of the power system is when the SBRT VSI greater than 0. When the value of SBRT VSI equal to 0, the power system is in collapse condition.

For the larger power system, the computation of SBRT VSI require network simplification. The first thing to do is to make the simplification of the power system network become simplified model. Figure 3.4 shows how the power system network can be simplified into load bus and equivalent source bus.

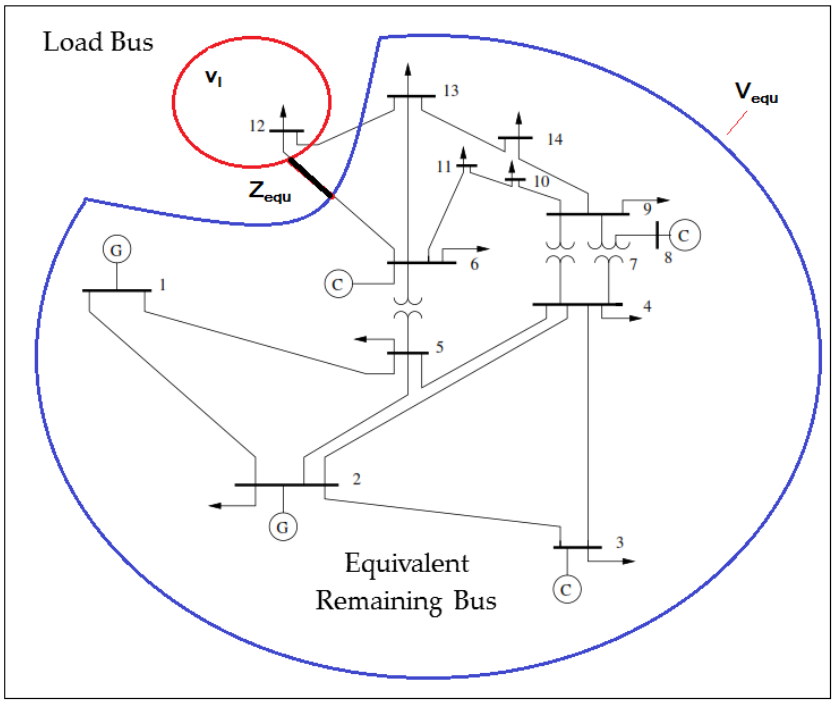

Figure 3.4 Network Simplification of Power System

SBRT-VSI is computed in every load bus in the power system network. In Figure 3.4 there is an IEEE 14 buses test system, that represent bus number 12 to be a load bus with voltage bus v_l propertiy. On the other hand, the other remaining busses are formulated to be equivalent bus with voltage v_{equ}. The line connecting the equivalent circuit is named by Z_{equ}. There are three properties that have to be considered for

make the network simplification there are v_l , v_{equ} and Z_{equ}. The Thevenin model is used to simplify the network.

In complex power system that has more than one load bus generator bus, simplification properties of v_l , v_{equ} and Z_{equ} for each load bus. Network simplification can be done by firstly rearranging the Y_{bus} equation into group of load bus and generator bus as seen in the equation (3.8). The Y_{bus} then rearrange using simple gauss elimination method.

$$\begin{bmatrix} I_L \\ I_G \end{bmatrix} = \begin{bmatrix} Y_{LL} & Y_{LG} \\ Y_{GL} & Y_{GG} \end{bmatrix} \begin{bmatrix} V_L \\ V_G \end{bmatrix}$$
$$\begin{bmatrix} V_L \\ I_G \end{bmatrix} = \begin{bmatrix} Z_{LL} & H_{LG} \\ F_{GL} & Y_{GG} \end{bmatrix} \begin{bmatrix} I_L \\ V_G \end{bmatrix} \tag{3.8}$$

Where

I_L is Load Bus Injected Current, $L \in$ Load Bus

I_G is Gen Bus Injected Current , $G \in$ Gen Bus

V_L is Load Bus Voltage

V_G is Load Gen Voltage

Y *i*s Y_{Bus}, $Y_{LL,}Y_{LG,}Y_{GL},Y_{GG} \in Y_{Bus}$

With the element of Z_{LL} and H_{LG} the equation above can be derive into the equation below

$$Z_{LL} = Y_{LL}^{-1}$$
$$H_{LG} = -Z_{LL}Y_{LG} \tag{3.9}$$

From the equation (2.25) and (2.26) the values of of v_{Lj} , v_{equ} and Z_{equ} can be calculated

$$v_{Lj} = Z_{LLjj}\left(\frac{-S_{Lj}}{V_{Lj}}\right)^* + \sum_{i=l,i\neq j}^{N} Z_{LLji}\left(\frac{-S_{Li}}{V_{Li}}\right)^* + \sum_{k=1}^{M} H_{LGjk}V_{Gk}$$
$$\sum_{i=l,i\neq j}^{N} Z_{LLji}\left(\frac{-S_{Li}}{V_{Li}}\right)^* + \sum_{k=1}^{M} H_{LGjk}V_{Gk} = Z_{LLjj}\left(\frac{S_{Lj}}{V_{Lj}}\right)^* + v_{Lj} \tag{3.10}$$

$$\left(\frac{v_{equj}-v_{Lj}}{Z_{equj}}\right)^{*} v_{Lj} = S_{Lj}$$

$$v_{equj} = Z_{equj}\left(\frac{S_{Lj}}{v_{Lj}}\right)^{*} + v_{Lj} \tag{3.11}$$

$$v_{equj} = \sum_{i=l,i\neq j}^{N} Z_{LLji}\left(\frac{-S_{Li}}{V_{Li}}\right)^{*} + \sum_{k=1}^{M} H_{LGjk}V_{Gk}$$

$$Z_{\text{equj}} = Z_{\text{LL}_{\text{jj}}} \tag{3.12}$$

Where

v_{lj} is voltage of load bus in network simplification

v_{equj} is voltage of equivalent network of load bus j

Z_{equj} is line connecting the load bus j and the equivalent network

V_{Lj} is load bus voltage $\forall\ i, j \in$ load bus

$S_{Lj}$is bus apparent power $\in Y_{Bus}$

With the assumption of constant v_{equ} and power factor in the load bus L_j. The maximum active power of the load bus can be calculated as following

$$P_{Lj\max} = \frac{-v_{equj}^2(X_{equj}\tan\theta_j + R_{equj})\left|Z_{equj}\right|v_{equj}^2\sqrt{\tan^2\theta_j - 1}}{2(X_{equj} - R_{equj}\tan\theta)^2} \tag{3.13}$$

Where

P_{Lj} is Maximum Active Power of load bus j

R_{equj} is equivalent line resistance of load bus j network simplification

X_{equj} is equivalent line reactance of load bus j network simplification

θ_j is power bus j angle

The power margin and the SBRT VSI for each load bus can be calculated using the following equation. The power margin is the power difference between the actual condition value and calculated maximum active power of each load bus. The power system is in the stable operating condition when the value of SBRT VSI for each load bus is greater than zero.

$$P_{Lj\text{margin}} = P_{Lj\max} - P_{Lj} \quad (3.14)$$

$$SBRT\ VSI_{Lj} = \frac{P_{Lj\text{margin}}}{P_{Lj\max}} \quad (3.15)$$

$$0 < \text{SBRT VSI}_{Lj} \leq 1 \quad (3.16)$$

Where

P_{Lj} is Actual power of Load Bus j

$P_{Lj\text{margin}}$ is Actual Power Margin Load bus j

VSI_{Lj} is voltage stability index of load bus j

The local value of SBRT VSI can be formulated to be a global index of VSI by taking the minimum value of VSI in load bus j:

$$\text{Global SBRT VSI} = \min(\text{SBRT } VSI_{Lj}) \quad (3.17)$$

3.3.2 PQ Voltage Stability Index

PQ Voltage Stability Index (PQVSI) is one of the voltage stability indexes (VSI) that can measure the voltage stability performance based on the line performance. PQVSI measure the distance between the actual condition and the collapse point for negative power flow in each line[24]. The detail process for computing the PQVSI can be started using the Figure 3.5 that represents the sending and receiving end of transmission-line.

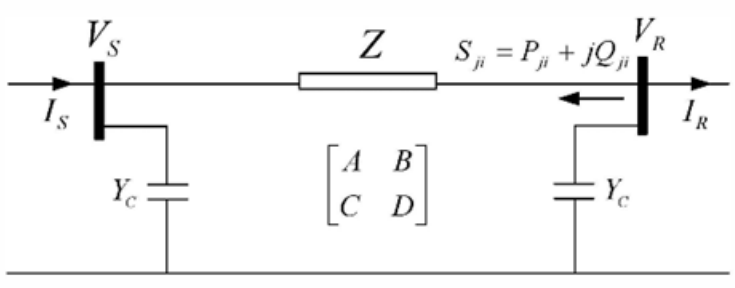

Figure 3.5 π Transmission-line Model [24]

V_S, V_R : the phasor bus voltage from bus and to bus

S_{ji} : the negative load flow to bus – from bus.

$$V_S = AV_R + BI_R \qquad \text{and} \qquad I_R = \left(\frac{-S_{ji}}{V_R}\right)^* \tag{3.18}$$

The transmission-line parameter of A, B, C and D are defined as below

$$A = 1 + ZY_c$$
$$B = Z$$
$$C = 2Y_c\left(1 + \frac{ZY_c}{2}\right)$$
$$D = A$$

From those two equations in equation (3.18) the following equation can be derived. The derivation is based on the equation of the negative power flow in the transmission-line.

$$V_S V_R^* - A\left|V_R\right|^2 = -B\left(P_{ji} - jQ_{ji}\right)$$
$$B^* V_S V_R = AB^*\left|V_R\right|^2 - \left|B\right|^2\left(P_{ji} - jQ_{ji}\right)$$
$$B^* V_S V_R = \left(\left|V_R\right|^2 \mathrm{Re}\left\{AB^*\right\} - \left|B\right|^2 P_{ji}\right) + j\left(\left|V_R\right|^2 \mathrm{Im}\left\{AB^*\right\} + \left|B\right|^2 Q_{ji}\right)$$
$$\left|B\right|^2\left|V_S\right|^2\left|V_R\right|^2 = \left(\left|V_R\right|^2 \mathrm{Re}\left\{AB^*\right\} - \left|B\right|^2 P_{ji}\right)^2 + \left(\left|V_R\right|^2 \mathrm{Im}\left\{AB^*\right\} + \left|B\right|^2 Q_{ji}\right)^2$$

The equation above can be transform into the quadratic equation with variable $|V_R|^2$ and the coefficient a, b, c can be formulated so that the value of each voltage can be calculated:

$$\left|V_R\right|^2 = \frac{-b \pm \sqrt{b^2 - 4ac}}{2a}$$
$$a = \mathrm{Re}\left\{AB^*\right\} + \mathrm{Im}\left\{AB^*\right\}$$
$$b = 2\,\mathrm{Im}\left\{AB^*\right\}\left|B\right|^2 Q_{ji} - \mathrm{Re}\left\{AB^*\right\}\left|B\right|^2 P_{ji} - \left|B\right|^2\left|V_S\right|^2$$
$$c = \left|B\right|^4 P_{ji}^4 + \left|B\right|^4 Q_{ji}^4$$

Based on the quadratic equation, there is two kind of value of $|V_R|^2$. The maximum negative power flow is reached when the determinant value of coefficient a, b and c is equal to zero (b^2-4ac=0). The equation of b^2 = 4ac is shown as the following.

$$\left(2\,\mathrm{Im}\left\{AB^{*}\right\}Q_{ji}^{NP^2}-2\,\mathrm{Re}\left\{AB^{*}\right\}P_{ji}^{NP^2}-\left|V_S\right|^2\right)^2=4\left|A\right|^2\left|B\right|^2\left(P_{ji}^{NP^2}+Q_{ji}^{NP^2}\right) \qquad (3.19)$$

P_{ji}^{NP} = active load at the collapse point

Q_{ji}^{NP} = reactive load at the collapse point

From the equation (3.19), the variable of V_s and the transmission-line network parameter A and B is known so that the equation to find the maximum negative power flow can be derived.

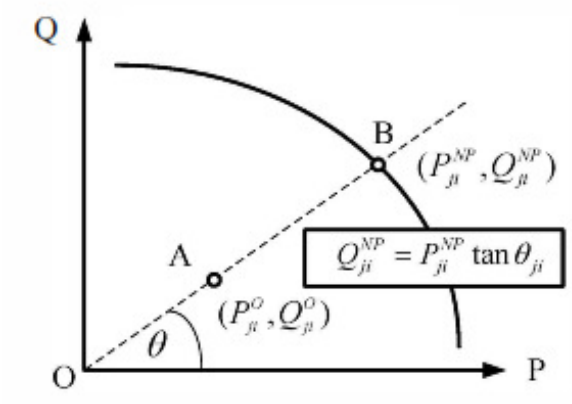

Figure 3.6 Predicted Maximum Power Flow in PQVSI [24]

To predict the maximum power the assumption of the power plow angle is constant is used as shown in the Figure 3.6 so that the reactive power flow can be represented as active power flow equation.

Rearranging the equation (3.19), the value of maximum negative active power flow can be derived by the equation (3.20) below.

$$P_{ji}^{NP}=\frac{\left|V_S\right|^2}{2\left[\,\mathrm{Im}\left\{AB^{*}\right\}\tan\theta_{ji}-\mathrm{Re}\left\{AB^{*}\right\}+\left|A\right|\left|B\right|\sec\theta_{ji}\right]} \qquad (3.20)$$

The PQVSI index for each line in the power system can be obtained by the equation:

$$PQVSI_{ji} = \frac{P_{ji}^{0}}{P_{ji}^{NP}}$$

where (3.21)

$\forall i, j \in$ bus number

The system is operated in the stable operating condition when the value of PQVSI index for all of the line is less than 1 ($0 \le PQVSI_{ji} < 1$). PQVSI can be treated as the global index for the power system by the equation (3.22) below.

$$Global\ PQVSI = \max(PQVSI_{ji}) \tag{3.22}$$

CHAPTER IV
PROBLEM FORMULATION AND METHODOLOGY

In chapter IV the problem formulation and methodology of conducting the research of **Application of Wide Area Monitoring System for Securing Voltage Stability** are elaborated into three sections that are problem formulation, solution method and simulated power system**.**

The problem formulation tells and elaborates further about the specific objective that has been described in the chapter one. Problem formulation identifies the detail in the input stage, process stage and output stage. The solution method part tells about the method and some assumptions used in this work. The method used in this worked has already been described in chapter II. The simulated power system describes the detail about the test system used and the machine model for real time simulation.

4.1 Problem Formulation

In completing this work, the specific objective must be elaborated to be the sequence process consisted of input, algorithm and output. Input, algorithm and output are described into several items so that what needed to do is seen obviously. Mapping of the input, process and the output is described the problem formulation as shown in Figure 4.1.

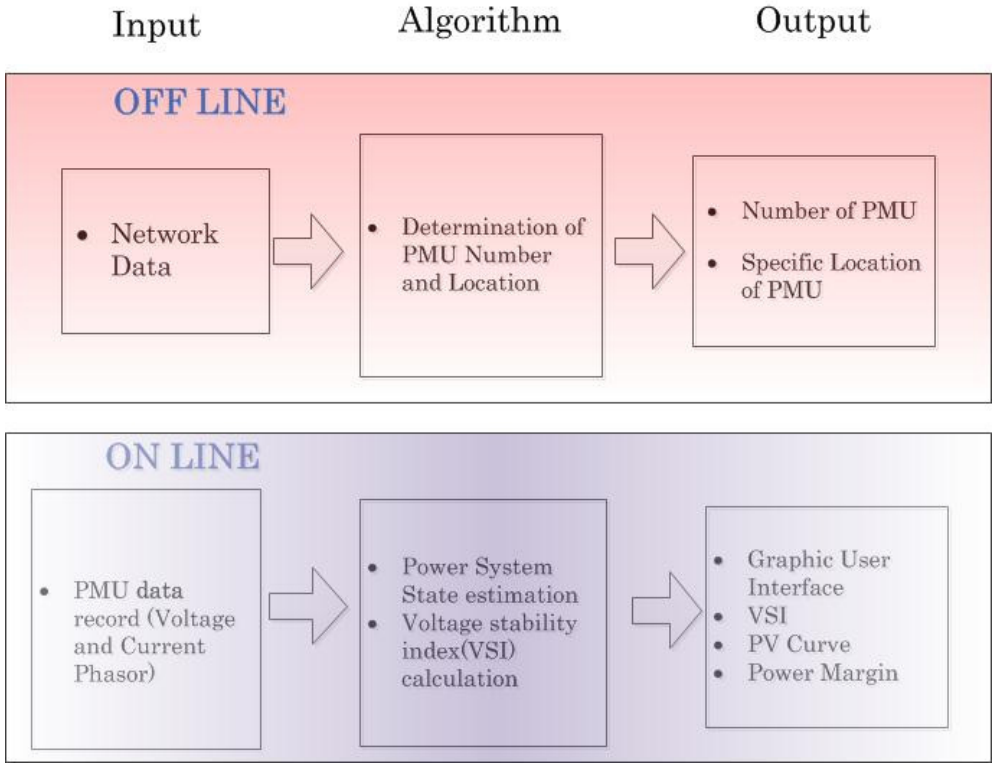

Figure 4.1 Problem Formulation

From Figure 4.1 above there are two kind of analysis needed to be used to formulate the problem. The analysis are off-line and on-line. Off-line analysis is used to find the solution related to the planning. In this work the off-line analysis is used to determine the sufficient number and location of PMU. The on-line analysis consists of the step to build the real time analysis based system.

In off-line analysis the power system network data such as the branch data that contain the power system parameter and the connection-line among the buses are used as the input. The algorithm needed is the algorithm that can determine the number and location of PMU in the power system. The outputs of the algorithm are the PMU number and location in power system. To verify that the result is optimum/sufficient verification method need to be applied.

In the on-line analysis the input are the PMU data record that consist of PMU bus voltage and line current from/to PMU bus. The data records are in phasor form so that they are ready to be directly computed.

The algorithms for on-line analysis are state estimation and voltage stability index (VSI) computation. State estimation is needed to estimate the non-PMU bus voltage that will be used as an input for VSI computation.

The output of the on-line analysis is Graphical User Interface (GUI), VSI, PV curve and power margin. GUI is built in single windows that contain information of VSI, PV Curve and power margin. VSI is useful to show the security level of the power system pertinent to the voltage stability. PV curve visualize the operating condition distance from the nose point. Power margin shows the remaining available active power (MW) from the allowable maximum active power.

4.2 Solution Method

The solution method is built based on the problem formulation. The solution method is built based on the blocks as describe in Figure 4.2. In Figure 4.2, there is WAMS block and simulated power system block. The solution method for WAMS algorithm is described by the WAMS blocks.

WAMS block is divided into two kinds of analysis, off-line and on-line analysis. In the off-line analysis contains one algorithm that is PMU Placement. In on-line analysis there are four series of algorithm/formulation that are PMU record, power system state estimation, VSI computation and user interface building. All of the algorithm/formulation is described in each subsection except the PMU record.

For PMU record part, there is assume that PMU has the capability to record every 10 ms. Another assumption is all of the PMU used in the power system has enough channel to record all of the data. The PMU recording process is simulated that the details is described in the appendix.

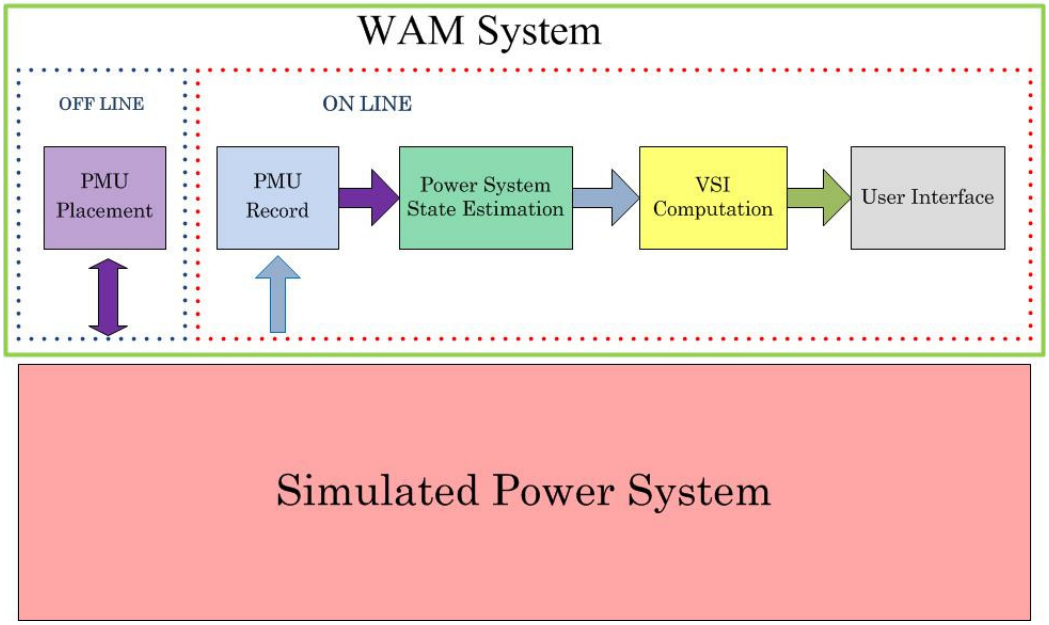

Figure 4.2 Solution Method

4.2.1 Phasor Measurement Unit Placement

In the PMU placement, some methods are used to determine the optimum solution. Graph theoretic procedure, Recursive N method [15] and Generalized Integer Linear Programming[17] are simulated to find the PMU number and location in power system.

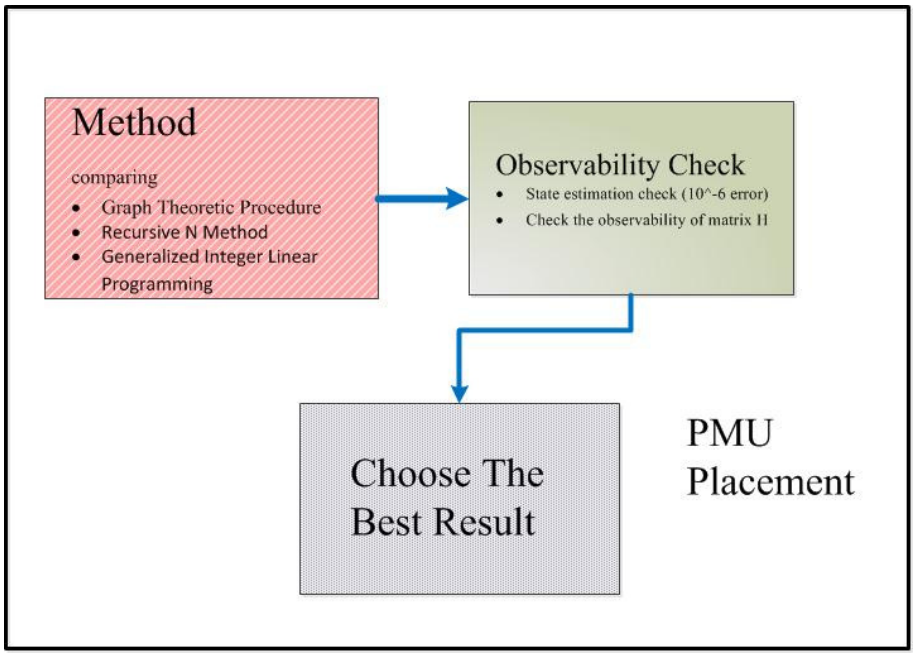

Figure 4.3 PMU Placement Block

The PMU placement results from those three methods are verified using the equation derivation from Linear Estimation for State Estimation method[19]. The verification is needed to determine the optimum solution among those three methods. The flow of the PMU Placement algorithm can be seen in Figure 4.3.

The determination of PMU placement using those three methods is tested into several test system such as IEEE 9-bus, IEEE 14-bus, IEEE 24-bus RTS, IEEE 30-bus and IEEE 57-bus. The input needed to perform those three methods is the network topography of each test systems. The determination result of those three methods is shown in Table 4.1 and Table 4.2. From Table 4.1 and Table 4.2, PMU number and location in various test system is different among three methods used in this work.

In IEEE 9-bus test system all of the three methods result the same number and location. But in the next test simulation the method Recursive N gives the least number of PMU compare to the Graph Theoretic procedure and Generalized Integer Linear Programming. The recursive N method gives the least amount of the PMU because this method considers that the non-load bus can be calculated with the Kirchhoff Current Law (KCL) estimation.

Table 4.1 Determination of PMU Number

IEEE Test System	Graph Theoretic Procedure	Recursive N Method	Generalized Integer Linear Programming
9- bus	3	3	3
14-bus	5	3	4
24-bus RTS	8	6	7
30-bus	11	7	10
57-bus	16	13	17

Table 4.2 Determination of PMU Location

IEEE Test System	Graph Theoretic Procedure	Recursive N Method	Generalized Integer Linear Programming
9-bus	4,6,8	4,6,8	4,6,8
14-bus	1,4,6,10,14	2,6,9	2,6,7,9
24- bus RTS	2,7,9,10,16,21, 23,24	2,8,10,15,17,20	2,3,8,10,16,21,23
30-bus	3,5,6,12,17,18,20,22,23,25,30	3,5,10,12,19,24,29	1,7,9,10,12,18,24,25,27,28
57-bus	1,4,10,13,19,24,29,30,32, 38,45,46,50,53,55,56	1,4,9,20,24,29,31,32, 44,47,51,54,56	1,4,6,13,19,22,25,27,29,32,36,39,41,45,47,51,54

The PMU location is located randomly in the power system. This phenomenon follows the concept of the topologically observable that the bus become observable when the PMU installed on that bus or the bus locate immediately adjacent to the PMU bus[16].

The verification of the PMU placement result from those three method can be evaluated determine the rank of Jacobian Matrix *H* that is used in Linear Formulation of State Estimation. The rank of matrix H represents the number of equation provided to find the number of the state variable. The minimum number of the equation needed to find the state variable is at least the same number as the number of the state variable.

In Linear Formulation of State Estimation, the state variables are the real part of bus voltage and imaginary part of bus voltage and the measurement function is consist of the equation to calculate the PMU buses and line current from/to PMU buses.

The optimum solution is reached when the rank of *H* is the same as the number of the state variable. When the rank of matrix *H* is less than the number of state variable the state estimation cannot be solved so that the number of PMU is not sufficient. When the rank of matrix *H* is greater than the state variable the state estimation can be solved so that it is sufficient but it is not the optimum solution.

Table 4.3 The rank of Jacobian Matrix *H* of the part of State Estimation

IEEE Test System	Number of State Variable	Rank of Matrix H		
		Graph Theoretic Procedure	Recursive N Method	**Generalized Integer Linear Programming**
9- bus	18	18	18	**18**
14-bus	28	26	26	**28**
24-bus RTS	48	48	42	**48**
30-bus	60	58	52	**60**
57-bus	114	100	96	**114**

From the result in Table 4.3, those three methods have different rank of Matrix H. The optimum solution is reached when Generalized Integer Linear Programming is used since the rank of Jacobian matrix *H* is equal to the number of state variable. In the on-line analysis, the PMU data record is come from the PMU installed on the selected buses as the result of Generalized Integer Linear Programming.

4.2.2 Power System State Estimation

In on-line analysis of the WAMS block state estimation computation is needed, after recording the PMU bus data and line current flowing from/to PMU bus. State estimation is needed since all of bus voltage is needed for the VSI calculation. Linear Formulation of State Estimation[19] is used to estimate all of the voltage bus value as shown in Figure 4.4.

In this state estimation method using the PMU bus voltage and line current flowing from/to PMU bus, the derivation of measurement functions are linear as described in the chapter II.

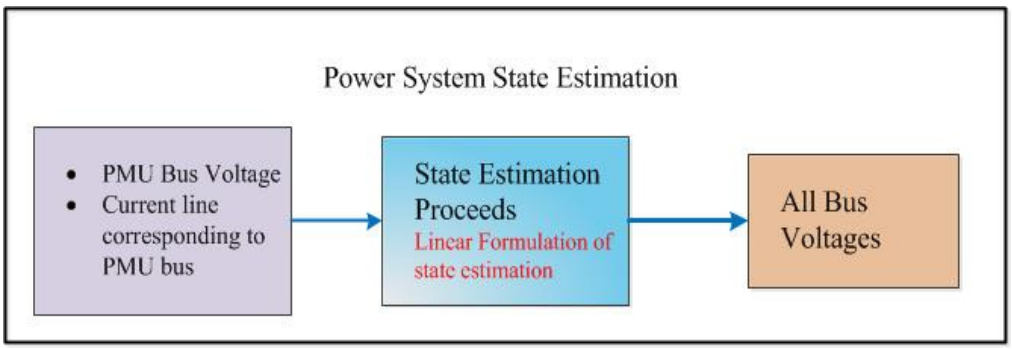

Figure 4.4 Power System State Estimation Block

The final solution is linear as shown in equation (2.17) in chapter II that described as follow:

$$\hat{x} = (H^T R^{-1} H)^{-1} H^T R^{-1} \hat{z}$$

Where:

H is the Jacobian Matrix of the derivation of measurement function

$\hat{z}$ is actual measurement vector

$\hat{x}$ is state variable vector

R is the weighted matrix

In this work, the weighted matrix R is represented the measurement error of the system. The measurement error is defined by r that is the standard deviation of set of data. The measurement error for each measurement is determined by taking the random value within the range of r in the form of $e = [\sigma_1^2, \sigma_2^2, \ldots, \sigma_n^2]$ with n is the number of measurement. Matrix R is formulated form the random error e with the mean 0 as described in chapter 2. In this work the value of r is set to be 10^{-10} to represent the accuracy of PMU that can measure the data with accuracy near to the real operating condition.

$$R = \begin{bmatrix} \sigma_1^2 & 0 & \cdots & 0 \\ 0 & \sigma_2^2 & \cdots & 0 \\ \vdots & \ddots & \ddots & \vdots \\ 0 & 0 & \cdots & \sigma_n^2 \end{bmatrix}$$

In the simulation the state estimation process is done on-line. Solving state estimation in linear form is suitable for real time simulation since no iterative process in each step.

The Linear Formulation for State Estimation is tested into IEEE test system such as IEEE 9-bus, IEEE 14-bus, IEEE 24-bus RTS, IEEE 30-bus and IEEE 57-bus using each initial condition. PMU placement result from Generalized Integer Linear Programming is applied into each test system.

Bus voltage and line current from/to PMU buses are recorded as PMU data record. PMU data record then estimated using Linear Formulation of State Estimation method. The voltage estimation is comparing with the voltage calculation from load flow. Assuming that the real condition is very near to the load flow calculation, the voltage calculation from load flow is used for the reference to determine the error. This procedure is tested for all test system.

Table 4.4 Voltage estimation in IEEE 9-bus

Bus Number	**$V_{Load\ Flow}$**		**$V_{estimated}$**		**Error ($x10^{-8}$)**	
	Vmag (p.u.)	Vang (deg)	Vmag (p.u.)	Vang (deg)	Vmag (%)	Vang (%)
1	1.0000	0.00	1.0000	0.00	0.353	15.649
2	1.0000	9.67	1.0000	9.67	0.355	13.314
3	1.0000	4.77	1.0000	4.77	0.366	19.468
4	**0.9870**	**-2.41**	**0.9870**	**-2.41**	**0.295**	**18.532**
5	0.9755	-4.02	0.9755	-4.02	0.370	18.882
6	**1.0034**	**1.93**	**1.0034**	**1.93**	**0.298**	**22.729**
7	0.9856	0.62	0.9856	0.62	0.297	18.231
8	**0.9962**	**3.80**	**0.9962**	**3.80**	**0.268**	**18.077**
9	0.9576	-4.35	0.9576	-4.35	0.332	16.457

* The bold font represent where the PMU installed on

** All of the variable error is less than 10^{-6} which is still acceptable

The state estimation result for IEEE 9-bus test system can be seen in Table 4.4. As we can see from the result that the difference between the load flow calculation and the state estimation for every bus voltages is still lesser than 10^{-6} for voltage magnitude and voltage angle.

In the IEEE 14-bus test system, the PMU installed in the power system network is increasing because of the complexity of the network comparing to the IEEE 9-bus test system. The number of PMU installed in this test system is 4 that is located in bus number 2, 6, 7 and 9.

State estimation results for IEEE 14-bus test system are shown in Table 4.5. In this simulation, the differences of voltage magnitude and voltage angle in load flow calculation to the state estimation result are still lesser than 10^{-6}. In this simulation the difference is still very small.

Table 4.5 Voltage estimation in IEEE 14-bus

Bus Number	$V_{Load\ Flow}$		$V_{estimated}$		Error ($x10^{-8}$)	
	Vmag (p.u.)	Vang (deg)	Vmag (p.u.)	Vang (deg)	Vmag (%)	Vang (%)
1	1.0600	0.00	1.0600	0.00	0.587	35.253
2	**1.0450**	**-4.98**	**1.0450**	**-4.98**	**0.490**	**39.569**
3	1.0100	-12.73	1.0100	-12.73	0.499	38.436
4	1.0177	-10.31	1.0177	-10.31	0.458	33.807
5	1.0195	-8.77	1.0195	-8.77	0.596	38.391
6	**1.0700**	**-14.22**	**1.0700**	**-14.22**	**0.415**	**46.876**
7	**1.0615**	**-13.36**	**1.0615**	**-13.36**	**0.237**	**42.134**
8	1.0900	-13.36	1.0900	-13.36	0.334	34.322
9	**1.0559**	**-14.94**	**1.0559**	**-14.94**	**0.221**	**42.188**
10	1.0510	-15.10	1.0510	-15.10	0.233	41.346
11	1.0569	-14.79	1.0569	-14.79	0.594	39.699
12	1.0552	-15.08	1.0552	-15.08	0.398	36.186
13	1.0504	-15.16	1.0504	-15.16	0.427	43.383
14	1.0355	-16.03	1.0355	-16.03	0.351	26.782

* The bold font represent where the PMU installed on

** All of the variable error is less than 10^{-6} which is still acceptable

In the IEEE 24-bus RTS The number of PMU installed in this test system is 7 that is located in bus number 2,3,8,10,16,21 and 23. In this test system there are 48 state variables which are estimated in with the Linear Formulation of State Estimation. Those state consist of the real value of voltage bus and imaginary value of the voltage bus. In IEEE 24-bus RTS test system estimation, the number of line current needed is 27 (which the total branch is 38).

State estimation results for IEEE 24-bus RTS test system are shown in Table 4.6. In this simulation, the differences of voltage magnitude and voltage angle in load flow calculation to the state estimation result are still lesser than 10^{-6}. In this simulation the difference is still very small.

The result for state estimation result verification for IEEE 30-bus and IEEE 57-bus test system are shown in appendix. In those two simulation, the differences of voltage magnitude and voltage angle in load flow calculation to the state estimation result are still lesser than 10^{-6}.

From the state estimation verification result comparing with the load flow calculation. The differences (error) between the estimation results and the load flow calculation are lesser than 10^{-6}. Since the differences are very small, the state estimation method using Linear Formulation of State Estimation can be applied to estimated the voltage using PMU data record and suitable applied in the real time simulation.

Table 4.6 Voltage estimation in IEEE 24-bus RTS

Bus Number	$V_{Load\ Flow}$		$V_{estimated}$		Error ($x10^{-8}$)	
	Vmag (p.u.)	Vang (deg)	Vmag (p.u.)	Vang (deg)	Vmag (%)	Vang (%)
1	1.0350	-7.28	1.0350	-7.28	0.501	34.158
2	**1.0350**	**-7.37**	**1.0350**	**-7.37**	**0.489**	**34.470**
3	**0.9894**	**-5.58**	**0.9894**	**-5.58**	**0.599**	**33.445**
4	0.9979	-9.69	0.9979	-9.69	0.555	30.620
5	1.0185	-9.96	1.0185	-9.96	0.649	32.258
6	1.0124	-12.42	1.0124	-12.42	0.532	30.902
7	1.0250	-7.36	1.0250	-7.36	0.593	30.649
8	**0.9927**	**-11.09**	**0.9927**	**-11.09**	**0.524**	**34.608**
9	1.0013	-7.43	1.0013	-7.43	0.618	30.190
10	**1.0285**	**-9.50**	**1.0285**	**-9.50**	**0.578**	**33.084**
11	0.9899	-2.15	0.9899	-2.15	0.681	25.879
12	1.0025	-1.52	1.0025	-1.52	0.695	24.941
13	1.0200	0.00	1.0200	0.00	0.670	22.988
14	0.9800	2.26	0.9800	2.26	0.726	27.554
15	1.0140	11.57	1.0140	11.57	0.800	21.059
16	**1.0170**	**10.45**	**1.0170**	**10.45**	**0.791**	**22.132**
17	1.0386	14.93	1.0386	14.93	0.819	16.827
18	1.0500	16.29	1.0500	16.29	0.820	16.704
19	1.0232	8.92	1.0232	8.92	0.792	22.471
20	1.0385	9.53	1.0385	9.53	0.725	17.377
21	**1.0500**	**17.12**	**1.0500**	**17.12**	**0.816**	**17.273**
22	1.0500	22.77	1.0500	22.77	0.831	9.400
23	**1.0500**	**10.57**	**1.0500**	**10.57**	**0.725**	**17.354**
24	0.9779	5.30	0.9779	5.30	0.706	22.258

* The bold font represent where the PMU installed on

** All of the variable error is less than 10^{-6} which is still acceptable

4.2.3 Voltage Stability Index Computation

VSI computation is calculated using two kinds of index that is Synchrophasor-Based Real-Time Voltage Stability Index (SBRT-VSI)[23] and PQ Voltage Stability Index (PQVSI)[24]. VSI computation is calculated using the voltage bus from the state estimation result. The detail process can be shown in Figure 4.5.

SBRT VSI predict the maximum loadable active power as one of the step as shown in the equation below. The load angle is assumed to be fixed to perform the following equation.

$$P_{Lj\max} = \frac{-v_{equj}^2 (X_{equj} \tan\theta_j + R_{equj}) \left| Z_{equj} \right| v_{equj}^2 \sqrt{\tan^2 \theta_j - 1}}{2(X_{equj} - R_{equj} \tan\theta)^2}$$

with

$$v_{equj} = \sum_{i=1, i\neq j}^{N} Z_{LLji}\left(\frac{-S_{Li}}{V_{Li}}\right)^{*} + \sum_{k=1}^{M} H_{LGjk} V_{Gk}$$

$$Z_{equj} = Z_{LLjj}$$

All of the voltage bus is computed to be the apparent power. Using the apparent power and network configuration data the voltage and impedance for the equivalent network can be calculated as shown in the equation before. To calculate the the apparent power the following Equation is needed.

$$S = V_{bus}.(Y_{bus}V_{bus})^{*}$$

With

S is vector of apparent power of all buses

V_{bus} is vector of estimated voltage from the state estimation

Knowing the apparent power at all bus, the load angle θ_j of the power/load in each bus can be calculated. The verification using the load flow data has been calculated that is shown in the appendix.

After calculating the predicted maximum active power P_{Ljmax}, the power margin and the SBRT VSI for each load bus can be calculated using equation (2.31) and (2.32). The power margin for each bus is one of the properties that can be extracted from the derivation of SBRT VSI.

$$P_{Ljmargin} = P_{Lj\max} - P_{Lj} \tag{2.31}$$

$$SBRT\ VSI_{Lj} = \frac{P_{Ljmargin}}{P_{Ljmax}} \tag{2.32}$$

The value of SBRT VSI for each load buses is $0 < \text{SBRT VSI}_{Lj} \leq 1$.

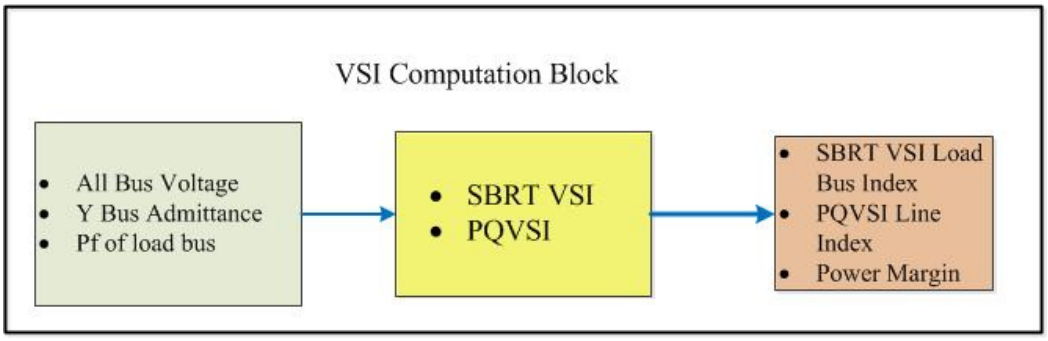

Figure 4.5 VSI Computation Block

When we know the value of the predicted maximum value of the certain load bus, the estimated PV curve can be derived, the first step to formulate the PV curve is varying the load value from 0 to the maximum active P_{max} value with the certain step.

$$\hat{P} = [0 \quad 10 \quad 20 \quad \cdots \quad (P_{\max} - 10) \quad P_{\max}]$$

Assuming that the power factor in the load buses and the equivalent network voltages for each load bus are constant as in each simulated step, PV curve can be derived using the equation below.

$$V_j = \sqrt{\frac{v_{equj}^{\ 2}}{2} - (Q_j X_{equj} + P_j R_{equj}) \pm \sqrt{\frac{v_{equ}^4}{4} - (Q_j X_{equj} + P_j R_{equj}) v_{equj}^2 - (P_j X_{equj} - Q_j R_{equj})^2}}$$

with :

V_{equj} is the Voltage at remaining bus for load bus j, $\forall\, j \in$ load bus

$Z_{equj} = R_{equj} + jX_{equj}$ is the equivalent lie between the load bus j with the remaining equivalent bus

P_j, Q_j are Active and Reactive load at bus j

The value of the reactive power can be represented as the function of vector $\hat{P}$ by assuming the constant power factor. Inserting the vector $\hat{P}$ in the equation above, the set of vector $\hat{V}$ can be derived as well. Plotting the data from vector $\hat{V}$ on vector $\hat{P}$, the PV curve can be derived.

Using the same assumption by varying the active power from zero to the maximum Pmax, P-V curve for each load bus can be created. The varying P between zeros to Pmax used as input value for the equation above. By considering those two assumptions the voltage at each load bus V_r can be calculated and the P-V curve can be plotted.

In calculating the PQVSI, the predicted maximum negative power flow can be calculated using the following equation.

$$P_{ji}^{NP} = \frac{|V_S|^2}{2\left[\mathrm{Im}\{AB^*\}\tan\theta_{ji} - \mathrm{Re}\{AB^*\} + |A||B|\sec\theta_{ji}\right]}$$

With

Vs is the voltage at the sending end bus

θ_{ji} is the negative power flow angle in each line

A and *B* is the transmission-line parameter that can be calculated from the power system network.

Using the data of all bus voltages the power flow in each line can be calculated using the equation.

$$S_{ji} = V_j . I_{ji}^*$$

The line current I_{ji} can be calculated using the equation below

$$\begin{bmatrix} I_{ij} \\ I_{ij} \end{bmatrix} = \begin{bmatrix} y_t & -\frac{y_t}{a} \\ -\frac{y_t}{a^*} & \frac{y_t}{|a|^2} \end{bmatrix} \begin{bmatrix} V_i \\ V_j \end{bmatrix}$$

With:

yt is the transmission-line admittance

a is the transformer tapping factor 1:*a* (from:to)

After calculating the negative power flow S_{ji} the power flow angle θ_{ji} can be calculated immediately as well so that the maximum predictive active power flow can be calculated. The verification using the load flow data has been calculated that is shown in the appendix.

The PQVSI for each line can be calculated using the equation below as derived from the chapter II.

$$PQVSI_{ji} = \frac{P_{ji}^0}{P_{ji}^{NP}}$$

With

P_{ji}^{NP} = active load at the collapse point

Q_{ji}^{NP} = reactive load at the collapse point

The value of PQVSI for each line is $0 \leq PQVSI_{ji} < 1$. When the value of any PQVSI line is reached 1, the power system is reached the collapse point.

The calculation of SBRT VSI, PQVSI, plotting the PV curve and calculate the power margin are done in real time simulation so that the value of each variable is updated following the simulation step.

SBRT VSI and PQVSI are used as the VSI in this WAMS design because of their simple calculation, the accuracy and the attributes. The computation of SBRT VSI and PQVSI is 5 ms, which is suitable with the WAMS requirement. The accuracy of both VSI is shown in another part of this thesis. From SBRT VSI the PV curve and the power margin can be also derived, this attribute is very useful information as WAMS output.

4.2.4 User Interface

User interface system is needed to show the meaningful information related to the voltage stability performance of WAMS. In this work, the user interface is built using MATLAB GUI. The process of user interface building is shown in Figure 4.6.

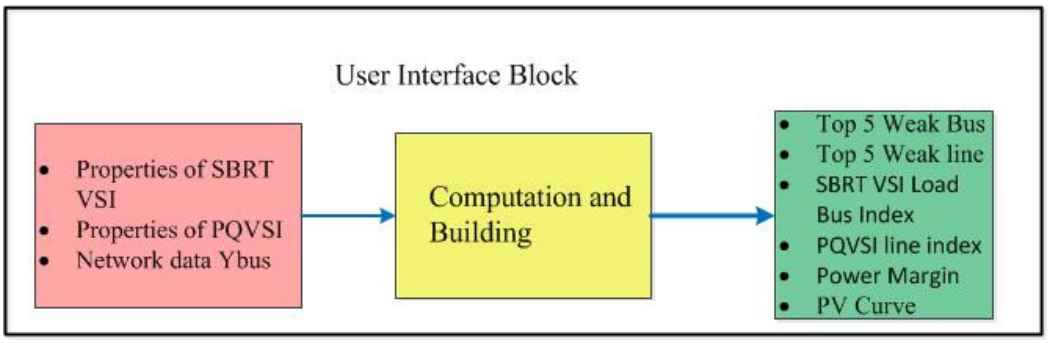

Figure 4.6 User Interface Block

The information shown in the user interface windows are the rank of the bus, the rank of the line, the SBRT VSI rank in the order of the bus rank, PQVSI rank in the order of the line rank, power margin from the ranked bus and the PV curve figure as can be seen in Figure 4.7.

The rank of the bus is done by ordering the SBRT VSI of the bus from the smaller to the bigger as shown in the first row of the windows. The rank of bus is needed to show which bus is the nearest to the collapse point. The top five buses in order (the left is the smallest) are shown in the first line of the user interface window.

The rank of the line is done by ordering the PQVSI of the line from the bigger to the smaller as shown in the second row of the windows. The rank of line is needed to show which lines is the nearest to the collapse point. The top five buses in order (the left is the smallest) are shown in the first line of the user interface window.

The value of SBRT VSI in order bus to the bus ranking is shown in third row of the windows. Then, the value of PQVSI in order to the line ranking is shown in the fourth row of the windows. The power margin according to the load bus rank is shown in the fifth row of the windows.

PV curve is shown as a graph in the bottom of the windows. There is a selection in the sixth row in the windows to show the PV curve of the load bus according to the bus rank. PV curve in the windows is shown comparing to the actual condition by showing the cross dot to the PV curve.

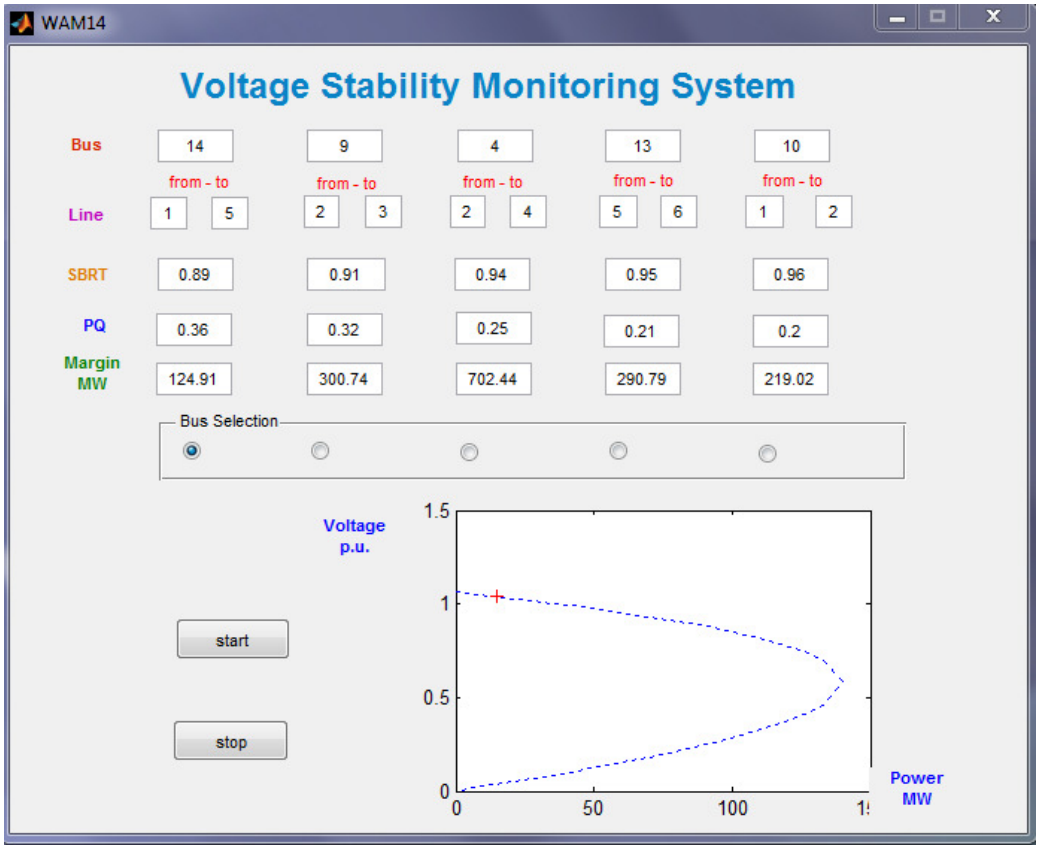

Figure 4.7 Main Windows of User Interface

4.3 Simulated Power System

The IEEE 14-bus test system is used to demonstrate the voltage stability performance. IEEE 14-bus test system has 14 buses with 5 generator bus and 9 load buses as shown in Figure 4.8. The detail value of the branch data and the loading condition is shown in the appendix.

Simulated Power System is the system that represents the real condition of power system network. The power system network consist of generators, loads, transmission topology and transmission-lines parameters. Modeling the power system network, the simulated power system block should be able to represent the real power system condition in order to simulate the real system network.

In this work, the generator, load and the transmission-lines have to be modeled as shown in Figure 4.8 and Figure 4.9. Generator at bus 1 is modeled as the infinite bus, generators at bus 3 and bus 6 are modeled as classical model with constant voltage and generator 2 and generator 8 are modeled as four state model. Load at bus number 4, 5, 9 and 13 are modeled as constant power. The other remaining loads are modeled as constant admittance. The detail of each model is described in the following subsection.

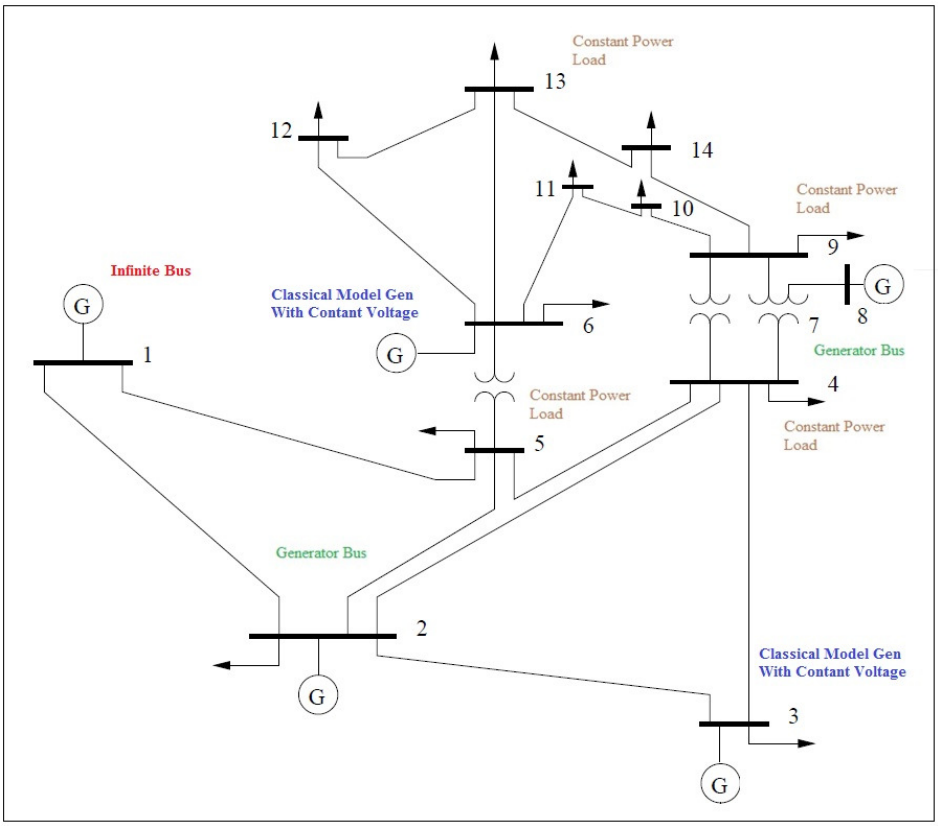

Figure 4.8 IEEE 14-bus Test System

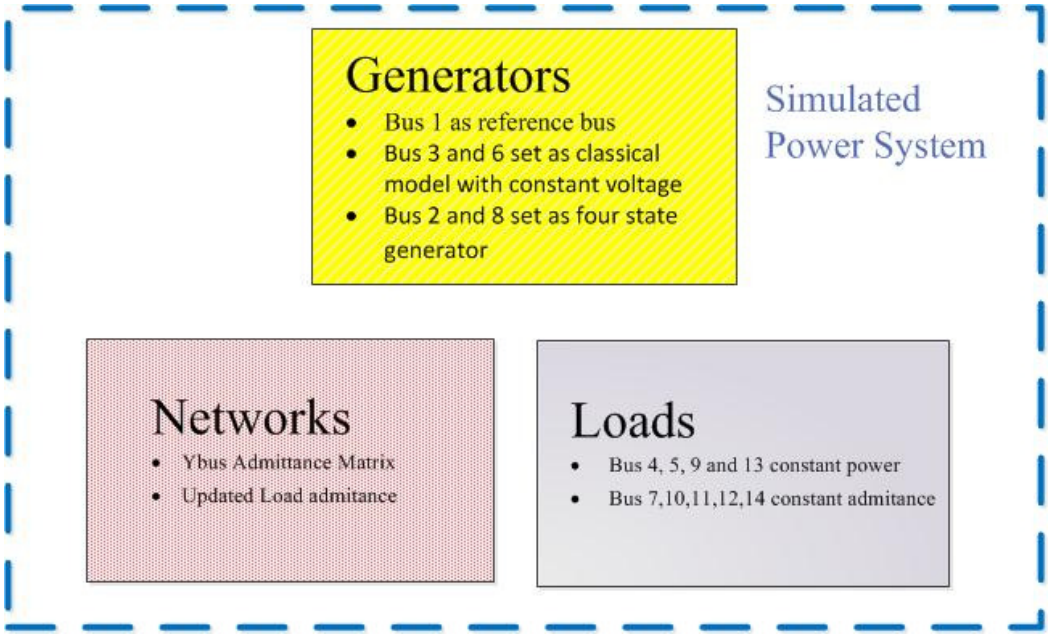

Figure 4.9 The Block Model of Simulated Power System

In this work, Simulated Power System should be built to be capable in simulating the real time manner. MATLAB m.file and MATLAB Simulink are used to build the power system so that the real time simulation can be done. MATLAB m.file is used to perform the static analysis of the power system such as load flow analysis, set up the branch data, set up the generator parameter and set up the calculation for the real time analysis (network calculation). S-function block is also used to solve the more complicated calculation.

4.3.1 Generator Model

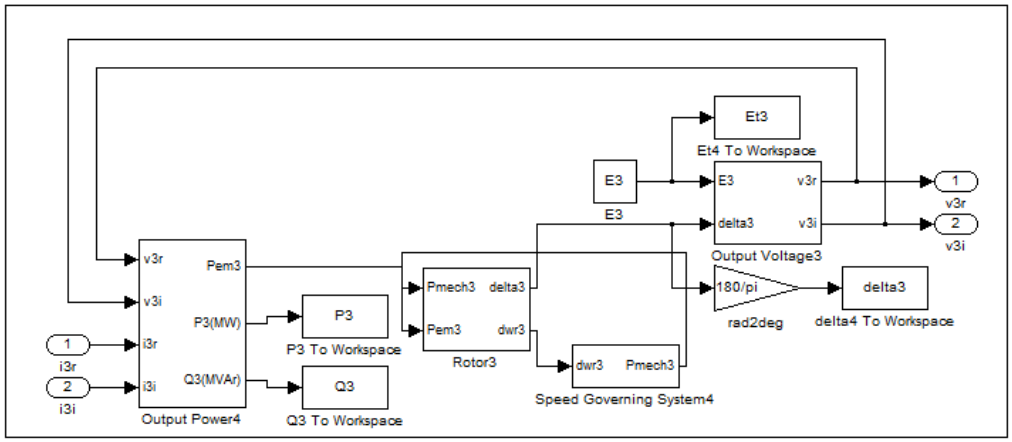

Figure 4.10 Classical Model of the Generator with the Constant Voltage

In this work there are five generators in IEEE 14-bus test system. There are generator at bus 1, 2, 3, 6 and 8. Generator at bus number 1 is modeled as an infinite bus so that the generator has the constant value of voltage magnitude and angle. Generator at bus number 3 and 6 are modeled as the classical model of generator with constant voltage so that the generator has the constant voltage magnitude. Generator at bus number 2 and 8 are modeled using the four states model of synchronous generator.

In the infinitive generator model the voltage magnitude and voltage angle is remains constant so that this generator can supply infinite power to the power system.

The Classical Model of the Generator with the constant voltage use the input of injected bus current and the output of bus voltage as can be seen in Figure 4.10. This model of the generator, calculate the P mechanical of the generator to calculate the voltage angle of bus terminal but keep the value of the voltage magnitude constant so that the voltage can be remained fixed while the angle is change

In four states generator model, the injected generator terminal current, the P mechanical and the constant excitation voltage E_{fd} use as the input as can be shown in Figure 4.11. In this four states generator model. The sub transient rotor winding is

neglected. The output of the four states generator model is the generator rotor angle and the generator terminal voltage. These output values are used as the input of the power system network model.

The other output such as the generator frequency, generator active power and generator reactive power also can be computed to be a certain data even though it is not used as the other input of the other model.

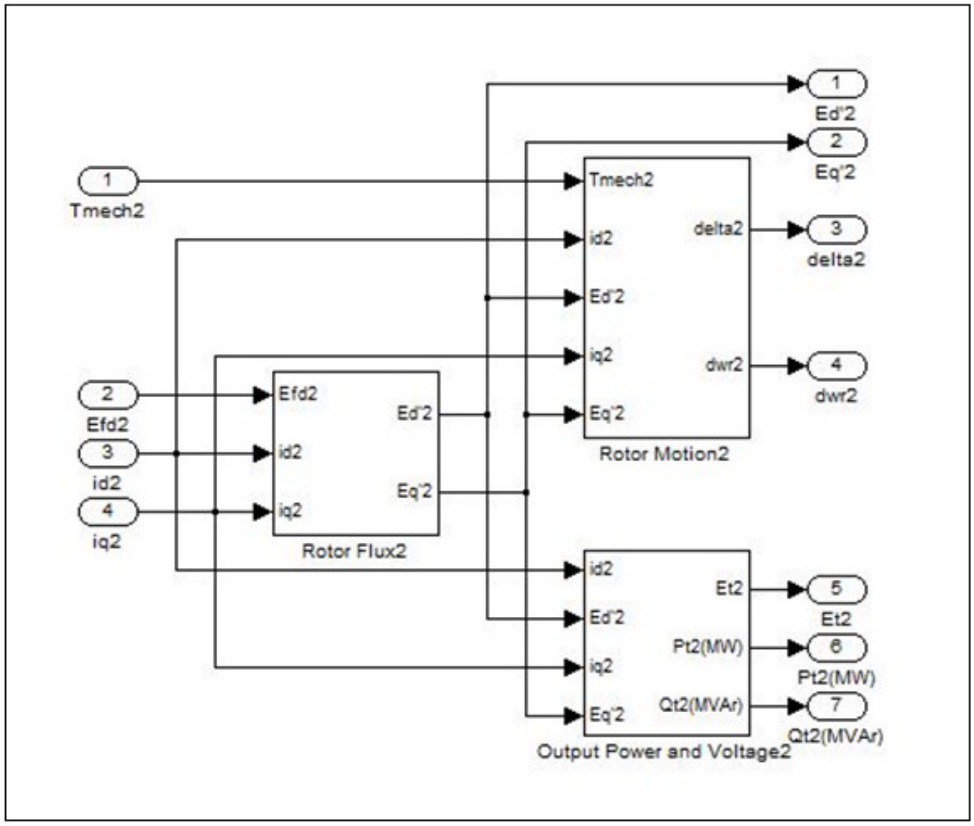

Figure 4.11 Four States Model of Synchronous Generator

4.3.2 Load Model

In IEEE 14-bus test system, there are 9 load buses. In this simulated power system, the load bus is grouped into two groups that are constant power load bus and fixed admittance load bus. Bus number 4, 5, 9 and 13 are belong to the constant power load while bus number 7, 10, 11, 12, 14 are belong to the fixed admittance load bus.

The admittance for the fixed admittance load bus is calculated at the initialization stage using the voltage at that load bus also the power. In constant load model load, the admittance is change during the load change. Constant load model load uses the

voltage magnitude and active power of that load bus as shown in Figure 4.12. The input of voltage magnitude is obtained from the power system network model while the active load input is get from the load demand.

Admittance of load bus is calculated form the active power input and the voltage magnitude input. In this simulation there is an assumption for the load bus, that the Power Factor (*Pf*) of this load bus is keeping constant so that the conductance (*g*) and the susceptance (*b*) are always linear. In the constant power model, the value of the admittance will change whenever the voltage bus is change even the power is remained constant.

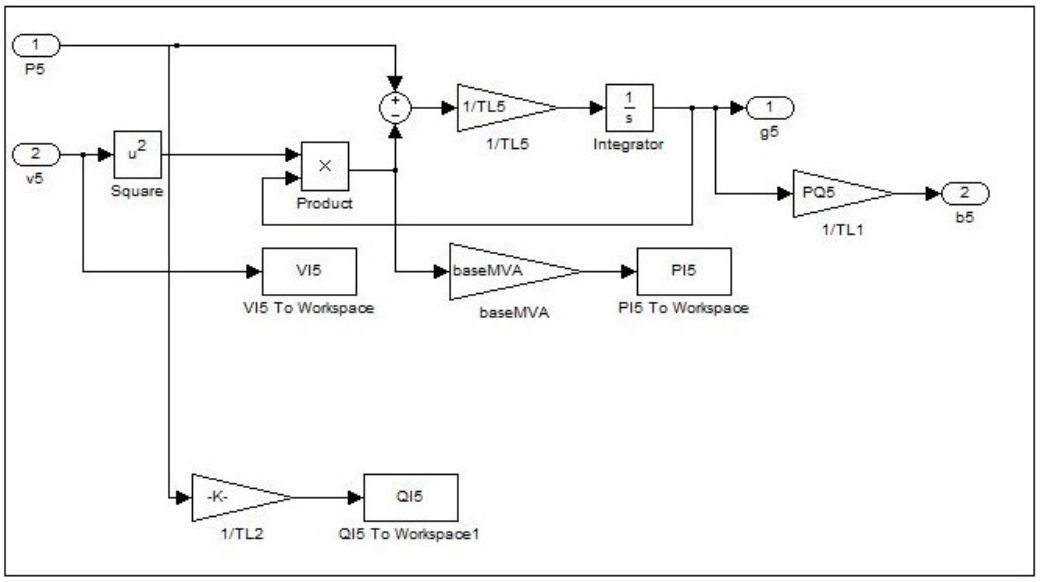

Figure 4.12 Constant Load Model

In some parts of simulation, the admittance of load is updated into the Y_{bus} admittance matrix. The detail parameter value and diagram of this load model is described further in the appendix.

4.3.3 Power System Network Model

Power system network model represent all of the computation related to the network. The network model used the reference bus voltage, fixed voltage bus voltage, generator terminal voltage and rotor angle of the four state models and admittance from all of load busses as the input data.

The power system network use S-Function in the Simulink model to compute the output values. The computation is to compute the generator terminal current, voltage magnitude as the input of load bus and the generator bus voltage of four states generator model as an input for the PMU.

CHAPTER V
TEST RESULT AND ANALYSIS

In chapter V the capability of WAMS is demonstrated by testing in to some scenario. Test procedure, results and discussion are elaborated further in this chapter.

5.1 Test Procedure

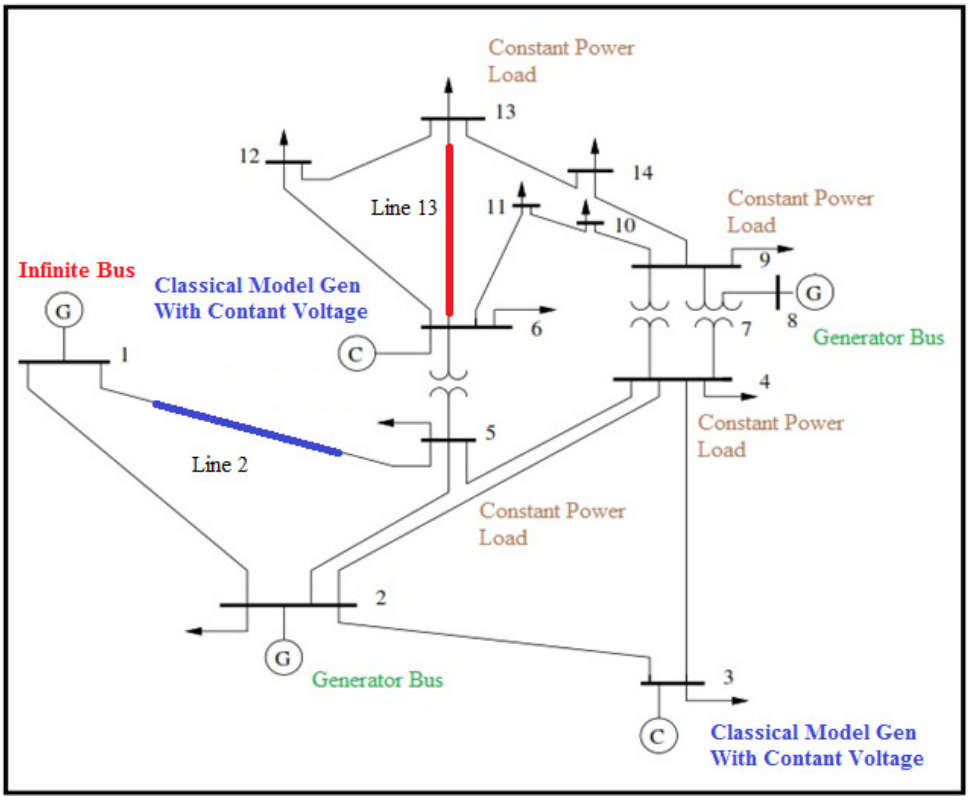

Figure 5.1 Test Procedure on IEEE 14-bus Test System

In performing this work about the application of WAMS to monitor the voltage stability of the power system, the explanation of test procedure is needed. The test procedure consists of four scenarios that are explained in the following subsection. The scenarios are applied in real time and trigger some disturbance in the power system. As described in the scope of work before that the disturbance in this work is the load changing or the set of the load changing.

The four kinds of scenario are used to show the capability of WAMS performance facing the various operating condition and disturbance.

5.1.1 Test Procedure in Scenario a

In scenario a, the set of disturbance is the combination of load increment in different buses and different time interval. This set of disturbance is to show the multiple actions that can probably happened in the real power system. The set of disturbance with the detail time interval is shown below.

- t = 0 - 3, Continuously Load Increment at Bus 4
- t = 3 - 6, Continuously Load Increment at Bus 5
- t = 6 - 9, Continuously Load Increment at Bus 9
- t = 9 - 12, Continuously Load Increment at Bus 13

The rate of increment of each load bus increment is 50 MW/second. After increment stop, the value of load set to be the final value of the increment. In the result, the effect of increase the load at each bus can be obtained.

Since in calculating the SBRT VSI and PQVSI the constant power factor is assumed, in scenario an initial power factor of each load bus is set to be 0.95 lagging. In the real time simulation the real power factor may change a bit since some of the load bus is modeled as the constant impedance.

5.1.2 Test Procedure in Scenario b

In scenario b, the set of disturbance is the combination of load increment in different buses and different time interval. This set of disturbance is to show the multiple actions that can probably happened in the real power system. The set of disturbance with the detail time interval is shown below.

- t = 0 – 3 s, Continuously Load Increment at Bus 4
- t = 3 – 6 s, Continuously Load Increment at Bus 5
- t = 6 – 9 s, Continuously Load Increment at Bus 9
- t = 9 – 12 s, Continuously Load Increment at Bus 13

The rate of increment of each load bus increment is 50 MW/second. After increment stop, the value of load set to be the final value of the increment. In the result, the effect of increase the load at each bus can be obtained.

Since in calculating the SBRT VSI and PQVSI the constant power factor is assumed, in this scenario an initial power factor of each load bus is set to be 0.95 leading. In the real time simulation the real power factor may change a bit since some of the load bus is modeled as the constant impedance. Setting the power factor leading in this scenario is used to confirm the voltage stability effect in the different operating power factor. Operating power factor in leading condition should shows the better voltage stability performance for the same case of disturbance.

5.1.3 Test Procedure in Scenario c

In scenario c, the set of disturbance is the combination of load increment in different certain bus and short circuit in certain line. This set of disturbance is to show the multiple actions that can probably happened in the real power system. The set of disturbance with the detail time interval is shown below.

- t = 0-4 s, Continuously Load Increment at Bus 4
- t = 3-7 s, There is no change due to the load increment and line reconfiguration.
- t = 7 s, Short Circuit at line 2 (bus 2 – bus5)
- t = 7.04 s, Disturbance is clear by removing line 2

The rate of increment of each load bus increment is 50 MW/second. After increment stop, the value of load set to be the final value of the increment. In the result, the effect of increase the load at each bus can be obtained. The power factor in the initial condition is set to be 0.95 lagging. In the real time simulation the real power factor may change a bit since some of the load bus is modeled as the constant impedance.

In performing the short circuit simulation, when the short circuit happened the line impedance value is decrease. The line 2 removal is applied after 40 ms (2 cycles). In applying the line removal, the impedance in the line (removed) is set to be very big value so that a little amount of current still flowing through this line. This assumption in removing line method is taken because of the network configuration constraint. Change the network configuration may change the observability of installed PMU in the power system.

5.1.4 Test Procedure in Scenario d

In scenario d, the set of disturbance is the combination of load increment in different certain bus and short circuit in certain line. This set of disturbance is to show the multiple actions that can probably happened in the real power system. The set of disturbance with the detail time interval is shown below.

The rate of increment of each load bus increment is 50 MW/second. After increment stop, the value of load set to be the final value of the increment. In the result, the effect of increase the load at each bus can be obtained. The power factor in the initial condition is set to be 0.95 lagging. In the real time simulation the real power factor may change a bit since some of the load bus is modeled as the constant impedance.

- t = 0-3, Continuously Load Increment at Bus 13
- t = 4-7, There is no change due to the load increment and line reconfiguration.
- t = 7, Short Circuit at line 13 (bus 6 – bus13)
- t = 7.04 second, Disturbance is clear by removing line 13

In performing the short circuit simulation, when the short circuit happened the line impedance value is decrease. The line 13 removal is applied after 40 ms (2 cycles). In applying the line removal, the impedance in the line (removed) is set to be very big value so that a little amount of current still flowing through this line. This assumption in removing line method is taken because of the network configuration constraint. Change the network configuration may change the observability of installed PMU in the power system.

5.2 Voltage Stability Performance Monitoring

Calculating the voltage stability index, the method of Synchronous Based on Real Time Voltage Stability Index (SBRT VSI) and PQ Voltage Stability Index (PQVSI) that has been described in the chapter II are used in this work. SBRT VSI calculate the voltage stability index based on calculate the power margin between the actual load bus value and the calculated maximum load bus value.

In this work, there are four scenarios that used to do the dynamic security assessment pertinent to voltage stability. The correlation between the voltage profile and the voltage stability index is described in this subchapter.

5.2.1 Voltage Stability Performance Monitoring in Scenario a

In scenario a the disturbance is a set of load increment in bus 4, 5, 9 and 13 in different interval time. At t = 0 – 5 second the snapshot of user interface (t = 5 second) is shown in Figure 5.3 and the voltage profile of five weakest bus is shown in Figure 5.3.

At t = 5, the weakest bus is bus number 4 with the voltage stability index value equal to 0.71. Voltage stability index for bus number 5 is equal to 0.85. For the comparison, the SBRT VSI value of bus 14, 9 and 10 that are not directly affected by the load increment are 0.89, 0.9 and 0.96 that are still quite secure.

At t = 5 the greater index of the line index PQVSI is at line that connected bus number 1 and 5 that have 0.75. In the second place, is at the line that connected bus 2 and 4 with the index 0.55. It seems that the load increment at this stage has already increased the load at the line.

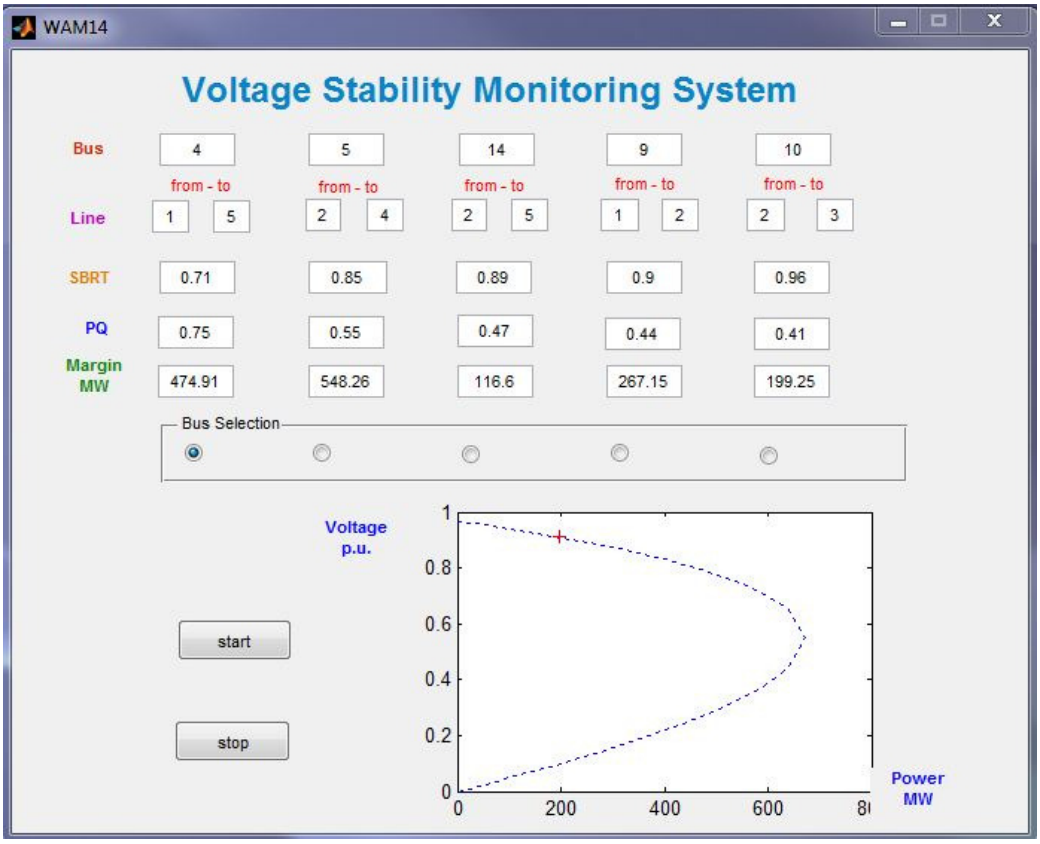

Figure 5.2 User Interface Monitoring of Scenario a at t = 5

Based on SBRT VSI and PQVSI, at t = 5 the voltage stability performance of the power system is still in the secure condition since there is no SBRT VSI bus index and PQVSI line index that exceed the limit.

The power margins for the top five load bus are still far from zero. However, the power margin is decreasing because of the load increment. Based on the PV curve display, load bus 4 still operates in the operating condition.

Voltage profiles for top 5 buses are shown in Figure 5.3. All of the top busses are decreasing as the effect of the load increment. From the figure, bus 4 has the biggest slope of decrement from t = 0 – 3 since the load increment at this time is happened in bus 4. Bus 5 has the biggest slope of decrement at t = 3 – 5 since the load increment at this period is happened in bus 5.

Generally the voltage profiles for all buses are still in stable operating condition even they are decreasing. So based on the SBRT VSI, PQVSI, Power Margin, PV curve and Voltage profile verification, at t = 0 -5 the power system is still in the secure condition.

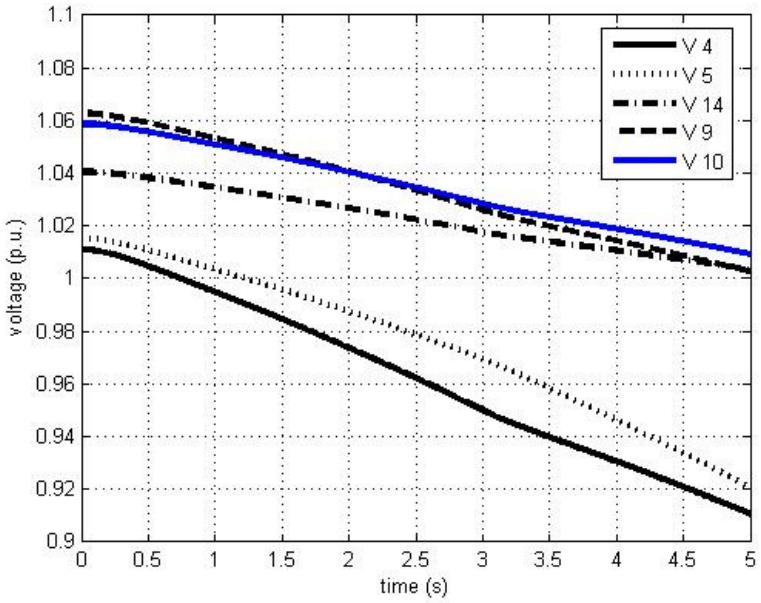

Figure 5.3 Voltage Profile of Scenario a during t = 0 – 5

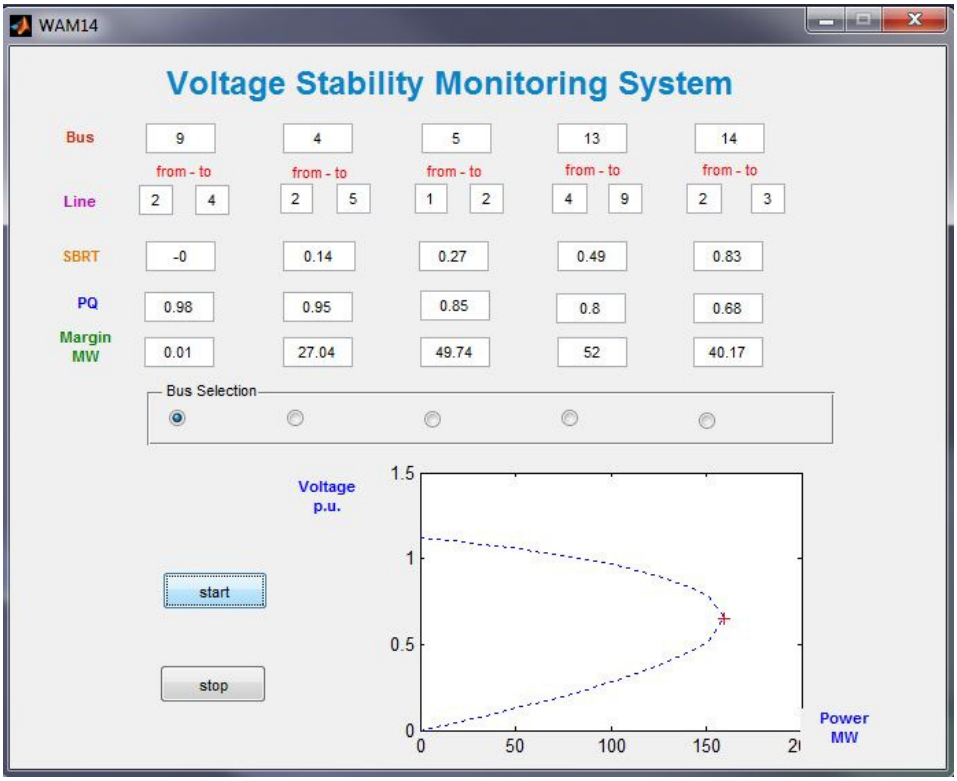

Figure 5.4 User Interface Monitoring of Scenario a at t = 10

At t = 5 – 10, the snapshot of user interface system is shown in Figure 5.4 (at t = 10) and the voltage profile for top five buses is shown in Figure 5.5. At this time the load increment is affected by the increment at bus 5, 9 and 13.

At t = 5, the weakest bus is bus number 9 with the voltage stability index value equal to 0. Voltage stability index for bus number 4, 5 and are equal to 0.14, 0.27 and 0.49. For the comparison, the SBRT VSI value of bus 14 that are not directly affected by the load increment are 0.83 that is still quite secure.

At t = 5 the greater index of the line index PQVSI is at line that connected bus number 2 and 4 that is 0.98. The PQVSI for line 2-5, 1-2, 4-9 and 2-3 are 0.95, 0.85, 0.8 and 0.68. It seems that the load increment at this stage have extremely affected some lines in the network such as line 2-4, 2-5, 1-2 and 4-9.

Based on SBRT VSI and PQVSI, at t = 10 the voltage stability performance of the power system is still in the insecure condition since there is a bus that has the SBRT VSI 0 and there is a line that has the PQVSI near to 1.

The power margins for the top five load bus are relatively near to zero. In bus 9 the power margin is zero so that the bus is loaded in the maximum predicted load. Based on the PV curve display, load bus 9 operates in the nose curve.

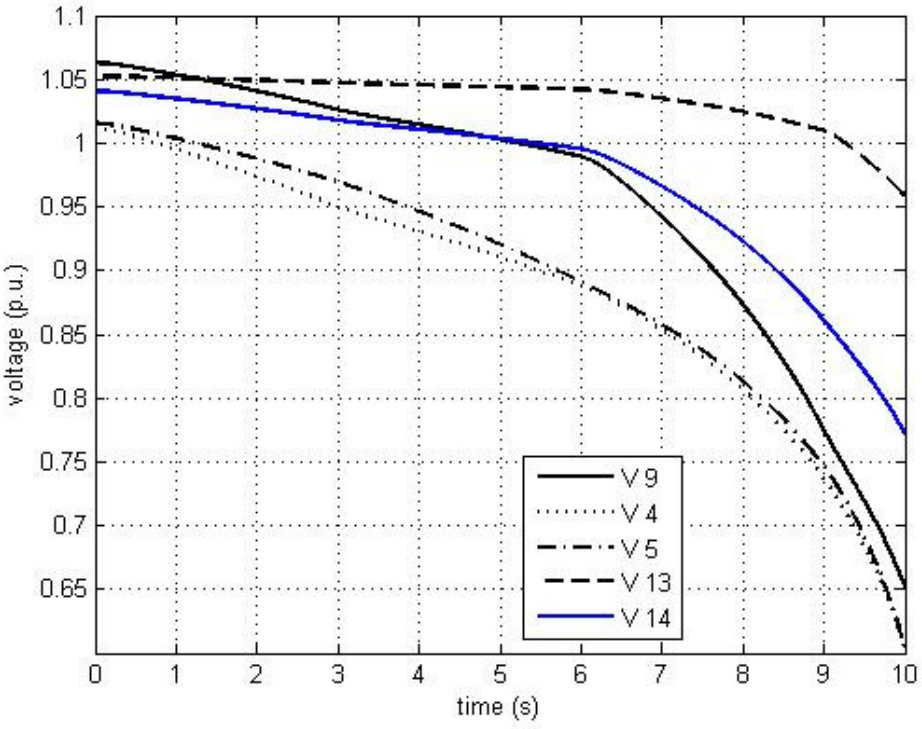

Figure 5.5 Voltage Profile of scenario a during t = 0 - 10 second

Voltage profiles for top 5 buses are shown in Figure 5.5. All of the top busses are decreasing extremely. Bus 9 has the bigger slope of load decrement in the duration of t = 5 – 10 since the load increment is happened at bus 9 at t = 6 - 9.

Generally the voltage profiles for all buses are still going to unstable operating condition. So based on the SBRT VSI, PQVSI, Power Margin, PV curve and Voltage profile verification, at t = 10 the power system is still in the insecure condition. The critical moment is happened between t = 5 – 10.

At t = 10 – 15, the snapshot of user interface system is shown in Figure 5.6 (at t = 15) and the voltage profile for top five buses is shown in Figure 5.7. At this time the load increment is affected by the increment at bus 13.

From the previous observation at t = 10, the system is already collapse. At t = 15, from the user interface windows it can be seen from the PV curve that bus 9 is operated under the nose curve that means the power system is in the insecure operating condition. It also can be confirm by looking at the SBRT VSI and PQVSI from the window at Figure 5.6

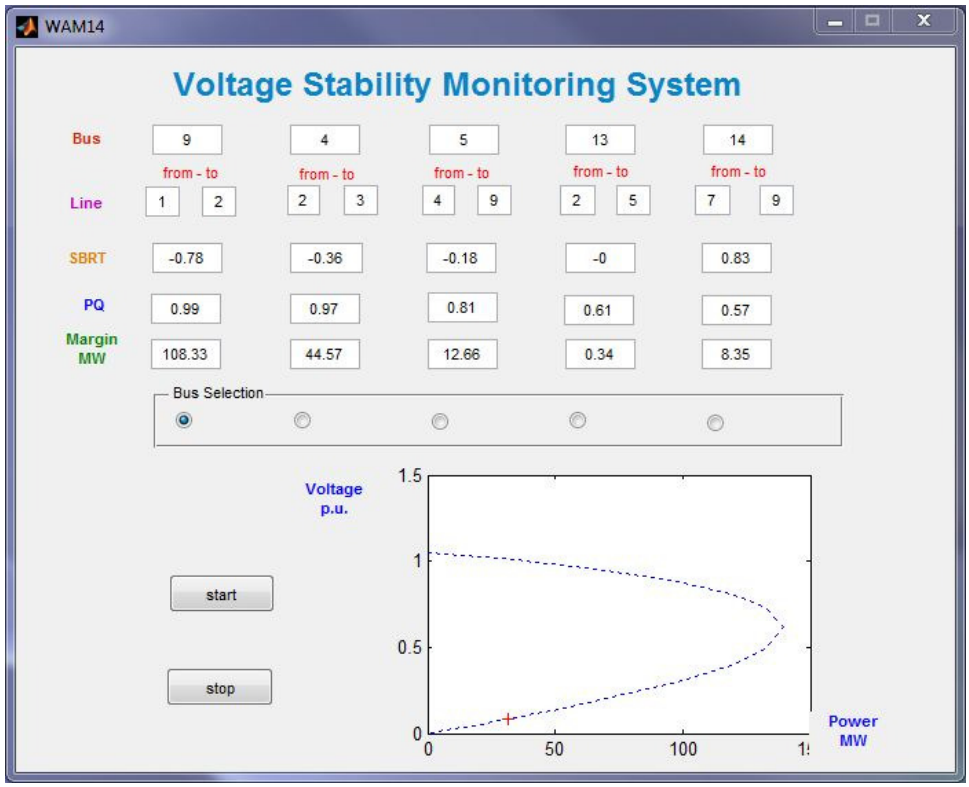

Figure 5.6 User Interface Monitoring of Scenario a at t = 15

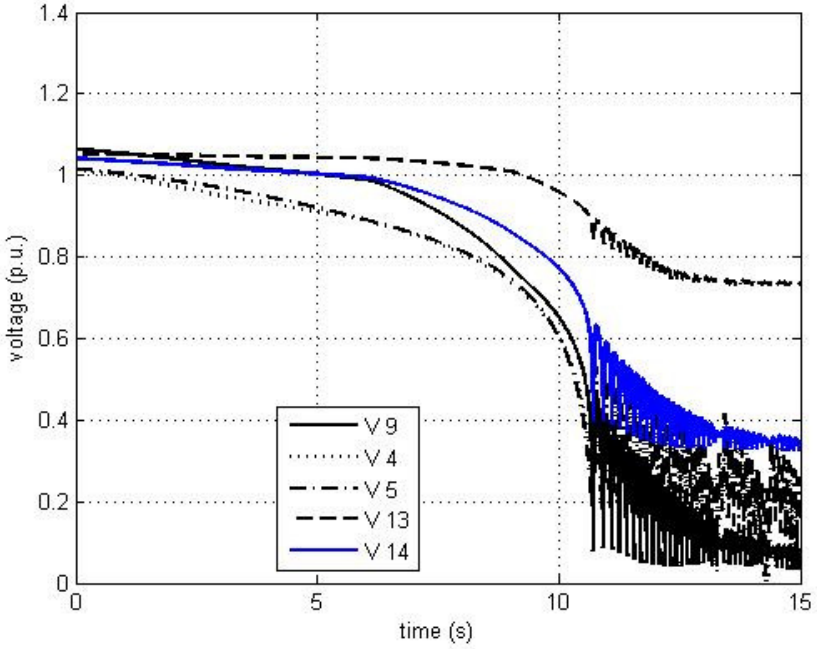

Figure 5.7 Voltage Profile in scenario a during t=0-15 second

The voltage profile of the scenario a will meet the unstable condition during the period t = 10 – 15. When t = 12 second bus voltage at bus number 4, 5, 9 and 13 go to unstable condition. So the effect of load increment in this scenario makes the system unstable after the load combination increment as shown in Figure 5.7.

Looking at the Figure 5.7, the voltage profiles of all buses are going into unstable condition after t = 10, the oscillations are happened at t = 10.5 and the oscillation is getting bigger.

5.2.2 Voltage Stability Performance Monitoring in Scenario b

In scenario b, the set of disturbance is the same of the scenario a that there is load increment at bus number 4, 5, 9 and 13. The difference is the power factor in the load bus is set as lagging 0.95. as seen below.

The first observation is at t = 0 – 5 s. The snapshot of user interface at t = 5 can be seen in Figure 5.8. The voltage profile of top five buses can be seen in the figure Figure 5.9.

At t = 5, the top five weakest buses in the scenario b are bus 4, 5, 14, 9 and 13. The values of SBRT VSI for the top five weakest buses are 0.83, 0.92, 0.93, 0.95 and 0.97. At this stage, it seems that the SBRT VSI for top five buses is still far away from the collapse point.

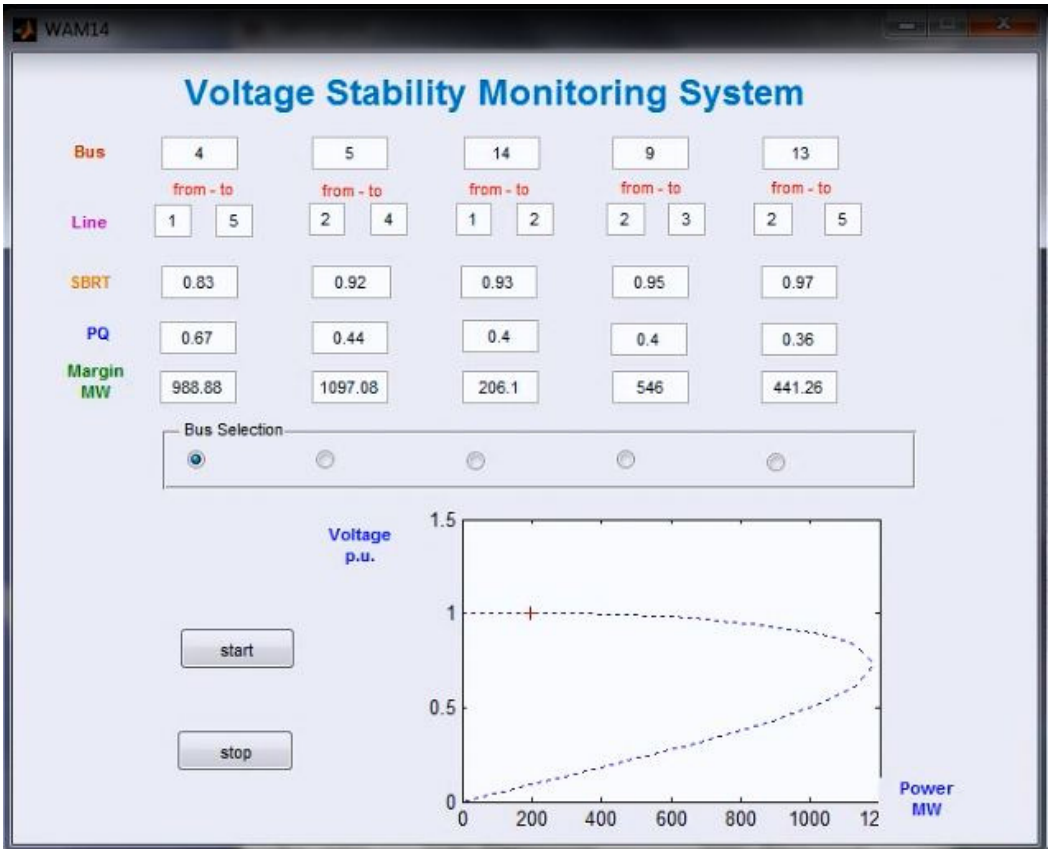

Figure 5.8 User Interface Monitoring of Scenario b at t = 5

For the line indexes, the top five weakest lines are line 1-5, 2-4, 1-2, 2-3 and 2-5 with the corresponding PQVSI index are 0.67, 0.44, 0.4, 0.4 and 0.36. It seems that the load increment increase the power flow at line 1-5. However the system still in the stable operating condition.

Power margin for the top five buses still maintain in high number. Moreover at t = 5 the PV curve for bus 4 shows that bus 4 is operated in the stable operating condition.

Based on the SBRT VSI and PQVSI the power system is still in the operating condition since there is not any index that exceeds the limit. Based on the PV curve it can be visually shown that the system is in the normal operating condition.

The voltage profile for the top five buses are shown in Figure 5.9. All of the voltages are decreasing because of the load increment. At t = 0-3 the slope decrement of bus 4 is the biggest since the load increment is happened in bus 4. At t = 3-5 the slope decrement of bus 5 is the biggest since the load increment is happened in bus5. However, generally the voltage profile view at t = 0-5 confirm the SBRT VSI and PQVSI that the system is in stable operating condition.

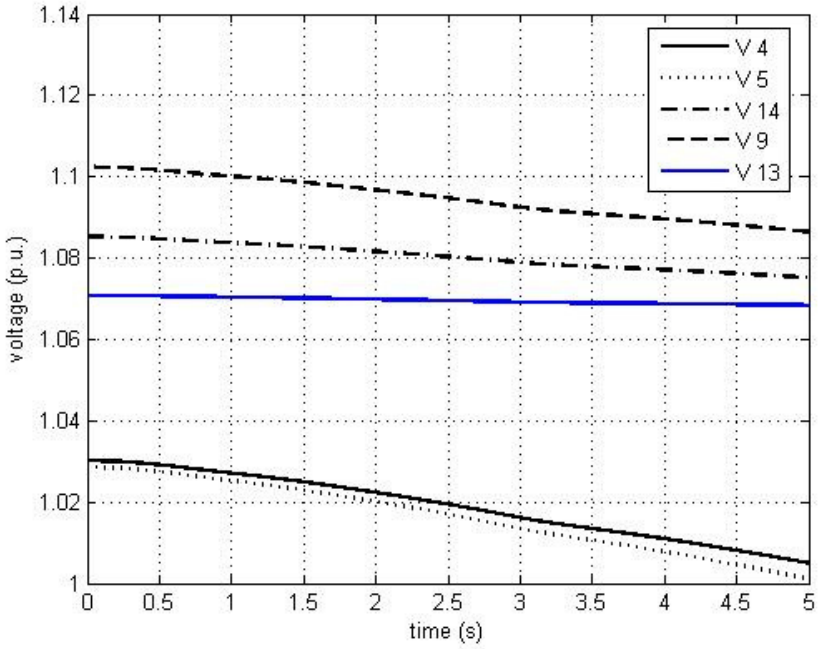

Figure 5.9 Voltage Profile in scenario b during t=0-5 second

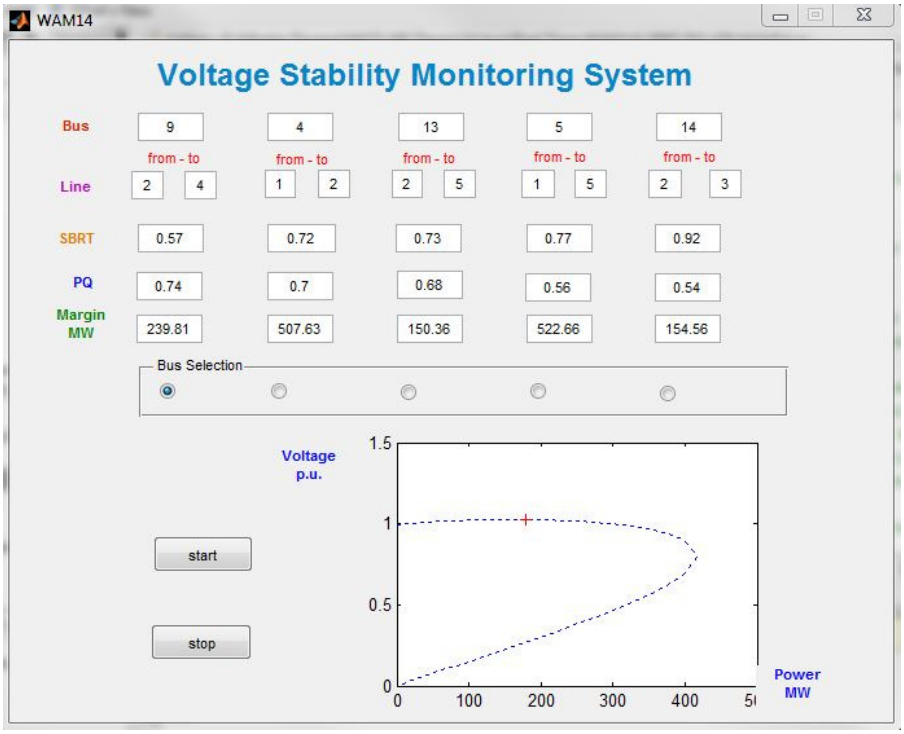

Figure 5.10 User Interface Monitoring of Scenario b at t = 10

In t = 5 – 10 second, the load increment is happened at bus 5, 9 and 13. The increment affect the power system as can be seen in Figure 5.10 for the snapshot overview of the user interface at t = 10. The voltage profile for for t = 0-10 can be seen in Figure 5.11.

Based on the WAMS user interface monitoring, the SBRT VSI at t = 10 shows that the bus 9, 4, 13, 5 and 14 as the top five buses. The SBRT VSI values for those buses are 0.57, 0.72, 0.72, 0.77 and 0.92. It seems that the load increment at bus 9 has affected the voltage stability performance much on bus 9.

The top five lines at t = 10 are line 2-4, 1-2, 2-5, 1-5 and 2-3. The PQVSI values for the corresponding lines are 0.74, 0.7, 0.68, 0.56 and 0.54. It seems that the load increment has been increased the power flow in those lines.

The power margins of the top five buses at t = 10 are decreasing as the effect of the load increment. Comparing to at t = 5, the power margin decrement is quite significant. However, form visual view of the PV plot, it seems that bus 9 still operate above the nose curve.

The voltage profile at t = 0 – 10 shows that the voltage of the top 5 buses are decreasing but still in the stable condition. Based on the SBRT VSI, PQVSI, power margin, PV curve and voltage profile observation it seems that at t = 10 the power system still in the secure operating condition.

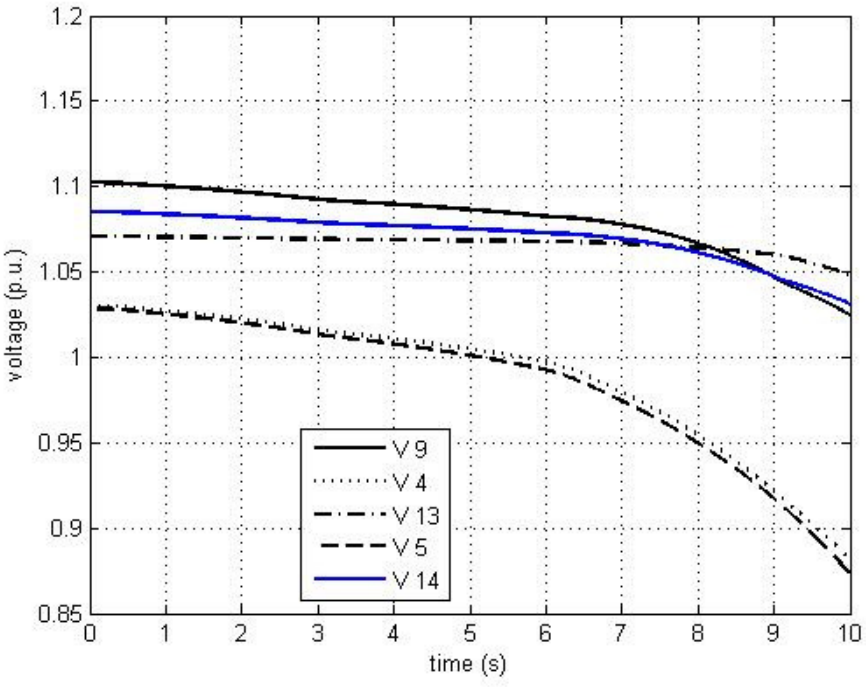

Figure 5.11 Voltage Profile in scenario b during t=0-10 second

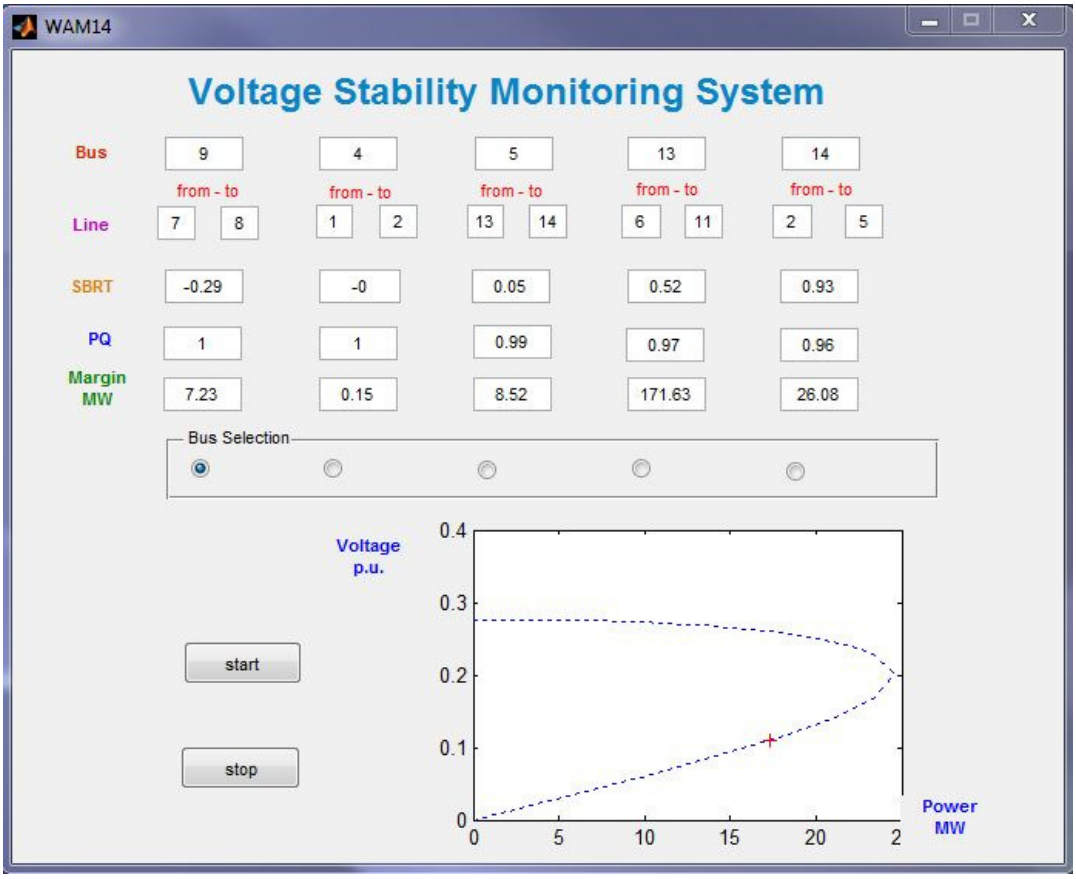

Figure 5.12 User Interface Monitoring of Scenario b at t = 15

The snapshot of WAMS at t = 15 can be shown in Figure 5.12. From the PV curve visualization it seems that at t = 15 the power system is in unstable operating condition since operated under the nose curve.

The top five buses at t = 15 are bus 9, 4, 5, 13 and 14 with the SBRT VSI value are -0.29, 0, 0.05, 0.52 and 0.93. The top five lines are line 7-8, 1-2, 13-14, 6 – 11 and 2-5 with the PQVSI values are 1, 1, 0.99, 0.97 and 0.96. The power margin is decreasing a lot comparing to at t = 10.

Based on the SBRT VSI, PQVSI, power margin and PV curve, it seems that the system has already been collapse. Bus 9, 4 5 have already violated the limit and all of the lines are violated.

Based on the voltage profile in the Figure 5.13, the voltages are started to be unstable in t = 12.5. It seems that the critical event is happened between t = 10 -12.5. The voltages profiles show that the system is unstable at t = 15 so that the voltages profiles confirm the assessment of SBRT VSI, PQVSI and the PV curve visualization of the WAMS.

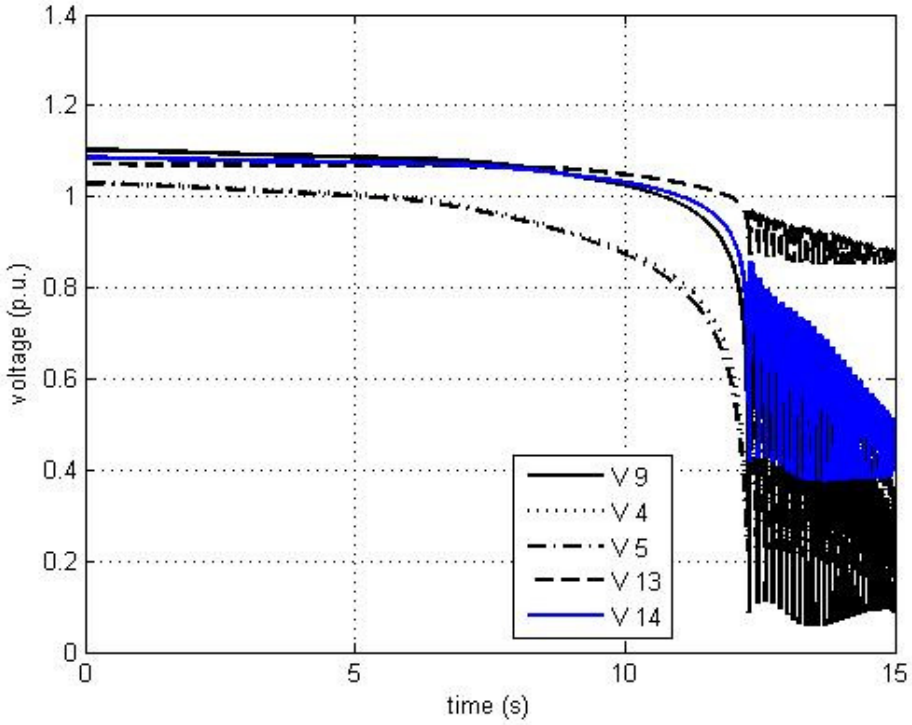

Figure 5.13 Voltage Profile in scenario b during t=0-15 second

5.2.3 Voltage Stability Performance Monitoring in Scenario c

In scenario c, set of disturbances is the combination of the load increment and the short circuit. Since there is any short circuit happened in power system, the line removal is needed to clear the short circuit. Since there is a line removal, there is a network changes.

In this scenario the first observation is when t = 0 – 5. The snapshot of user interface at t = 5 is shown in Figure 5.14. During this interval the value in the user interface is changes due to the load increment at bus 4 when t = 0 – 3.

At t = 5 the rank of the top five load buses based on the SBRT VSI is bus 4, 14, 9, 13 and 10. The SBRT VSI values for each load buses are 0.65, 0.89, 0.9, 0.95 and 0.96. The decrement is happened much in SBRT VSI at bus for as the load increment at bus 4.

The top five lines rank based on PQVSI index are 1-5, 2-4, 1-2, 2-3 and 2-5 with the PQVSI values 0.68, 0.54, 0.41, 0.41 and 0.39. Those lines are loaded more as the load increment in bus 4.

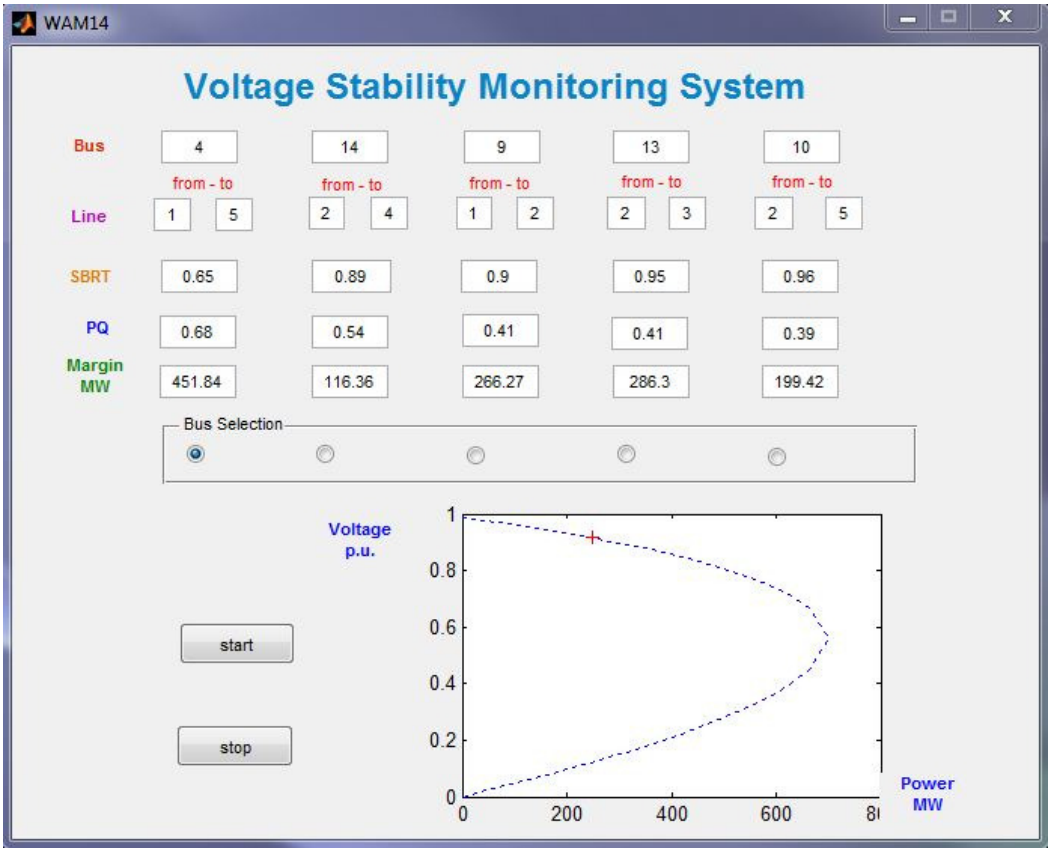

Figure 5.14 User Interface Monitoring of Scenario c at t = 5

Power margins for the top five buses are still plenty as shown in the PV curve visualization. In PV curve visualization, the distance between the actual condition and the nose curve is still far for bus 4.

The voltage profiles for the top five buses are decreasing during t = 0 – 5. The decrement is happened in the t = 0 – 3 second as the load increment at t = 0 – 4 second. Bus 4 has the bigger slope of decrement since the increment is in bus 4. After t = 4, the voltage profiles is go to the steady state values.

At the t = 4 – 5, there is no change in the power system load nor the power system configuration. However, there is a small decrement in each voltage profile of the top five buses. The effect of the disturbance still can be suffered for a little longer time and the WAMS can record that effect.

At the t = 0 - 5, based on SBRT VSI, PQVSI, power margin, PV curve and voltage profile visualization. The power system is still in the stable operating condition since there is no SBRT VSI index and PQVSI index has been violated. Since at t > 4 there is no disturbance so the user interface does not change to much form t = 4 – 5.

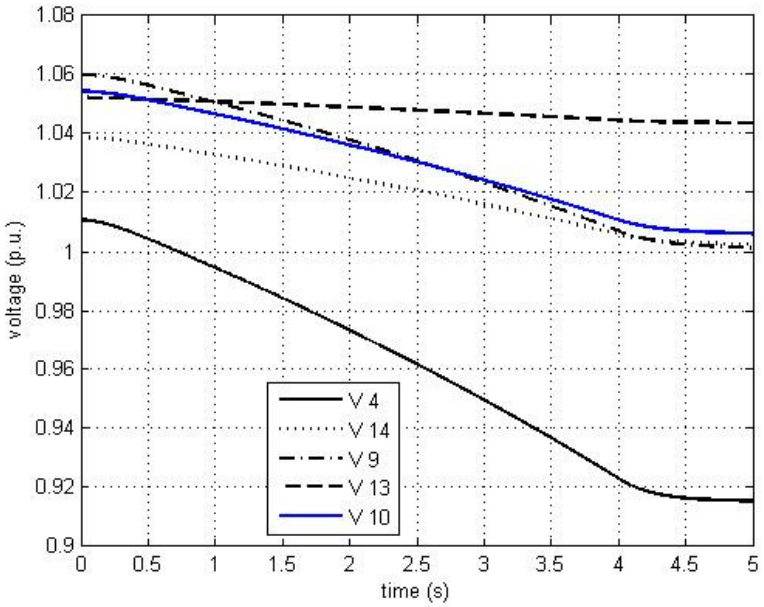

Figure 5.15 Voltage Profile in scenario c during t=0-5 second

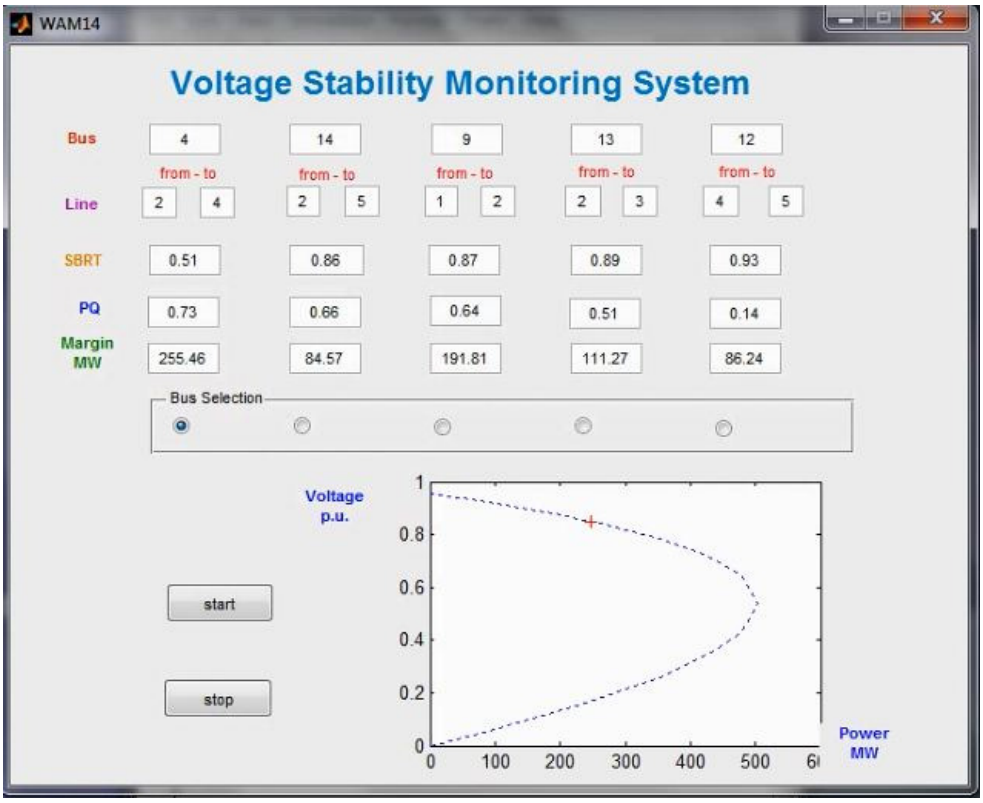

Figure 5.16 User Interface Monitoring of Scenario c at t = 10

The second observation time is at the t = 5 – 10 second. At this period the snapshot of the user interface of WAMS can be seen in Figure 5.16. The voltage profile for t = 0 – 10 can be shown in Figure 5.17. In this observation time, there is short circuit at t = 7 at line 2-5 and the line 2-5 removal at t = 7.04.

The top five buses in the in the WAMS user interface at t = 10 are bus 4, 14, 9, 13 and 12 with the SBRT VSI values are 0.51, 0.86, 0.87, 0.89 and 0.93. The top five lines are 2-4, 2-5, 1-2, 2-3 and 4-5 with the PQVSI values are 0.73, 0.66, 0.64, 0.51 and 0.14. The values of SBRT VSI index and PQVSI index are going more severe as the line 2-5 removal at t = 7.04.

The power margin and the PV visualization are still in the secure range since the distance of the actual condition is far from the nose curve at bus 4. The nearest distance is the PV curve visualization at bus 4 since this bus has the severest SBRT VSI bus index.

Voltage profiles at the top five buses are shown in Figure 5.17. The voltage profile at t = 5 – 10 are fluctuate as the short circuit and the line 2 – 5 removal. The most fluctuates bus is bus number 4 bust after the line removal, the voltage profiles can go to the stable operating condition.

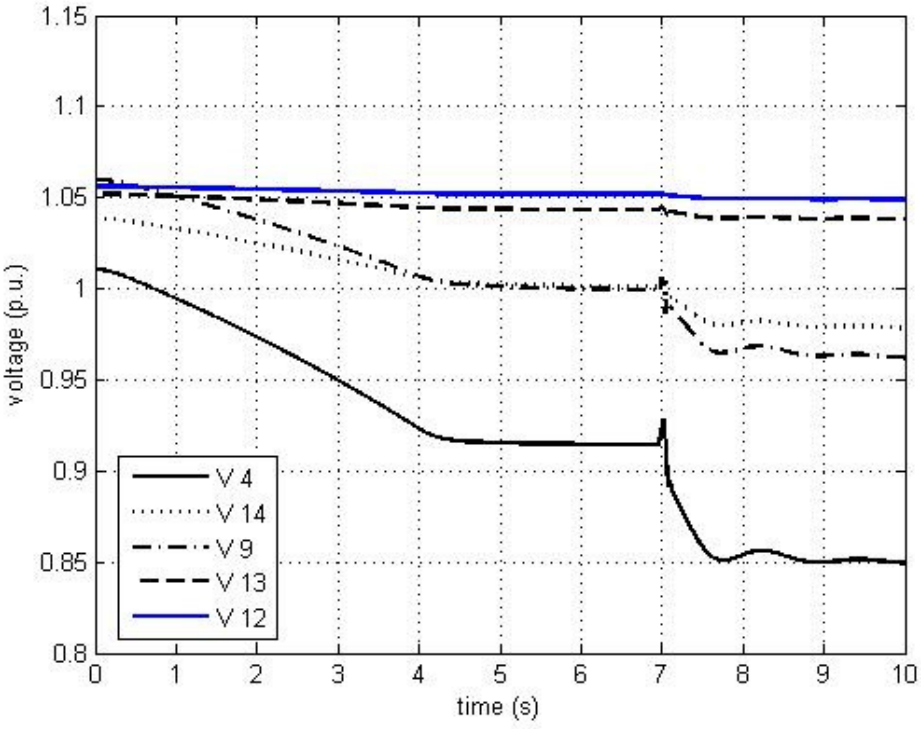

Figure 5.17 Voltage Profile in scenario c during t=0-10 second

Based on the SBRT VSI, PQVSI, power margin, PV curve visualization and voltage profile verification, the power system can reach the stable operating condition after line 2-5 removal. After the line 2-5 removal, it seems that the other lines can handle the power flow.

5.2.4 Voltage Stability Performance Monitoring in Scenario d

In scenario d, the WAMS will monitor the combination event consist of load increment and short circuit even. In the first observation time for t = 0 – 5 second. The snapshot of WAMS user interface can be seen in Figure 5.18. The voltage profile for t = 0-5 is shown in Figure 5.19.

At t = 5 the top five buses shown in WAMS user interface are bus 13, 14, 9, 4 and 10. The SBRT VSI at bus number 13 is 0.46 and the value is much lesser than the SBRT VSI of another top five buses which are 0.89, 0.9, 0.93 and 0.96 (for bus 14, 9, 4 and 10).

The top five lines in WAMS user interface are lines 1-5, 6-13, 5-6, 2-4, 2-5 with the PQVSI value 0.64, 0.55, 0.54, 0.42 and 0.39. Power margin and the PV curve visulaization are still far from the limit since the distance between the actual condition and the nose point is still far.

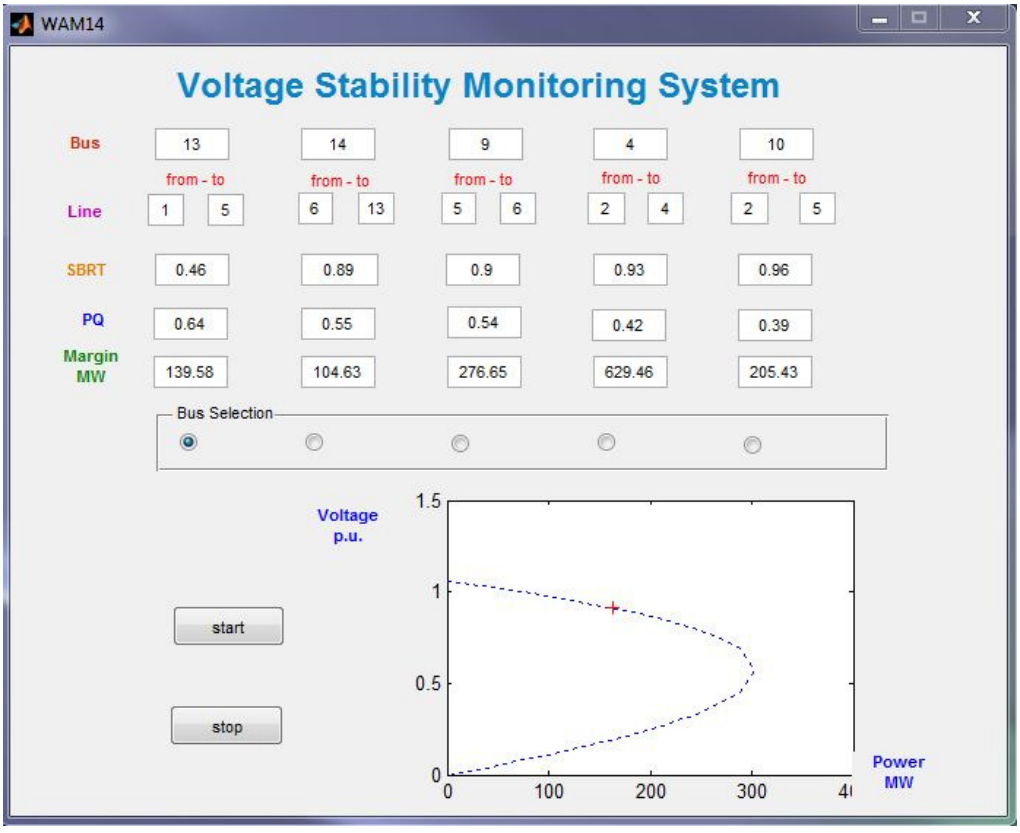

Figure 5.18 User Interface Monitoring of Scenario d at t = 5

The voltage profiles for t = 0 – 5 are shown in Figure 5.19. The voltages of all top five buses are decreasing in this period. The decrement is happened at t = 0-3 as the increment of load at bus 13 at t = 0-3. After t = 3 the voltage profile is going to the steady state values for all buses.

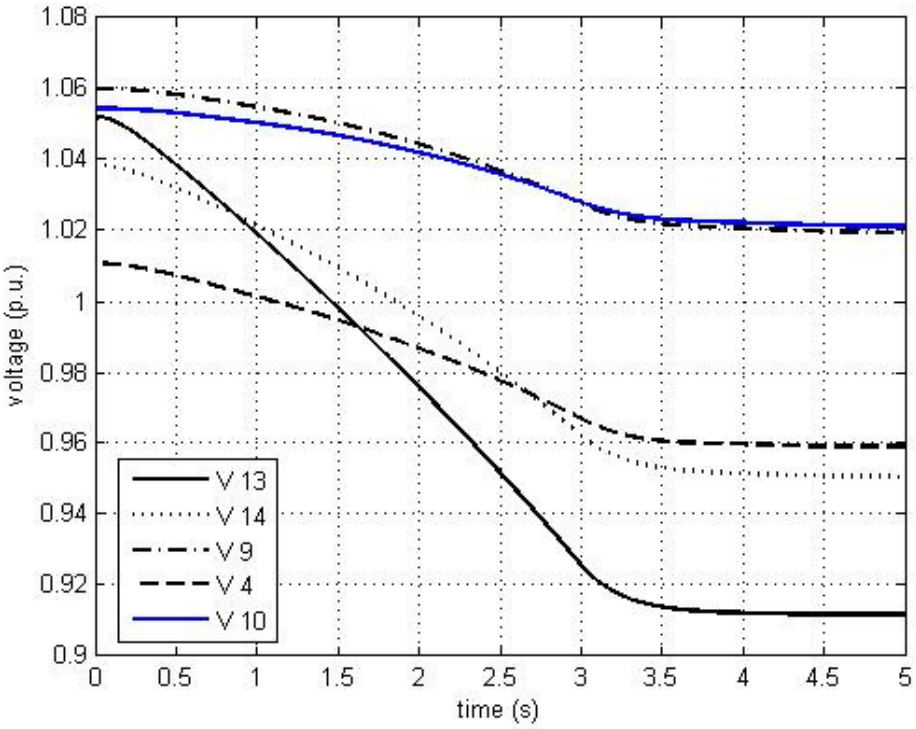

Figure 5.19 Voltage Profile in scenario d during t=0-5 second

The second observation time is at t = 5 – 10. The user interface snapshot for t = 7.1 s is shown in Figure 5.20. The voltage profile at t = 0-10 is shown in Figure 5.21. On those two figures the dynamic of the power system can be observed.

In Figure 5.20, it shows the monitoring of scenario d when the power system is in the collapse condition. Short circuit happen in line 6 - 13 that connecting bus number 6 and 13 at t = 7. The SBRT VSI of bus 13 has reached zero and the PQVSI index of the line 12 -13 is 0.94. The power margin and the PV curve visualization show that the bus 13 is in the nose point.

As can be seen in Figure 5.21 the voltage profile value, when the disturbance happened, the transient happened in all of the voltage bus in the power system. And when the short circuit clear by removing the line number 13, the voltage goes down so rapidly and the system is going to collapse at t ~= 7.04. From the voltage profile verification it shown that the system is in the collapse condition at t ~=7.04.

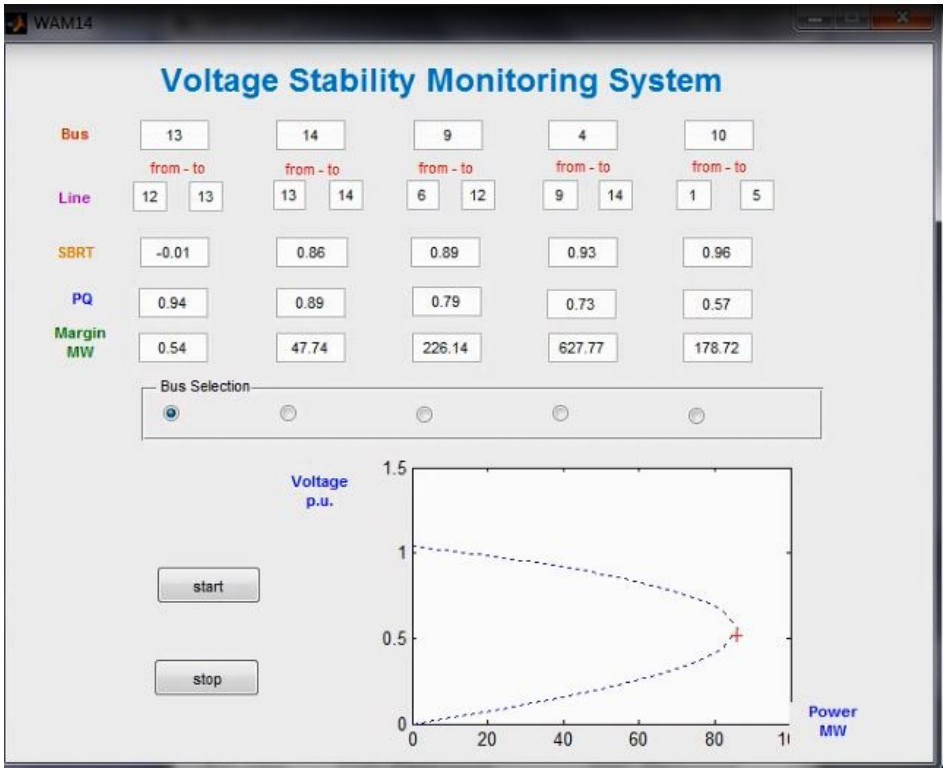

Figure 5.20 User Interface Monitoring of Scenario d at t = 7.1

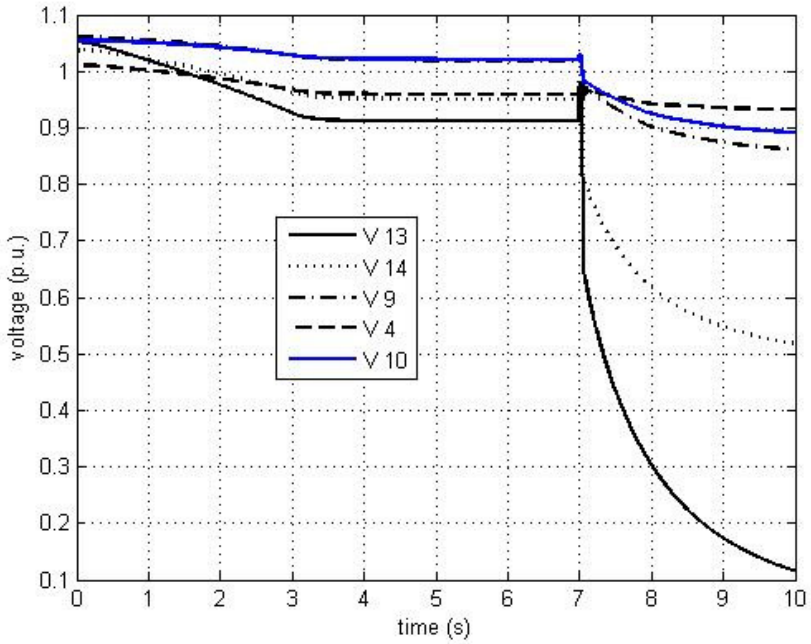

Figure 5.21 Voltage Profile in scenario d during t=0 - 10 second

5.3 Verification

SBRT VSI and PQVSI are calculated based on some assumptions described in chapter IV. For monitoring the voltage stability performance in the power system, the accurate calculation of VSI is required. SBRT VSI and PQVSI calculation can be verified using the actual values obtained from the simulation.

Verification against the result of the SBRT VSI and PQVSI in the critical point has been done in the precious section, which when the value of SBRT VSI and PQVSI are reached the limit, the voltage profile show the unstable condition.

In the graphic user interface display, the PV curve visualization is plotted using the estimated formulation using the assumption that during the PV curve plotting, the value of the remaining equivalence network voltage is remain constant while the voltage value of the load buses is changing. Thus, the verification on the SBRT VSI and PQVSI against the critical condition is needed.

In the graphic user interface display, the power margin value is calculated by find the difference between the predicted maximum loadable load in the corresponding bus and the actual condition.

5.3.1 Verification of the Voltage Stability Indexes against the Critical Point

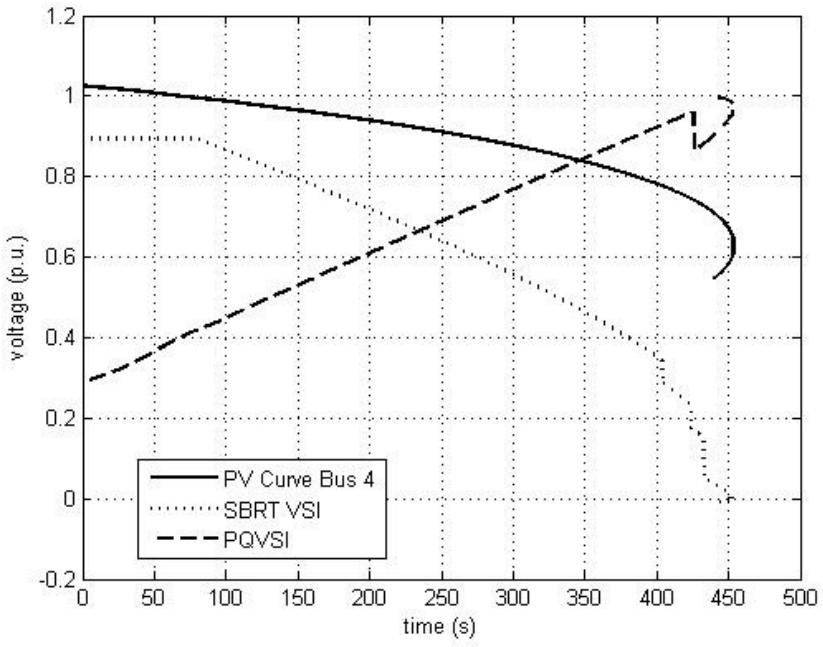

Figure 5.22 SBRT VSI and PQVSI again PV curve at bus 4

In verifying the SBRT VSI and PQVSI computation against the critical collapse point, two different scenarios are developed. The scenarios using to demonstrate the WAMS performance cannot be used since consist of multiple events, which the simulated PV curve in specified bus cannot be plotted. The first scenario is increase the load at bus 4 continuously. The second scenario is increase the load at bus 5 continuously.

In Figure 5.22, it shown that both of the SBRT VSI and PQVSI can show the critical point accurately since the value of SBRT VSI is 0 and PQVSI is 1 when the critical point at bus 4 is reached. The global indexes of SBRT VSI and PQVSI are used in this scenario to confirm that the most severe local index is used.

In Figure 5.23, it shown that both of the SBRT VSI and PQVSI can show the critical point accurately since the value of SBRT VSI is 0 and PQVSI is 1 when the critical point at bus 5 is reached.

From both scenarios, the SBRT VSI and PQVSI is well suit to use in the WAMS since the accuracy of both index is high in showing the critical point.

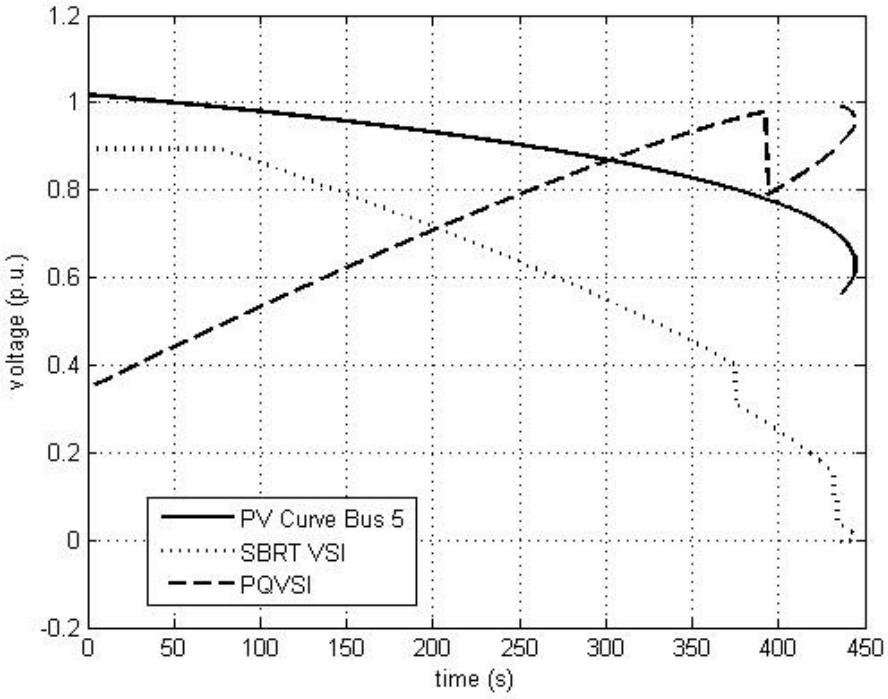

Figure 5.23 SBRT VSI and PQVSI again PV curve at bus 5

5.3.2 Verification of the Power Margin Calculation

In the GUI display, the power margin information for the top five weak buses is shown. However, the value of the power margin is calculated based on the difference between the predicted maximum loadable load in the corresponding bus and the actual condition.

To verify the power margin calculation, the first scenario, which the load at bus 4 is continuously increased is selected to explain the accuracy of the power margin. Actual PV curve, Actual Condition and predicted PV curve are compared in two different periods.

The first period is when t = 3.5 second when the bus 4 still have margin 490 MW. Figure 5.24 can show the calculated margin between the actual condition and the critical points of the predicted PV curve. On the other hand, the actual values from the dynamic simulation also can be obtained in the same figure. There is some mismatch between the actual PV curve and the predicted PV curve, which by deriving the predicted PV curve, the power margin for bus 4 is higher.

This mismatch is happened because of the assumption used in predicting the maximum load P_{max}, which the equivalent network voltage is kept constant since the pattern of the disturbance is assumed unknown as well.

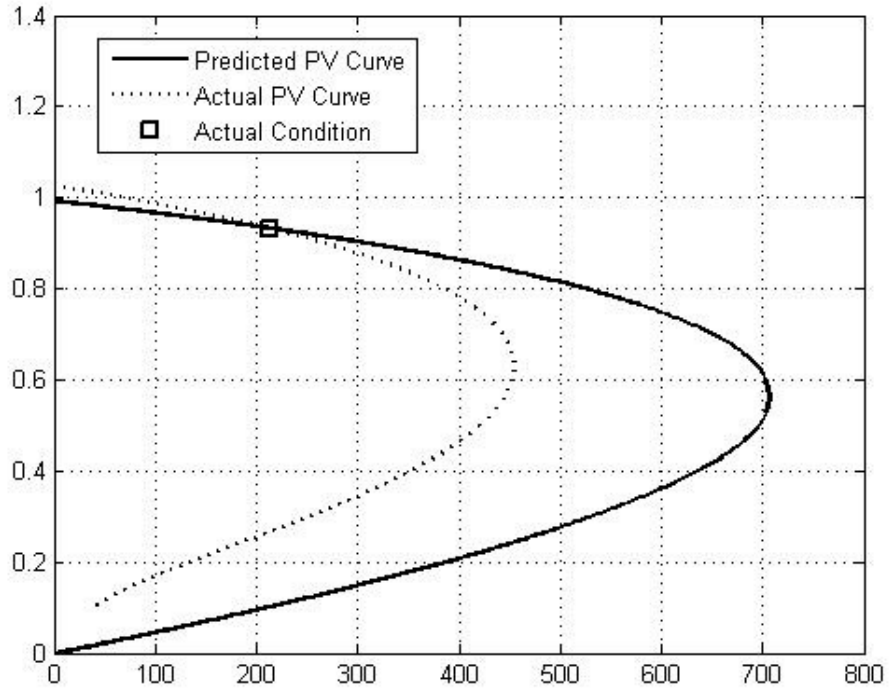

Figure 5.24 Actual PV Curve against Predicted PV Curve when t = 3.5 s

The second period time in when the t = 8.46 second, when the system is predicted near the critical point with the power margin for bus 4 is 20.5 MW. From Figure 5.25, it seems that the actual PV curve and the predicted PV curve are close, especially when showing the area near the critical point. The power margin mismatch is not huge and tolerable.

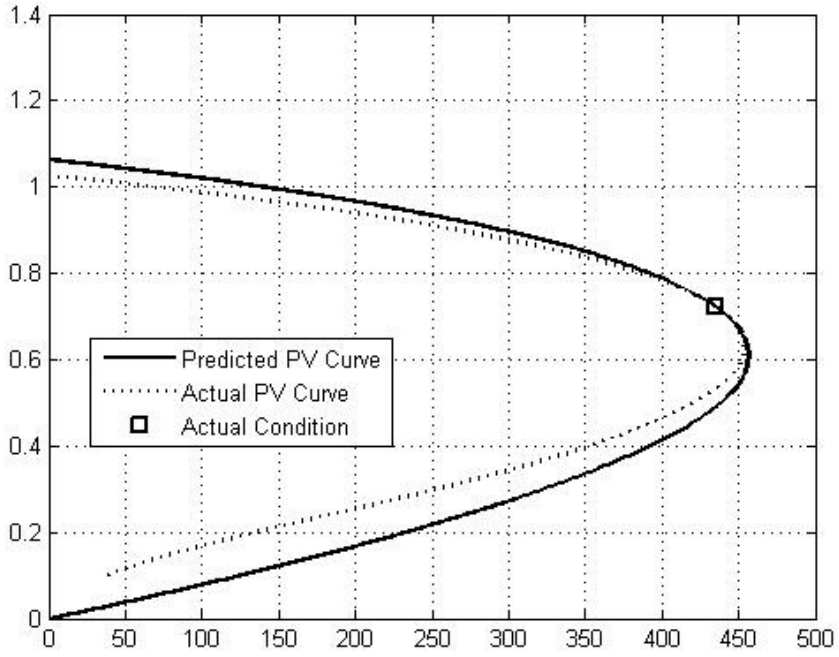

Figure 5.25 Actual PV Curve against Predicted PV Curve when t = 8.46 s

Based on those two period times observation, the accuracy of the predicted PV curve is more accurate when the power system is nearer to the critical point. The power margin calculation is more accurate as well when the power system nearer to the critical point since it calculated from the predicted PV curve.

5.4 Discussion

In voltage stability performance monitoring the properties of SBRT VSI and PQVSI can be used as well to set the monitoring system. From the voltage monitoring result some interesting point can be pointed out.

1. In voltage stability performance monitoring there is some cases that the disturbance can be monitored for longer time as shown in scenario a and scenario b. At those scenarios, the trend of VSI can be obtained in the real time. Knowing the weakest buses, the possible action can be taken when the VSI is

near the collapse point. The popular action related directly to the bus is load shedding.

2. There is a case that the disturbance cannot longer detected by the WAMS like happened in scenario d. In this scenario when the short circuit happened at t = 7 s, the action is clear the short circuit by remove the line 6-13 at t = 7.1 s. Immediately after the line removal the system is collapse with the violation of SBRT VSI and the PQVSI in bus 13 and line 12-13 while the others bus and lines still in the secure operating condition. It also can be seen in the voltage profiles of all buses. In this case, the line removal action has to be evaluated as the action. In this case removing the line 6-13 is made the voltage stability performance worse. The feasible observation whether the line is important or not at the current operation condition should be done.

CHAPTER VI
CONCLUSION AND FUTURE WORK

6.1 Conclusion

In the work of Application of Wide Area Monitoring System for Securing Voltage Stability several processes have been done to finish the work. There are several conclusions that can be taken from the process.

1. The number of the PMU used in the power system is depend on the power system network itself, more complex the power system the more PMU needed in the power system.
2. Assuming that the PMU has enough channels to record the bus voltage and power system line current related to the bus that PMU installed on. The value of PMU record can be estimated using the Linear Programming of State Estimation, which has the linear solution and does not need the iterative computation. The Linear Programming of State Estimation estimates all of the voltage bus in the power system and the result of estimation is acceptable after verified by the load flow analysis
3. Synchronized Based Real Time Voltage Stability Index (SBRT VSI) compute the voltage stability index for each load bus. Moreover the maximum power in each load bus also can be computed so that the power margin in each load bus can be computed. From this basic equation of the SBRT VSI, the PV curve in each load bus can be derived. The properties given by the derivation of SBRT VSI give the measurable information from the voltage collapse so that SBRT VSI is applicable for the on-line VSI monitoring. Moreover the computation time of SBRT VSI is still acceptable for on-line monitoring.
4. PQ Voltage Stability Index (PQVSI) computes the VSI for each line in the power system network. The other properties that can be extracted from the PQVSI are the maximum power flow in each line. PQVSI is suitable to apply in the on-line VSI monitoring system since the computation time of PQVSI is acceptable for on-line monitoring.
5. SBRT VSI and PQ VSI can synchronously show the voltage stability performance. The synchronous result of both VSI has been shown through the simulation in this work.
6. To build the advance WAMS, some factors like the speed of the computation, measurement model, state estimation, communication and the user interface have to be considered in order to perform the dynamic analysis.

6.2 Future Work

In this work some assumptions are considered to perform some parts computation of WAMS. In practical solution, the computation with some assumptions may not been met the acceptable accuracy. To increase the accuracy for the practical solution the suggestion below can be considered to conduct the future work:

1. Develop the studied to give the zone classification based on the SBRT VSI and PQVSI calculation so that the warning procedure can be applied before the voltage collapse happened.
2. In the PMU placement technique, there is an assumption that the determination of PMU number and location is for the system with the normal operating condition. The determination method does not consider the network change due to the disturbance effect. In the real system there is a probability that the line removal of the power system when the short circuit happen.
3. Network simplification in calculating SBRT VSI is using Gauss elimination and Thevenin method. This method is approximation that is suitable for constant power source. This network simplification method is used because of the accuracy is still good and time computation consideration. In the next work, the network simplification having better accuracy than this method should be applied.
4. In determining the PV curve for the user interface display, the data used is updated whenever the data form the state estimation is gotten. There is an assumption used that the voltage of the equivalent remaining circuit is the same in extrapolating the other operating condition.

The availability to develop this work in some aspect is still plenty since the WAMS can be developed into Wide Area Protection System (WAPS). Some aspect that can be developed to conduct the future work:

1. SBRT VSI can give the information about the active power margin in the load bus. This information can be developed to be the scheme of load shedding. Probably the level of margin can be elaborated further to make the use of SBRT VSI to be more practical.
2. PQVSI also can give the information about the calculated maximum power flow in each line. From this information the future study can be elaborated to be practical action. Probably the generation re-dispatches or parameter setting of FACTS controller can be applied.
3. Interdisciplinary research can be conducted by considering the communication problem in the WAMS such as the signal delay, data sampling rate etc.

REFERENCES

1. Begovic, M., et al., Summary of "System protection and voltage stability". IEEE Transactions on Power Delivery 10 (April 1995): 631 - 638.
2. Zima, M., et al., Design Aspects for Wide-Area Monitoring and Control Systems. Proceeding of the IEEE Energy Infrastructure Defense Systems 93 (May 2005): 980 - 996.
3. Begovic, M., et al., Wide-Area Protection and Emergency Control. Power Systems Conference and Exposition IEEE PES 93(April 2005): 1776-1791.
4. Terzija, l., et al., Wide-Area Monitoring, Protection, and Control of Future Electric Power Networks. Proceedings of the IEEE Network System Engineering: Meeting The Energy & Environmental Dream 99 (January 2011): 80 - 93.
5. Machowski, J., et al., Power System Dynamics: Stability and Control. England: John Wiley and Sons, 2008.
6. Eissa, M.M., et al., A Novel Back Up Wide Area Protection Technique for Power Transmission Grids Using Phasor Measurement Unit. **I**IEEE Transactions on Power Delivery 25 (January 2010): 270 - 278.
7. Westermann, D. and H. Sauvain, Experience with Wide Area Monitoring and FACTS Control in A Real Time Simulator. IEEE Transactions on Power Tech Russia (June 2005): 1 - 6.
8. Mustafa, M.A., N.S.N. Yusuf, and V.V. Terzija, Development of wide area monitoring and control applications in Malaysia. Power & Energy Society General Meeting (July 2009): 1 - 8**.**
9. Donolo, M.A. and V.A. Centeno, A Fast Quality Assessment Algorithm for Phasor Measurements. IEEE Transactions on Power Delivery Transmission and Distribution Conference and Exhibition 20 (May 2006): 1099 - 1105.
10. Darren McCrank, P.E., Phasor Measurement Unit Requirement. Alberta Electric System Operator, 2010.
11. Ouadi, A., H. Bentarzi, and J.C. Maun, A New Computer Based Phasor Measurement Unit Framework. 6th International Multi-Conference on Systems, Signals and Devices (March 2009): 1 - 6.
12. Xu, B. and A. Abur, Optimal Systems Engineering Research Center. Power System Engineering Research Center, 2005.
13. Nuqui, R.F. and A.G. Phadke, Phasor measurement unit placement based on incomplete observability. Power Engineering Society Summer Meeting 2 (July 2002):888 - 893.
14. Denegri, G.B., M. Invernizzi, and F. Milano, A Security Oriented Approach to PMU Positioning for Advanced Monitoring of a Transmission Grid. IEEE PowerCon International Conference on Power System Technology 2(2002): 798 - 803.
15. Venugopal, G., R. Veilumuthu, and P.A. Theresa, Optimal PMU Placement and Observability of Power System using PSAT. International Journal ofComputer Network and Security (2010).
16. Baldwin, T.L., et al., Power System Observability with Minimal Phasor Measurement Placement. IEEE Transactions on Power System 8 (May1993):707 - 715.

17. Gou, B., Generalized Integer Linear Programming Formulation for Optimal PMU Placement. IEEE Transactions on Power Systems 23 (August 2008). 1099 - 1104.
18. Abur, A. and A.G. Exposito, Power System State Estimation, Theory and Implementation. New York: Marcel Dekker,2005.
19. Abdollahzadeh, S.H., A.M. T, and M.M. R, The Effect of Phasor Measurement Unit on the Accuracy of the Network Estimated Variables. Second International Conference on Developments in eSystems Engineering (DESE) (December 2009): 66 - 71.
20. Simon, D., Optimal State Estimation. New Jersey: J Wiley & Sons, 2006.
21. Cutsem, V. and Vournas, Voltage stability of electric power systems. Boston:Kluwer academic publisher, 1998.
22. Kundur, P., Power system stability and control, New York: McGraw-Hill, 1994.
23. Gong, Y., A. Guzman, and N. Schulz, Synchrophasor-Based Real-Time Voltage Stability Index. Power Systems Conference and Exposition, (November 2006): 1029 - 1036.
24. Tiabrat, P., W. Yokyong, and K. Udomwongseree, PQ Voltage Stability Index (PQVSI) for Voltage Stability Analysis. EECON 31 (October 2008).

APPENDICES

APPENDIX A

Network data, Initial Loading Condition and System Configuration of IEEE 14-bus Test System

Bus Data

Table A.1. Bus Data for IEEE 14-bus Test System

Bus	type	Pload	Qload	Gs	Bs	Area	Vmagnitude	Vangle	base kVA	Zone	Vmax	Vmin
1	3	0	0	0	0	1	1.06	0	0	1	1.06	0.94
2	2	21.7	12.7	0	0	1	1.045	-4.9937	0	1	1.06	0.94
3	2	94.2	19	0	0	1	1.01	-12.778	0	1	1.06	0.94
4	1	47.8	15.7111	0	0	1	1.0106586	-10.23	0	1	1.06	0.94
5	1	7.6	2.498	0	0	1	1.0150122	-8.7171	0	1	1.06	0.94
6	2	11.2	7.5	0	0	1	1.07	-14.144	0	1	1.06	0.94
7	1	0	0	0	0	1	1.0616281	-13.32	0	1	1.06	0.94
8	2	0	0	0	0	1	1.09	-13.32	0	1	1.06	0.94
9	1	29.5	9.69618	0	19	1	1.0599585	-14.905	0	1	1.06	0.94
10	1	9	5.8	0	0	1	1.0543249	-15.057	0	1	1.06	0.94
11	1	3.5	1.8	0	0	1	1.0586167	-14.735	0	1	1.06	0.94
12	1	6.1	1.6	0	0	1	1.0561111	-15.009	0	1	1.06	0.94
13	1	13.5	4.43724	0	0	1	1.0521203	-15.119	0	1	1.06	0.94
14	1	14.9	5	0	0	1	1.0386151	-15.993	0	1	1.06	0.94

Branch Data

Table A.2 Branch data for IEEE 14-bus Test System

From	To	r	x	b	rate A	Rate B	rate C	ratio	angle	status	angle min	angle max
1	2	0.01938	0.05917	0.0528	9900	0	0	0	0	1	-360	360
1	5	0.05403	0.22304	0.0492	9900	0	0	0	0	1	-360	360
2	3	0.04699	0.19797	0.0438	9900	0	0	0	0	1	-360	360
2	4	0.05811	0.17632	0.034	9900	0	0	0	0	1	-360	360
2	5	0.05695	0.17388	0.0346	9900	0	0	0	0	1	-360	360
3	4	0.06701	0.17103	0.0128	9900	0	0	0	0	1	-360	360
4	5	0.01335	0.04211	0	9900	0	0	0	0	1	-360	360
4	7	0	0.20912	0	9900	0	0	0.978	0	1	-360	360
4	9	0	0.55618	0	9900	0	0	0.969	0	1	-360	360
5	6	0	0.25202	0	9900	0	0	0.932	0	1	-360	360
6	11	0.09498	0.1989	0	9900	0	0	0	0	1	-360	360
6	12	0.12291	0.25581	0	9900	0	0	0	0	1	-360	360
6	13	0.06615	0.13027	0	9900	0	0	0	0	1	-360	360
7	8	0	0.17615	0	9900	0	0	0	0	1	-360	360
7	9	0	0.11001	0	9900	0	0	0	0	1	-360	360
9	10	0.03181	0.0845	0	9900	0	0	0	0	1	-360	360
9	14	0.12711	0.27038	0	9900	0	0	0	0	1	-360	360
10	11	0.08205	0.19207	0	9900	0	0	0	0	1	-360	360
12	13	0.22092	0.19988	0	9900	0	0	0	0	1	-360	360
13	14	0.17093	0.34802	0	9900	0	0	0	0	1	-360	360

Generator Data

Table A.3. Generator Data of IEEE 14-bus Test System

Gen (bus)	Pgen	Qgen	Qmax	Qmin	Vg	mbase	status	Pmax
1	232.443	-14.517	10	0	1.06	100	1	332.4
2	40	50.3745	50	-40	1.045	100	1	140
3	0	29.272	40	0	1.01	100	1	100
6	0	12.2083	24	-6	1.07	100	1	100
8	0	17.5563	24	-6	1.09	100	1	100

Generator Data parameter for SIMULINK Model

Table A.4. Generator Data for Simulink Model

Generator	MVA	kV	x_l (p.u.)	r_s (p.u.)	x_d (p.u.)	x'_d (p.u.)	T'_{do}	x_q (p.u.)	x'_q (p.u.)	T'_{qo}	H	D
Gen 2	60	100	0	0.0031	1.05	0.185	6.1	0.98	0.36	0.3	6.54	2
Gen 8	60	100	0	0.0031	1.05	0.185	6.1	0.98	0.36	0.3	6.54	2

APPENDIX B

State Estimation Result for IEEE 30-bus and 57-bus Test System

Table B.2 Voltage Estimation in IEEE 30-bus Test System

Bus Number	V Load Flow		V estimated		Error ($x10^{-8}$)	
	Vmag (p.u.)	Vang (deg)	Vmag (p.u.)	Vang (deg)	Vmag (%)	Vang (%)
1	**1.0000**	**0.00**	**1.0000**	**0.00**	**0.769**	**50.765**
2	1.0000	-0.42	1.0000	-0.42	0.814	49.394
3	0.9831	-1.52	0.9831	-1.52	0.745	45.712
4	0.9801	-1.79	0.9801	-1.79	0.596	11.363
5	0.9824	-1.86	0.9824	-1.86	0.546	12.648
6	0.9732	-2.27	0.9732	-2.27	0.527	18.726
7	**0.9674**	**-2.65**	**0.9674**	**-2.65**	**0.474**	**21.307**
8	0.9606	-2.73	0.9606	-2.73	0.643	18.375
9	**0.9805**	**-3.00**	**0.9805**	**-3.00**	**0.437**	**19.316**
10	**0.9844**	**-3.37**	**0.9844**	**-3.37**	**0.401**	**19.849**
11	0.9805	-3.00	0.9805	-3.00	0.584	18.469
12	**0.9855**	**-1.54**	**0.9855**	**-1.54**	**0.382**	**21.579**
13	1.0000	1.48	1.0000	1.48	0.471	13.238
14	0.9767	-2.31	0.9767	-2.31	0.398	10.963
15	0.9802	-2.31	0.9802	-2.31	0.446	18.930
16	0.9774	-2.64	0.9774	-2.64	0.462	7.871
17	0.9769	-3.39	0.9769	-3.39	0.405	16.047
18	**0.9684**	**-3.48**	**0.9684**	**-3.48**	**0.520**	**32.752**
19	0.9653	-3.96	0.9653	-3.96	0.562	29.029
20	0.9692	-3.87	0.9692	-3.87	0.541	10.361
21	0.9934	-3.49	0.9934	-3.49	0.433	18.462
22	1.0000	-3.39	1.0000	-3.39	0.541	14.404
23	1.0000	-1.59	1.0000	-1.59	0.461	4.471
24	**0.9886**	**-2.63**	**0.9886**	**-2.63**	**0.432**	**21.552**
25	**0.9902**	**-1.69**	**0.9902**	**-1.69**	**0.532**	**26.654**
26	0.9722	-2.14	0.9722	-2.14	0.516	20.181
27	**1.0000**	**-0.83**	**1.0000**	**-0.83**	**0.477**	**24.249**
28	**0.9747**	**-2.27**	**0.9747**	**-2.27**	**0.484**	**21.886**
29	0.9796	-2.13	0.9796	-2.13	0.433	2.459
30	0.9679	-3.04	0.9679	-3.04	0.292	1.590

Table B.2. State Estimation in IEEE 57-bus Test System

Bus Number	V Load Flow		V estimated		Error (x10^{-8})	
	Vmag (p.u.)	Vang (deg)	Vmag (p.u.)	Vang (deg)	Vmag (%)	Vang (%)
1	1.0400	0.00	1.0400	0.00	0.740	30.584
2	1.0100	-1.19	1.0100	-1.19	0.742	32.030
3	0.9850	-5.99	0.9850	-5.99	0.366	34.454
4	0.9808	-7.34	0.9808	-7.34	0.334	35.483
5	0.9765	-8.55	0.9765	-8.55	0.315	31.286
6	0.9800	-8.67	0.9800	-8.67	0.294	34.966
7	0.9842	-7.60	0.9842	-7.60	0.306	29.773
8	1.0050	-4.48	1.0050	-4.48	0.455	29.742
9	0.9800	-9.58	0.9800	-9.58	0.848	29.239
10	0.9862	-11.45	0.9862	-11.45	0.254	3.520
11	0.9740	-10.19	0.9740	-10.19	0.739	33.532
12	1.0150	-10.47	1.0150	-10.47	0.705	31.995
13	0.9789	-9.80	0.9789	-9.80	0.699	34.752
14	0.9702	-9.35	0.9702	-9.35	0.716	33.629
15	0.9880	-7.19	0.9880	-7.19	0.747	31.768
16	1.0134	-8.86	1.0134	-8.86	0.840	32.363
17	1.0175	-5.40	1.0175	-5.40	0.748	29.543
18	1.0007	-11.73	1.0007	-11.73	0.716	33.629
19	0.9702	-13.23	0.9702	-13.23	0.674	22.128
20	0.9638	-13.44	0.9638	-13.44	0.495	56.345
21	1.0085	-12.93	1.0085	-12.93	0.747	47.272
22	1.0097	-12.87	1.0097	-12.87	0.691	48.769
23	1.0083	-12.94	1.0083	-12.94	0.699	48.014
24	0.9992	-13.29	0.9992	-13.29	0.747	47.272
25	0.9825	-18.17	0.9825	-18.17	0.719	49.683
26	0.9588	-12.98	0.9588	-12.98	0.287	16.806
27	0.9815	-11.51	0.9815	-11.51	0.197	34.416
28	0.9967	-10.48	0.9967	-10.48	0.269	30.828
29	1.0102	-9.77	1.0102	-9.77	0.236	32.488
30	0.9627	-18.72	0.9627	-18.72	0.887	34.511
31	0.9359	-19.38	0.9359	-19.38	0.724	25.266
32	0.9499	-18.51	0.9499	-18.51	0.608	26.547
33	0.9476	-18.55	0.9476	-18.55	0.596	24.352
34	0.9592	-14.15	0.9592	-14.15	0.723	6.171
35	0.9662	-13.91	0.9662	-13.91	0.179	44.241
36	0.9758	-13.63	0.9758	-13.63	0.169	46.747
37	0.9849	-13.45	0.9849	-13.45	0.196	43.634
38	1.0128	-12.73	1.0128	-12.73	0.691	47.744
39	0.9828	-13.49	0.9828	-13.49	0.171	44.955
40	0.9728	-13.66	0.9728	-13.66	0.169	44.011
41	0.9962	-14.08	0.9962	-14.08	0.472	50.071

Bus Number	V Load Flow		V estimated		Error (x10^{-8})	
	Vmag (p.u.)	Vang (deg)	Vmag (p.u.)	Vang (deg)	Vmag (%)	Vang (%)
42	0.9665	-15.53	0.9665	-15.53	0.502	43.336
43	1.0096	-11.35	1.0096	-11.35	0.547	44.789
44	1.0168	-11.86	1.0168	-11.86	0.786	34.960
45	1.0360	-9.27	1.0360	-9.27	0.738	35.430
46	1.0598	-11.12	1.0598	-11.12	0.725	7.587
47	1.0333	-12.51	1.0333	-12.51	0.678	12.603
48	1.0274	-12.61	1.0274	-12.61	0.667	11.452
49	1.0362	-12.94	1.0362	-12.94	0.821	33.849
50	1.0233	-13.41	1.0233	-13.41	0.257	6.752
51	1.0523	-12.53	1.0523	-12.53	0.244	7.149
52	0.9804	-11.50	0.9804	-11.50	0.359	20.838
53	0.9709	-12.25	0.9709	-12.25	0.352	53.338
54	0.9963	-11.71	0.9963	-11.71	0.424	63.452
55	1.0308	-10.80	1.0308	-10.80	0.368	51.623
56	0.9684	-16.07	0.9684	-16.07	0.729	15.707
57	0.9648	-16.58	0.9648	-16.58	1.318	66.407

APPENDIX C
PMU Data Record Modeling

In this work the PMU data record is done using the calculation. The voltages of the PMU bus is computed using the real time data of the generator voltage and the load admittance. Using the equation:

$$\begin{bmatrix} I_L \\ I_G \end{bmatrix} = \begin{bmatrix} Y_{LL} & Y_{LG} \\ Y_{GL} & Y_{GG} \end{bmatrix} \begin{bmatrix} V_L \\ V_G \end{bmatrix}$$

$$\begin{bmatrix} V_L \\ I_G \end{bmatrix} = \begin{bmatrix} Z_{LL} & H_{LG} \\ F_{GL} & Y_{GG} \end{bmatrix} \begin{bmatrix} I_L \\ V_G \end{bmatrix}$$

Where

$$Y_{\text{bus updated}} = \begin{bmatrix} Y_{LL} & Y_{LG} \\ Y_{GL} & Y_{GG} \end{bmatrix}$$

The value of the $Y_{\text{bus updated}}$ is the Y_{bus} add with the load admittance value of the load bus. By adding the load admittance into the Y_{bus} the value of the element of vector I_L is equal to zero so that the value of vector V_L can be derived from the V_G only.

Line current value can be calculated using the equation 4.2. With the a is the tap transformer ratio 1:a (from:to) and the y_t is the line admittance. When all of the bus voltage is known by calculating the voltage using the equation 4.1, the line current can be calculated.

$$\begin{bmatrix} I_{ij} \\ I_{ij} \end{bmatrix} = \begin{bmatrix} y_t & -\frac{y_t}{a} \\ -\frac{y_t}{a^*} & \frac{y_t}{|a|^2} \end{bmatrix} \begin{bmatrix} V_i \\ V_j \end{bmatrix}$$

Bus voltage data and line current data are recorded by PMU installed on the buses. The recording data is taken directly from the calculation result of equation 4.1 and 4.2.

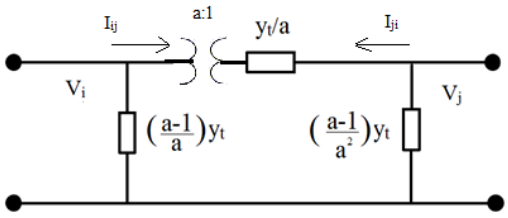

Figure C.1. Representation of from and to bus at with the tap factor a of transformer

BIOGRAPHY

Lesnanto Multa Putranto was born in Yogyakarta, Indonesia, in 1985. He received his Bachelor's degree in electrical engineering from Gadjah Mada University, Indonesia, in 2007. He has been granted a scholarship by the AUN/SEED-Net (www.seed-net.org) to pursue his Master's degree in electrical engineering at Chulalongkorn University, Thailand, since 2010. He conducted his graduate study with the Power System Research Laboratory, Department of Electrical Engineering, Faculty of Engineering, Chulalongkorn University. His research interest focuses on Application of Wide Area Monitoring System for Securing Voltage Stability.